TURUN YLIOPISTO
UNIVERSITY OF TURKU

CHILD BRAIN DEVELOPMENT: EXPLORING PRENATAL IMPACTS AND EMOTIONAL PERCEPTION THROUGH ADVANCED NEUROIMAGING

– Findings from the FinnBrain Birth Cohort Study

Niloofar Hashempour

TURUN YLIOPISTON JULKAISUJA – ANNALES UNIVERSITATIS TURKUENSIS
SARJA – SER. D OSA – TOM. 1815 | MEDICA – ODONTOLOGICA | TURKU 2024

TURUN YLIOPISTO
UNIVERSITY OF TURKU

CHILD BRAIN DEVELOPMENT: EXPLORING PRENATAL IMPACTS AND EMOTIONAL PERCEPTION THROUGH ADVANCED NEUROIMAGING

– Findings from the FinnBrain Birth Cohort Study

Niloofar Hashempour

TURUN YLIOPISTON JULKAISUJA – ANNALES UNIVERSITATIS TURKUENSIS
SARJA – SER. D OSA – TOM. 1815 | MEDICA – ODONTOLOGICA | TURKU 2024

University of Turku

Faculty of Medicine
Institute of Clinical Medicine
Department of Psychiatry
Doctoral Programme in Clinical Research

Supervised by

Professor, Hasse Karlsson, MD, PhD
FinnBrain Birth Cohort Study
Department of Clinical Medicine
University of Turku
Turku, Finland

Associate Professor, Jetro J Tuulari, MD, PhD
FinnBrain Birth Cohort Study
Department of Clinical Medicine
University of Turku
Turku, Finland

Associate Professor, Harri Merisaari, PhD
FinnBrain Birth Cohort Study
Department of Clinical Medicine
University of Turku
Turku, Finland

Reviewed by

Associate Professor, Isabelle M. Rosso, PhD
Department of Psychiatry
Harvard Medical School
Boston, MA, USA

Kiran Thapaliya, PhD
National Centre for Neuroimmunology and Emerging Diseases (NCNED)
Griffith University
Gold Coast, QLD, Australia

Opponent

Associate Professor, Predrag Petrovic, MD, PhD
Department of Clinical Neuroscience
Karolinska Institute
Stockholm, Sweden

The originality of this publication has been checked in accordance with the University of Turku quality assurance system using the Turnitin OriginalityCheck service.

Cover Image: Niloofar Hashempour

ISBN 978-951-29-9863-0 (PRINT)
ISBN 978-951-29-9864-7 (PDF)
ISSN 0355-9483 (Print)
ISSN 2343-3213 (Online)
Painosalama, Turku, Finland 2024

In every child's smile, a light shines bright,
No matter their color, no matter their race,
Their dreams and their fears, deserve care and kindness.

-*For the mental wellness of all children worldwide.*

UNIVERSITY OF TURKU
Faculty of Medicine
Department of Clinical Medicine
Psychiatry
NILOOFAR HASHEMPOUR: Child brain development: exploring prenatal impacts and emotional perception through advanced neuroimaging – Findings from the FinnBrain Birth Cohort MRI Study
Doctoral Dissertation, 154 pp.
Doctoral Programme in Clinical Research (DPCR)
September 2024

ABSTRACT

The amygdala, a key player in emotional processing, undergoes rapid growth and development prenatally and in infancy. Environmental factors, such as prenatal maternal depressive symptoms, can alter the structure of the amygdala. The altered structure of the amygdala can influence neural and functional development, contributing to negative outcomes in offspring. However, identifying limbic system structures, such as the amygdala and hippocampus, in infants' brain magnetic resonance (MR) images is challenging. This difficulty arises from the small size of these structures, the lower resolution of the scans, and the lack of accurate segmentation methods. This thesis encompasses three studies involving mothers and infants from the FinnBrain Birth Cohort Study. In study I, a manual segmentation protocol tailored to neonatal MR images was established, focusing on the amygdala and hippocampus in healthy infants. In study II, we investigated the links between prenatal maternal depressive symptoms (PMDS) at different gestational stages and infant amygdala microstructure using diffusion tensor imaging (DTI). Sex-specific responses to PMDS were revealed, with boys showing a stronger positive association between PMDS and the left amygdala DTI parameter (mean diffusivity). In study III, we explored the neural basis of emotional perception in infancy, correlating amygdala microstructure with infants' recognition of emotional faces using eye-tracking. Increased right amygdala mean diffusivity was associated with reduced disengagement from fearful faces, while sex differences revealed that girls with elevated amygdala mean diffusivity exhibited greater disengagement from scrambled non-face control pictures. These studies advance our understanding of early neurodevelopment by examining the development of the amygdala, a crucial element in emotional processing and regulation.

KEYWORDS: amygdala, diffusion tensor imaging, maternal prenatal depression, fear processing, brain development

TURUN YLIOPISTO
Lääketieteellinen tiedekunta
Kliininen laitos
Psykiatria
NILOOFAR HASHEMPOUR: Lapsen aivojen kehitys: synnytystä edeltävien vaikutusten ja emotionaalisen havainnoinnin tutkiminen kehittyneen neurokuvantamisen avulla – FinnBrainin syntymäkohortti -tutkimuksen tuloksia
Väitöskirja, 154 s.
Turun kliininen tohtoriohjelma (TKT)
Syyskuu 2024

TIIVISTELMÄ

Mantelitumake kasvaa ja kehittyy nopeasti raskauden sekä vauvaiän aikana ja on myöhemmissä ikävaiheissa keskeinen aivorakenne muun muassa masennukseen ja pelkoon liittyvässä emotionaalisessa käsittelyssä. Ympäristötekijät, kuten synnytystä edeltävät äidin masennusoireet, voivat vaikuttaa mantelitumakkeen kasvuun ja kehitykseen, millä voi olla pitkäkestoisia vaikutuksia lapsen kehitykseen. Mantelitumakkeen tunnistaminen imeväisten aivojen magneettiresonanssi – kuvissa (MRI) on osoittautunut kuitenkin haastavaksi MRI-kuvien alhaisemman erotustarkkuuden rajoitteiden vuoksi. Tämä opinnäytetyö sisältää kolme tutkimusta, joissa on mukana FinnBrain Birthsyntymäkohorttitutkimuksen äitejä ja vauvoja. Väitöskirjan ensimmäisessä osatyössä I kehitettiin vastasyntyneiden MRI-kuville manuaalinen segmentointiprotokolla mantelitumakkeelle ja aivotursolle. Osatutkimuksessa II tutkittiin yhteyksiä synnytystä edeltävien äidin masennusoireiden eri raskausvaiheissa ja vauvan amygdalan mikrorakenteen välillä, käyttämällä diffuusiotensorikuvausta (DTI). Äidin oireisiin löytyi sukupuolispesifisiä yhteyksiä, ja pojilla oli vahvempi positiivinen yhteys äidin synnytystä edeltävien masennusoireiden ja vasemman amygdalan keskimääräisen diffusiviteetin välillä. Tutkimuksessa III tutkittiin emotionaalisen tarkkaavaisuuden hermoperustaa vauvaiässä. DTI-kuvista arvioitu oikeanpuoleisen mantelitumakkeen keskimääräinen diffusiviteetti oli yhteydessä vähentyneeseen irrottautumiseen pelokkaista kasvojen ilmeistä, kun taas sukupuolierot osoittivat suurempaa irrottautumista kasvoja sisältämättömistä kontrollikuvista tytöillä, joilla oli kohonnut mantelitumakkeen keskimääräinen diffusiviteetti. Yhdessä nämä tutkimukset edistävät ymmärrystämme varhaisesta hermoston kehityksestä tarkastelemalla amygdalan kehitystä, jolla on tärkeä osa tunteiden käsittelyssä ja säätelyssä.

AVAINSANAT: amygdala, diffuusiotensorikuvantaminen, äidin synnytystä edeltävä masennus, pelon käsittely, aivojen kehitys

Table of Contents

Abbreviations

DTI	Diffusion Tensor Imaging
MR	Magnetic Resonance
PMDS	Prenatal Maternal Depressive Symptoms
MD	Mean Diffusivity
FA	Fractional Anisotropy
AD	Axial Diffusivity
GW	Gestational Weeks
CNS	Central Nervous System
SSRI	Selective Serotonin Reuptake Inhibitor
SNRI	Serotonin and Norepinephrine Reuptake Inhibitor
EPDS	Edinburgh Postnatal Depression Scale
iBEAT	Infant Brain Extraction and Analysis Toolkit
TE	Echo Time
TR	Repetition Time
TSE	Turbo Spin Echo
MPRAGE	Magnetization Prepared Rapid Acquisition Gradient Echo
TI	Inversion Time
NIFTI	Neuroimaging Informatics Technology Initiative
FSL	Fmrib Software Library
MINC	Medical Imaging Netcdf
AAL	Automatic Anatomical Labeling
MNI	Montreal Neurological Institute
GCI	Generalized Conformity Index
DWI	Diffusion-Weighted Imaging
EPI	Echo Planar Imaging
SD	Standard Deviation
DSD	Dice Similarity Coefficient
ICC	Intraclass Correlation Coefficient
FDR	False Discovery Rate
DP	Disengagement Probability
CS	Scrambled Non-Face Control Picture

NE	Neutral
HA	Happy
FE	Fearful
HPA	Hypothalamic-Pituitary-Adrenal
1β-HSD2	11-Beta Hydroxysteroid Dehydrogenase 2

List of Original Publications

This dissertation is based on the following original publications, which are referred to in the text as studies I-III. The original publications have been reproduced with the permission of the copyright holders.

I Hashempour N, Tuulari JJ, Merisaari H, Lidauer K, Luukkonen I, Saunavaara J, Parkkola R, Lähdesmäki T, Lehtola S, Keskinen M, Lewis J, Scheinin N, Karlsson L, Karlsson H. (2019). A Novel Approach for Manual Segmentation of the Amygdala and Hippocampus in Neonate MRI. Frontiers in Neuroscience, 13.

II Hashempour N, Tuulari JJ, Merisaari H, Acosta H, Lewis JD, Pelto J, Scheinin NM, Fonov VS, Collins DL, Lehtola SJ, Saunavaara J, Lähdesmäki T, Parkkola R, Karlsson L, Karlsson H. (2023). Prenatal maternal depressive symptoms are associated with neonatal left amygdala microstructure in a sex-dependent way. European Journal of Neuroscience, January 2022, 1–18.

III Hashempour N, Tuulari JJ, Merisaari H, Lewis JD, Häikiö T, Scheinin NM, Nolvi S, Korja R, Karlsson L, Karlsson H, Kataja EL. Neonatal amygdala mean Diffusivity: a potential predictor of emotional face perception. (Manuscript)

1 Introduction

Brain development is a complex and intricate process that unfolds across prenatal and postnatal stages, resulting in profound changes in brain structure and function. It is during the prenatal period that the foundation for many of these developmental changes is laid, including the early formation of key structures such as the amygdala and hippocampus. The limbic system, with the amygdala and hippocampus at its core, plays a central role in shaping emotional and cognitive responses (Ressler, 2010; Ruiz et al., 2018; Saghir et al., 2018). Over recent years, advanced neuroimaging techniques, such as diffusion tensor imaging (DTI), have emerged as invaluable tools for exploring the complexities of brain structures (Basser et al., 1994). DTI, notable for its ability to provide detailed information about both white and gray matter microstructures, holds promise for studying the development of brain regions (Stebbins, 2010). However, there is a scarcity of studies conducted on amygdala and hippocampus development using DTI, due to challenges in studying neonatal brain development. These challenges include the smaller size of infant brains, the lower resolution of DTI scans (Weisenfeld et al., 2006), and the difficulty in accurately identifying brain structures in neonatal brain scans. Therefore, there is a need for manual segmentation protocols for studying the amygdala and hippocampus of the developing brain.

Furthermore, environmental factors like prenatal maternal depressive symptoms (PMDS) play a role in amygdala development, resulting in enduring effects from the prenatal period into adulthood (Susser et al., 2016). PMDS have emerged as a noteworthy concern, with far-reaching implications for both mothers and their offspring (Bonari et al., 2004; Davalos et al., 2012; Douros et al., 2017). These symptoms have been associated with adverse birth outcomes, neurodevelopmental issues, and neuropsychiatric disorders in children (Kinney et al., 2008; Ronald et al., 2011). Moreover, PMDS may exert a significant influence on the structure and function of the amygdala in offspring, potentially contributing to emotional and behavioral challenges (Wen et al., 2017). Research has also begun to uncover that the effects of PMDS can differ between males and females, indicating that sex-specific factors may play a role in how these symptoms impact neurodevelopment. Additionally, the timing of PMDS exposure during different stages of prenatal development may result in varying effects on the amygdala and subsequent behavior. Yet, our understanding of the sex-specific effects of PMDS at different stages of prenatal exposure remains incomplete, with gaps in knowledge.

It is known that infants have a preference for emotional facial expressions over alternative stimuli, a tendency that is closely linked to the maturation and functioning of the amygdala (Prunty et al., 2020). This preference, holds critical importance in understanding infants' socio-emotional development (Reynolds & Roth, 2018). While it is known that infants exhibit longer fixation times on fearful faces, yet the origins and neural underpinnings of this bias remain unknown (Peltola et al., 2013). While neuroimaging studies have revealed amygdala activation in response to fearful stimuli, the examination of potential microstructural changes in the amygdala related to attentional bias towards fearful facial stimuli during infancy remains unclear (Zhao et al., 2017). Exploring this relationship might provide insights into the underlying neurological mechanisms of fear regulation and their potential long-term consequences in the developing brain.

To these ends, this thesis presents a manual segmentation protocol for identifying the amygdala in infant brain MRI scans. Additionally, by employing DTI, we examined the connections between amygdala microstructure and PMDS at various gestational stages, as well as emotional perception during infancy. Furthermore, our research delved into potential sex differences. These investigations may potentially address gaps in our understanding of the developing amygdala.

2 Review of the Literature

2.1 Embryonic brain development

The developing brain goes through a series of processes during pregnancy that shape its neural architecture and set the foundation for future cognitive and emotional functions. The development of the central nervous system (CNS) is a complex and prolonged process that spans across various stages of prenatal and postnatal life (Figure 1) (de Graaf-Peters & Hadders-Algra, 2006). The total brain volume in the neonatal phase is roughly 35% of what is reported in adults brains (Mortamet et al., 2005). Overall brain size doubles within the first year of life, reaching around 73% of the adult brain (Gilmore et al., 2007). Brain maturation continues beyond the embryonic period, extending until around age 25 (Hochberg & Konner, 2020).

2.1.1 Neurulation

During the first trimester, the foundation of the CNS is laid. A significant event in this period is dorsal induction, which leads to neurulation, which occurs around week 3 of the postconceptional weeks (Singh & Munakomi, 2023). The neural plate begins to fold inward, forming the neural tube, which eventually becomes the brain and spinal cord (Singh & Munakomi, 2023). As the neural tube closes, foundational brain structures like the forebrain, midbrain, and hindbrain initiate their development (Ackerman, 1992). At the 4th postconceptional week, the forebrain is divided into two cerebral hemispheres and the optic vesicles, and related facial features are formed (Leibovitz et al., 2022).

2.1.2 Proliferation

In the 8th postconceptional week to late second trimester, neuronal and glial proliferation takes place in the brainstem and spinal cord (Leibovitz et al., 2022; Prado & Dewey, 2014; Thomason, 2020). It is believed that overproduction of neurons and glial cells occurs. This mechanism initiates apoptosis, leading to the elimination of excess neurons (Fricker et al., 2018). This elimination helps prevent the formation of communication pathways that might lack specific, accurate communication networks (Saxena & Caroni, 2007).

2.1.3 Neural migration

Neurons originating in the subventricular zone migrate toward the outer brain zones (O'Rahilly & Muller, 2006). A majority of neurons undergo sequential waves of migration between the 12th and 20th gestational weeks (GW), leading to the formation of the six-layered cortex (neocortex) (Leibovitz et al., 2022; Stiles & Jernigan, 2010).

2.1.4 Cortical organization

Cortical organization begins around 22–24 postconceptional weeks, and includes the maturation of the six-layered cortex as well as axon and dendrite growth from cortical neurons, which contributes to the development of inter-neuronal synapses during infancy (Leibovitz et al., 2022).

2.1.5 Myelination

Myelination marks the brain's final developmental phase. Neuronal axons are enveloped by fatty cells, enhancing neuronal communication by accelerating electrical signal transmission compared to unmyelinated axons (Tierney & Nelson, 2009). Myelination timelines vary across brain regions. At 25 weeks, myelination begins in the pallidothalamic fibers of the posterior internal capsule that connect the globus pallidus and the thalamus (Hasegawa et al., 1992). The majority of myelination occurs after birth and continues into early adulthood (Barnea-Goraly et al., 2005; Govaert et al., 2020).

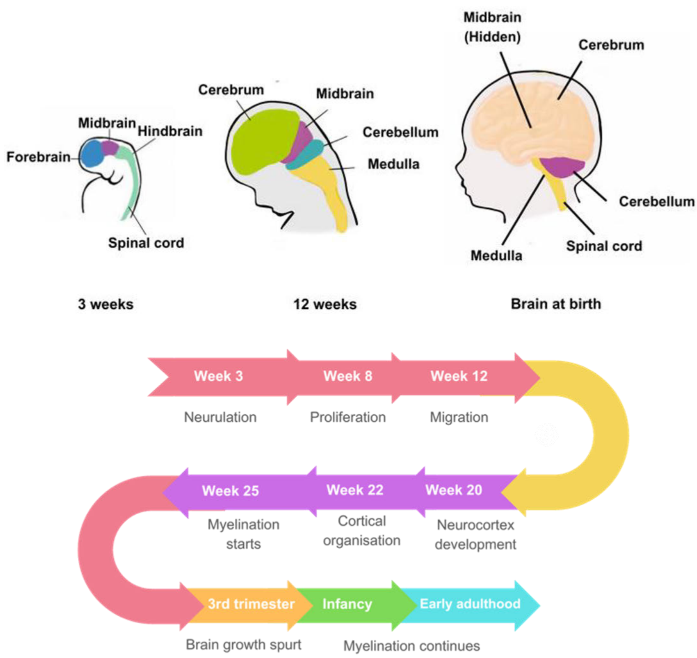

Figure 1. Schematic illustrations outlining the critical period and specific brain components relevant to the early phases of brain development (the timeframes are measured at postconceptual age). Author's illustration.

2.1.6 White matter and gray matter maturation

Cortical gray matter volume undergoes a remarkable 21-fold increase, while white matter volume sees a 22-fold growth, and deep subcortical structures expand by 10-fold between the 18th and 39th GW (Andescavage et al., 2017). The expansion of white matter and deep subcortical structures is particularly notable during the second trimester compared to the third. However, the third trimester sees a doubled growth rate in cortical gray matter compared to the second trimester (Andescavage et al., 2017; Munakata et al., 2013). Around the 19th to 20th GW, at birth, and at 6 years of age, the development of white matter shows a pattern where limbic fibers mature first, followed by association fibers (Huang et al., 2006). In the early weeks following birth, gray matter matures at a faster pace in sensory and motor regions than in prefrontal regions (K. Konrad et al., 2013). The findings from available research indicate that the volume growth of white and gray matter during the prenatal period and early life is subject to variations across brain regions and developmental stages. Overall, comprehensive studies on gray and white matter development, particularly gray matter, remain scarce.

2.2 Brain asymmetry

A variety of factors influence brain macro- and micro-structural asymmetry, including sex, age, and brain region (Kivilevitch et al., 2010; Liu et al., 2021; Tanaka et al., 2013). This asymmetry emerges from the prenatal stages into adulthood. During the 20-22-week gestation period, the left hemisphere has a larger volume than the right hemisphere in both male and female fetuses, with this disparity being more prominent in males (Hering-Hanit et al., 2001). A rightward hemisphere asymmetry becomes apparent as individuals age into older children and adults (Giedd et al., 1996). Brain asymmetry extends to other areas of the brain, such as left-greater-than-right asymmetry in the lateral ventricles, which can even be detected through prenatal ultrasonography (Achiron et al., 1997). Before the 28th GW, the left hemisphere of the brain has larger subcortical volumes than the right hemisphere. However, by the time of term birth, these changes were no longer discernible (Andescavage et al., 2017).

In the first half of life, DTI indicates a central-peripheral asymmetry pattern in MD, showing leftward lateralization in the neocortex and rightward asymmetry in deep brain regions (Liu et al., 2021). Infant brains exhibit greater brain asymmetry compared to adults (Matsuzawa et al., 2001). Neonatal brains display a 5% difference in left-to-right gray matter, whereas adults exhibit a 0.19% right-to-left difference (Gilmore et al., 2007; Gur et al., 1999).

When compared to the temporal lobes, the frontal lobes grow at a faster rate during the first two years of life. The right-left asymmetry is higher in the temporal lobes than in the frontal lobes, and gray matter volume growth is faster than white matter growth in the temporal lobes (Matsuzawa et al., 2001). Neonatal brain asymmetry patterns arise from prenatal genetic programs, with early gene expression evidence starting at GW 12 (Sun & Walsh, 2006). In adults, genetic programming intertwines with postnatal development and environmental factors to shape asymmetry patterns (Gilmore et al., 2007).

2.3 Brain sexual dimorphism

Differences between sexes are evident in both neonatal and adult brain structures. In the case of adults, women demonstrate a higher ratio of gray matter, while men exhibit a larger proportion of white matter (Gur et al., 1999). Signs of sexual dimorphism are already evident at the time of birth (Gilmore et al., 2007). Notably, variations in head circumference associated with sexual dimorphism appear as early as the second trimester of pregnancy (Joffe et al., 2005).

Furthermore, disparities in total intracranial volumes and cortical gray matter volumes become apparent right from birth. In neonates, males display roughly 9% more growth in intracranial volumes and a 10% increase in cerebral gray matter in comparison to females, mirroring the distinctions identified in both childhood and adulthood (Giedd et al., 1999; Gur et al., 1999; Raz et al., 2004). The brains of infant boys display a 6% greater amount of cortical white matter, though this dissimilarity is not as pronounced as the difference observed in adults (Gur et al., 1999).

2.4 Limbic system

The limbic system integrates cognitive and emotional responses, shaping human behavior and physiological responses to various stimuli (Hariri et al., 2000; Tyler J. & Abdijadid, 2023). The limbic system is located lateral to the thalamus, underneath the cerebral cortex, and above the brainstem (Tyler J. & Abdijadid, 2023). The development of the limbic system typically takes place during the initial phases of gestation, and the formation of limbic fibers becomes evident approximately between the 19th and 20th weeks (Huang et al., 2006). During the embryonic period, the midbrain and forebrain form elements of the limbic system (Gupta, 2017). The limbic system includes the olfactory bulbs, hippocampus, amygdala, anterior thalamic nuclei, fornix, column of fornix, mammillary body, septum pellucidum, anteriror commissure, cingulate gyrus, parahippocampal gyrus, limbic cortex, limbic midbrain areas, and pons (Figure 2) (Gupta, 2017).

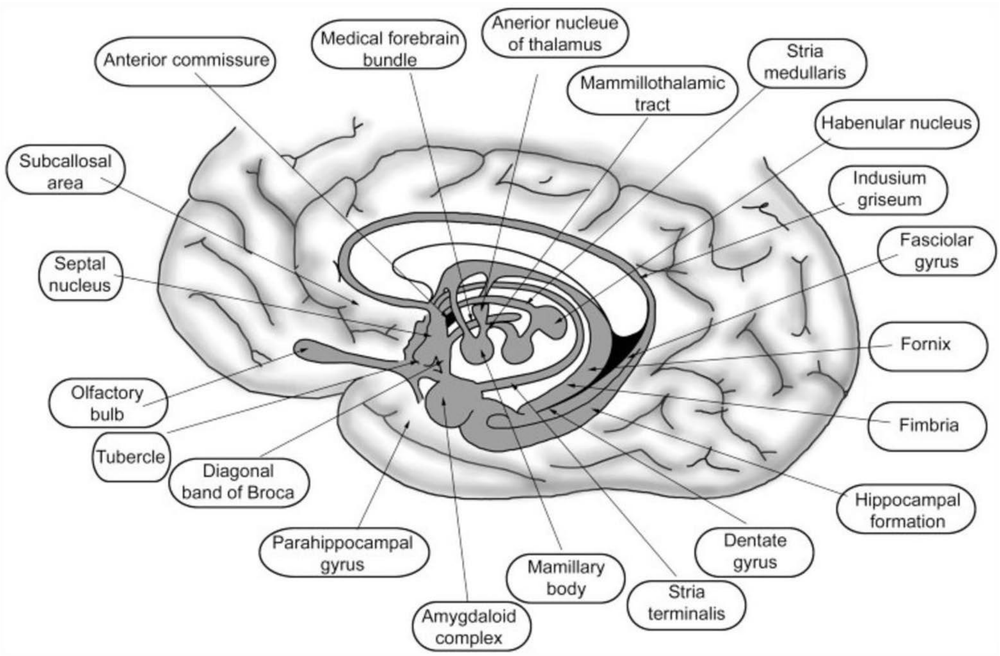

Figure 2. Illustration of the limbic system. The figure is adapted from Gupta, 2017 and is reprinted with the permission of the copyright holders.

2.5 Amygdala and hippocampus

Subcortical brain structures constitute approximately a quarter of the entire human brain volume and encompass a diverse collection of gray matter nuclei (Forstmann et al., 2017). These nuclei encompass the thalamus, basal ganglia, hippocampus, amygdala, and nucleus accumbens (Forstmann et al., 2017). The hippocampus is a seahorse-like curved shape, a feature that is functionally significant. This unique form allows for a high degree of connectivity within the hippocampal formation and between the hippocampus and other regions of the brain (Duvernoy et al., 2005). The hippocampus begins its rapid growth phase around 32 weeks of gestation, continuing this development for at least the first 18 postnatal months (Albi et al., 2022). The maturation and development of the hippocampus during the prenatal period and after birth are critical for cognitive function and memory formation (Zeidman & Maguire, 2016). The amygdala is situated within the medial temporal lobe and is recognized for its pivotal role in processing emotional reactions, particularly those linked to fear, anxiety, depression, and aggression (Ressler, 2010; Ruiz et al., 2018; Saghir et al., 2018). The earliest migration of cells that contribute to the creation of the striatal complex occurs near the interventricular foramen, close to the developing hippocampus formation (Humphrey, 1968). Because of its distinctive topographical position, the amygdala is the first component of the human striatal complex to develop embryologically (Humphrey, 1968). The amygdaloid nuclei form as a result of neuroblast migration from the germinal epithelium (Humphrey, 1968). Throughout GW 7, all amygdala cells arise from the lateral striatal ridge, and by GW 8, neuroblasts from the medial striatal ridge also contribute to amygdala formation (Humphrey, 1968). The three principal subdivisions of the amygdala, namely, the basolateral complex of the amygdala, the central amygdala, and the medial amygdala, begin to take shape around the 5th week of gestation (Figure 3) (Müller & O’Rahilly, 2006). By the 8th week, crucial amygdala connections are established with pathways that link parts of the forebrain to the hindbrain (such as the medial forebrain bundle), as well as with the neighboring formations of the hippocampus, hypothalamus, and thalamus, which collectively form the limbic system (Müller & O’Rahilly, 2006). The amygdala's rapid growth throughout pregnancy and infancy emphasizes the relevance of this time period for neural and functional development.

Previous research findings have shown amygdala lateralization. Magnetic resonance imaging (MRI) and post-mortem analyses have found that adults generally exhibit greater rightward asymmetry in amygdala volumes (G. M. J. Murphy et al., 1987; Pedraza et al., 2004). Interestingly, a study found that only boys aged 8 to 11 years old had rightward amygdala asymmetry, suggesting a potential link between androgens and amygdala volume asymmetry (Lombardo et al., 2012). Additionally, it was observed that the volumes of the left amygdala undergo significant growth exclusively in males, indicating sex-specific developmental changes between the ages of 4 and 18 years (Giedd et al., 1996). When considering developmental patterns, the right amygdala experiences prolonged growth, whereas the left amygdala's growth rate is more pronounced during early childhood, irrespective of sex (Uematsu et al., 2012). The period of the amygdala reaching its largest volume occurs between the ages of 9 and 11 (Uematsu et al., 2012). Notably, the female bilateral amygdala reaches its peak volume around 18 months prior to the male amygdala (Uematsu et al., 2012).

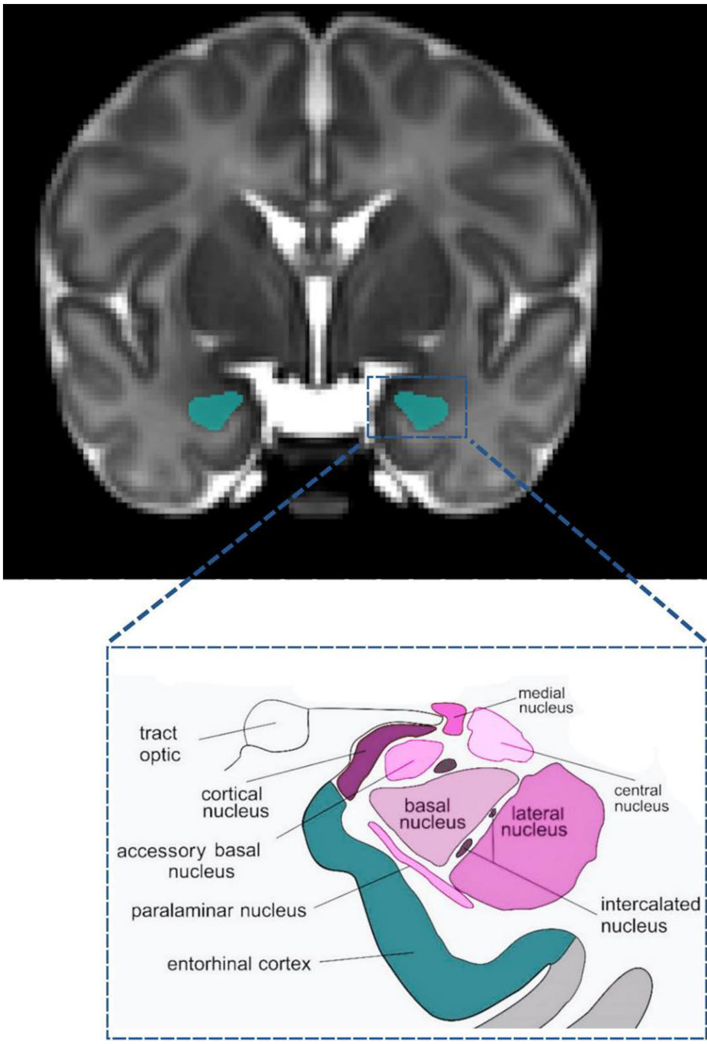

Figure 3. The manually segmented amygdala of an infant and its nuclei are presented. Author's illustration.

2.6 Neonatal amygdala segmentation

Neuroimaging studies have been used to investigate the structure of the amygdala across different stages of life, both in adult and pediatric populations (Bethlehem et al., 2022). Neuroimaging techniques mostly use MRI to study amygdala morphology (Bertoni, 2012). MRI is a safe and valuable tool for investigating postnatal brain structure changes in infants (Jernigan et al., 2011).

MRI in infants is difficult due to insufficient signal strength and low image resolution, which differ from adult MRI. This is potentially due to variations in anatomy, the requirement for specialized procedures, and distinct imaging techniques (Barkovich et al., 2019; Thukral, 2015). Even after successfully obtaining high-quality brain MRI scans in infants, the task of accurately identifying and segmenting the desired anatomical structures remains challenging.

While automated and semi-automated software for segmenting adult brains is widely accessible, the availability of tools designed for infant brain segmentation is comparatively limited. The process of manually segmenting an infant's brain is recognized as the gold standard—an accurate approach for comprehending and exploring brain structure (Devi et al., 2017; Morey et al., 2009). Within the initial two years of life, brain segmentation is challenging due to the rapid structural development and movement of infants during scanning (Weisenfeld et al., 2006). While certain studies have developed manual segmentation protocols for infants, it's important to note that these protocols do not specifically pertain to the amygdala within the healthy full-term newborn population. Several studies have outlined manual segmentation techniques applicable to MR images of healthy adults. However, the distinct contrast and reduced resolution of MR images of infant brains hinder the direct application of adult methods to segment infant brains (Gousias et al., 2012). Nonetheless, the identification of the amygdala offers the possibility of further research into its role in a wide range of physiological and behavioral responses (Aggleton et al., 1980).

2.7 Magnetic resonance imaging

MRI is an invaluable tool for studying the brain, particularly in infants. Its non-invasive nature, coupled with its ability to produce high-resolution images without the use of ionizing radiation, makes it especially suitable for pediatric populations (Thukral, 2015). MRI provides detailed insights into the structure and function of the infant brain (Rosenbloom & Pfefferbaum, 2008). A diverse array of MRI sequences is available, such as T1- and T2-weighted imaging, which provide detailed volumetric properties of different brain regions. These sequences enable the precise assessment of brain volume changes (Dieleman et al., 2017). Microscopic characteristics of brain structures can be studied using DTI (Basser et al., 1994; Salo et al., 2018). DTI is another commonly used MRI sequence that facilitates the visualization of tissue architecture by tracking the diffusion of water molecules, which subsequently generates a three-dimensional (3D) representation for each voxel via a 3×3 matrix known as a diffusion tensor (Stebbins, 2010). Within each voxel, the diffusion tensor offers insights into diffusion magnitude and direction (Stebbins, 2010). Within gray matter voxels, including regions like the amygdala, the diffusion is lower and more random, displaying an isotropic nature. This stands in contrast to voxels containing fiber bundles, where diffusion is higher along the axis of the fibers (Batalle et al., 2019). DTI facilitates the examination of tissue metrics such as mean diffusivity (MD), axial diffusivity (AD), radial diffusivity (RD), and fractional anisotropy (FA) (Tae et al., 2018). The FA metrics serve as an indicator of the orientation of molecular water displacement and exhibit sensitivity to various factors such as axonal diameter, myelin sheath thickness, fiber density, and directionality (Tao et al., 2017). Conversely, AD metrics measure the movement of water molecules parallel to axonal tracts (Klawiter et al., 2011). However, when it comes to the analysis of gray matter structures like the amygdala, the interpretation of FA and AD metrics can prove challenging and potentially misleading. This is due to the isotropic nature of diffusivity within gray matter, meaning that alterations in diffusion occur randomly across all three directions (Gillespie et al., 2017; Jeurissen et al., 2013; Yrondi et al., 2019). Consequently, a more precise understanding of the microstructure of the amygdala and other gray matter structures might be better achieved through the measurement of MD. MD represents the average of the three eigenvalues and quantifies overall water diffusion, regardless of its orientation (Stebbins, 2010). It is worth noting that this limitation primarily applies to conventionally available imaging resolutions. In ultra-high field MRI, it is possible to observe the fiber orientations inside the gray matter due to the higher spatial resolution, potentially offering additional insights into the microstructure of these regions (Tax et al., 2023; Vachha & Huang, 2021). MD metrics are influenced by the number of barriers and constraints to water motion within tissues, with higher values indicating fewer restrictions and lower values signifying greater barriers within the underlying tissue composition (Clark et al., 2011; Tao et al., 2017). Patients with anxiety, impaired cognitive performance, and neurovegetative diseases show elevated MD in the amygdala (Cherubini et al., 2010; Juranek et al., 2012). The increase in MD values was correlated with a decrease in neurons and synapses, alongside tissue degeneration and immaturity (Cherubini et al., 2010; De Gennaro et al., 2011; Gillespie et al., 2017; Kantarci et al., 2005). Conversely, in healthy individuals, MD value was decreased in gray matter throughout normal brain development, beginning as early as 26 weeks of gestation and continuing through developmental stages ranging from infancy to adolescence (Batalle et al., 2019; Lebel et al., 2010; Moura et al., 2016; Pohl et al., 2016; Taki et al., 2013). These observations imply that elevated MD in the amygdala could be a shared characteristic among diverse psychiatric conditions and dysregulation of fear.

2.8 Prenatal maternal depressive symptoms

The prenatal period is critical for brain development (E. Fitzgerald et al., 2020). The psychological and physiological changes during pregnancy can culminate in the emergence of prenatal maternal distress, including stress, anxiety, and depression. Recent research has shown that prenatal distress exposure is a global public health issue (Marecková et al., 2019). A global range of 10% to 35% of children face prenatal distress exposure (Maselko et al., 2015). Evolving evidence underscores that prenatal distress may negatively influence fetal development, with repercussions spanning the entire lifespan (Bennett et al., 2004; Douros et al., 2017; Lupien et al., 2009; Nazzari et al., 2019; Sidebottom et al., 2020). Adverse birth outcomes have particularly been linked with high maternal depression, in addition to anxiety (Douros et al., 2017; Loomans et al., 2013). Prior investigations indicate that the incidence of PMDS during pregnancy is estimated to be 7.4%, 12.8%, and 12% in the first, second, and third trimesters, respectively (Bennett et al., 2004; Sidebottom et al., 2020). However, since a substantial number of pregnant women (half of the pregnancies) experiencing depression remain undiagnosed, these data may understate the extent of the problem (Ko et al., 2012). PMDS has been correlated with a spectrum of health complexities for both expectant mothers and their offspring.

In infants, PMDS correlates with outcomes such as low birth weight (Bonari et al., 2004; Davalos et al., 2012), premature birth (Diego et al., 2009; Sandman et al., 1994), as well as neurodevelopmental conditions like autism and attention deficit hyperactivity disorder (Kinney et al., 2008; Ronald et al., 2011). These adversities extend to negative emotional, behavioral, and cognitive disorders, along with psychiatric conditions, with effects that reverberate into adolescence and, in some instances, adulthood (Kinney et al., 2008; Ronald et al., 2011). In mothers, increased risks of suicide attempts (Bonari et al., 2004; Sidebottom et al., 2020), substance use, alcohol consumption (Zuckerman et al., 1989), emergency operative deliveries (Chung et al., 2001), and postpartum depression (Stowe & Nemeroff, 1995) have been associated with PMDS.

Depressive symptoms in pregnant women may alter amygdala anatomy and function in their offspring. The amygdala is a key anatomical component for understanding how PMDS affects infants' mental health and brain development (Wen et al., 2017). Several studies have reported the volumetric changes of the amygdala in offspring and its association with PMDS, with some investigations highlighting sexual dimorphisms in the amygdala (Acosta, Tuulari, et al., 2020; Buss et al., 2012; Wen et al., 2017). In a study, higher cortisol concentrations during early pregnancy were correlated with larger amygdala volumes in 7-year-old girls, and with more affective problems in girls compared to boys (Buss et al., 2012). Certain studies have indicated that PMDS during the second trimester exhibits a more pronounced association with the amygdala in girls compared to boys, affecting both macrostructural and microstructural aspects (Wen et al., 2017). Furthermore, an escalation in depressive symptoms during the second trimester was associated with reduced right amygdalar volumes, specifically in infant boys as opposed to girls (Acosta, Kantojärvi, et al., 2020).

To the best of our knowledge, no studies have explored the sex-specific impacts of PMDS measured across different stages of pregnancy on amygdala microstructure. Studying PMDS in association with microscopic features of the amygdala in infants is limited to one study (Rifkin-Graboi et al., 2013), and further investigations could help to better understand the neurobiological processes by which PMDS confers risk for developing a range of neuropsychiatric disorders. In the study conducted by (Rifkin-Graboi et al., 2013), findings revealed that among infants (n = 157) aged 6 to 14 days, increased PMDS during the second trimester were linked to a lower FA in both the right and left amygdala, as well as lower AD in the right amygdala. Wen et al., 2017 have reported higher right amygdala FA in the overall sample (n = 235) and girls (n = 122) at the age of 4.5 years in relation to increased maternal prenatal depression during the second trimester. Maternal prenatal depression asassed during the third trimester has been linked to decreased FA and increased MD in the amygdala-frontal tract and cingulum in 4-year-old children (Hay et al., 2019). However, it's important to note that the studies mentioned above have not examined PMDS throughout all trimesters of pregnancy. PMDS was assessed specifically at 26 weeks gestation using the Edinburg Postnatal Depression Scale (EPDS) questionnaire. As a result, there remains a lack of evidence regarding the effects of PMDS on the amygdala microstructure. The relevance of PMDS may depend on the developmental stage at the time of exposure (Buss et al., 2012). Therefore, studying how the timing of PMDS is related to measures of brain development in offspring can be beneficial for understanding the influence of PMDS on brain structures (Buss et al., 2012).

2.9 Fear regulation in infancy

The preference for social stimuli, particularly faces, is a fundamental prerequisite for human social and emotional growth (Prunty et al., 2020; Reynolds & Roth, 2018). Right from birth, infants display a preference for faces and exhibit a tendency to sustain their visual attention on faces more than non-social stimuli (Farroni et al., 2005; Johnson et al., 1991; Libertus et al., 2017). Infants from 7 months look longer at fearful faces than at happy or neutral faces (Peltola et al., 2008, 2009, 2013). The exact origin of the bias towards fearful facial expressions in infants remains yet to be fully understood. Yet, this bias might be due to the infrequent exposure of infants to fearful stimuli compared to other emotions within their environment (Nelson & Dolgin, 1985).

Amygdala function involves responding to fear-inducing stimuli, such as fearful facial expressions and fear-conditioned cues (Marschner et al., 2008; Whalen et al., 2001; Zhao et al., 2017). Neuroimaging studies have shown the activation of the amygdala when exposed to fearful stimuli (Phan et al., 2002). Moreover, evidence supports the notion that individuals who have experienced amygdala lesions display abnormal responses to fear stimuli such as fearful faces (Adolphs et al., 1999; Cardinale et al., 2021). Additionally, the amygdala was activated when emotional responses were induced through visual stimuli such as fear (Phan et al., 2002). These findings demonstrate the significance of the amygdala in regulating the fear response (Ressler, 2010).

Multiple sensory modalities, including auditory, visual, and olfactory inputs, convey information to the amygdala (Baysal Akin & Onat, 1995; Morrow et al., 2019). The amygdala facilitates the appropriate behavioral response by either activating the hypothalamic-pituitary-adrenal axis and releasing stress hormones or by directly triggering autonomic and behavioral reactions (Smith & Wylie, 2006; Watson et al., 2010). The amygdala exhibits a reaction to various emotional facial expressions (D. A. Fitzgerald et al., 2006). However, it has been observed that expressions of fear is more pronounced compared to other emotional expressions (Morris et al., 1996; Tuulari et al., 2020). So far, only one study has examined the correlation between amygdala macrostructural alterations and attentional bias towards facial stimuli in infants (Tuulari et al., 2020). This study highlights that a larger volume of the left amygdala is associated with an increased tendency to shift attention away from fearful facial expressions as opposed to happy and neutral ones. However, no studies have investigated potential microstructural changes in infants or adults. Investigating the relationship between the microstructure of the amygdala and the attentional bias towards emotional facial stimuli has the potential to offer valuable insights into the neurological mechanisms involved in the regulation of fear during early infancy, as well as its possible long-term implications.

2.10 Conclusions based on the literature

Brain development is a complex process that encompasses various prenatal and postnatal stages, leading to significant changes in brain size and structure. Brain asymmetry patterns emerge and evolve from prenatal stages to adulthood, influenced by genetic programming and environmental factors. Sexual dimorphism in brain structures is noticeable in both neonatal and adult brains. The limbic system, including the amygdala, plays a vital role in emotional and cognitive responses.

Advanced neuroimaging methodologies like DTI serve as invaluable tools for examining brain development. DTI, through the measurement of water molecule diffusion via MD metrics, can unveil details of gray matter structures like the amygdala. However, the identification and delineation of brain structures in infants pose challenges due to the smaller size of their brains and the lower image resolution of MR scans, underscoring the significance of straightforward yet precise manual segmentation protocols.

PMDS are notably prevalent, affecting not only mothers but also their offspring. PMDS can result in unfavorable birth outcomes, neurodevelopmental issues, and neuropsychiatric disorders in children. Furthermore, PMDS might influence the structure and function of the amygdala in offspring, potentially contributing to emotional and behavioral challenges. The sex-specific influences of PMDS may vary with the developmental stage of exposure. Current studies have not examined PMDS across all pregnancy trimesters, leaving a gap in our understanding of its effects on the amygdala microstructure.

The amygdala is a key player in responding to fear-inducing stimuli, including fearful facial expressions and conditioned fear cues. Neuroimaging studies demonstrate amygdala activation in response to fearful stimuli, and individuals with amygdala lesions show reduced fear responses, particularly to fearful faces. While one study in infants has linked a larger left amygdala volume to an attentional bias away from fearful faces, no research has explored potential microstructural changes in this context. Investigating the connection between amygdala microstructure and attentional bias toward emotional facial stimuli could provide valuable insights into the neurological mechanisms of fear regulation during infancy and its potential long-term effects.

3 Aims of the Study

This PhD thesis examines brain development, facial emotional perception, and PMDS impacts through three investigations. In study I, a manual segmentation protocol was developed for neonatal MR images, with a specific focus on the amygdala and hippocampus in healthy neonates. Study II explored the correlation between prenatal PMDS at different gestational stages and the microstructure of the infant's amygdala. Study III examined infants' amygdala microstructure and emotional face recognition using eyetracking. Studies II and III used advanced DTI techniques while also investigating sex-specific differences. This thesis aims to advance pediatric neuroimaging by providing novel insights into the complexities of early brain development through three studies.

I. To establish a novel manual segmentation protocol for the amygdala and hippocampus in neonatal MR images. Furthermore, manual segmentations were compared to automated segmentations performed with the infant brain extraction and analysis toolkit (iBEAT toolbox).

II. Assess how PMDS affects infant amygdala microstructure and explore potential gender-specific effects by examining the interaction between PMDS and infant sex.

III. To explore potential links between the microstructure of the amygdala and infants' perception of emotional facial expressions, with an additional investigation into sex-specific differences.

4 Materials and Methods

4.1 Ethical considerations

All studies incorporated into this thesis were carried out in adherence to the principles outlined in the Declaration of Helsinki. The studies I, II, and III received ethical approval from the Joint Ethics Committee of the University of Turku and the Hospital District of Southwest Finland (ETMK: 31/180/2011). Families were provided with oral and written information about the studies. Informed consent was obtained from the parents, acting as representatives for their children.

4.2 Participants

The participants of this thesis were mothers and infants of Caucasian ethnicity, drawn from the ongoing FinnBrain Birth Cohort Study located in South-Western Finland (www.finnbrain.fi) (Karlsson et al., 2018). The recruitment period spanned from December 2011 to April 2015 and yielded a total of 3,808 pregnant women who voluntarily enrolled during their initial ultrasound examination at GW12. Among them, 367 families chose to discontinue their participation due to time constraints, miscarriage or stillbirth observed in 35 cases. The cohort included 3,837 children, including 29 twin pairs. The primary aim of the cohort is to explore neurodevelopmental aspects and identify biomarkers linked to prenatal and early life stress. Additionally, it aims to characterize trajectories for psychiatric and somatic conditions, encompassing depression, anxiety, and cardiovascular illnesses. A total of 189 mother-newborn dyads voluntarily participated in an MRI visit, with 180 completing scanning procedures successfully. Of the 189 participants, 64 were excluded due to motion artifacts in the MR images. Table 1 provides an overview of the demographic data from the sub-studies. Newborns' inclusion criteria were birth weights > 2500 g and gestational ages > 36 weeks. Exclusion criteria included congenital abnormalities diagnosed prior to the study and abnormal findings in a prior MRI scan. The study included singleton pregnancies only. Among the newborns, 19 were identified as having mild asphyxia. Among them, one newborn underwent cardiopulmonary resuscitation and received respiratory treatment, while another scored 4 out of 10 in the 5-minute Apgar evaluation. Mothers with a background of alcohol or drug misuse, severe psychiatric conditions, epilepsy, or medication use for psychosis were excluded from the study. Background information was assessed via the mothers' self-report questionnaires at GW 14 and/or 34. Obstetric data were gathered from the Finnish Medical Birth Register of the National Institute for Health and Welfare (http://www.thl.fi).

Table 1. The participant's' characteristics.

Maternal characteristics	Study I (n = 31)	Study II (n = 84)	Study III (n = 40)
Pre-pregnancy BMI, mean (SD)	25.44 (5.00)	24.6 (4.2)	24.89 (3.82)
Age at due date (years), mean (SD)	29.70 (5.09)	30.0 (4.6)	30.70 (5.01)
Education (%)			
low (high school or lower)	29.03	28.6	30.8
middle (vocational degree)	22.58	34.5	38.5
high (master's degree or higher)	35.48	35.7	30.8
Economic situation, %			
very good	8.7	7.1	2.6
fairly good	43.5	52.4	48.7
not good	39.1	29.8	41
fairly bad	8.7	9.5	7.7
very bad	0	0	0
SSRI/SNRI medication use, % yes	6.45	6	5.11
CNS medication use % yes	3.23	0.91	0
Smoking, %	0	0	0
Alcohol, %	0	8.7	5.1
Infant characteristics, mean (SD)			
Gestational age (weeks) at birth	39.87 (1.18)	39.9 (1.1)	39.83 (1.03)
Age (days) at MRI from birth	28 (6.24)	25.43 (7.8)	25.60 (6.90)
Head circumference (cm)	35.03 (1.43)	34.91 (1.2)	35.01(1.42)
Birth weight (grams)	3639.48 (417.81)	3491.9 (464.2)	3505.65 (460)

Table 1 footnote | Abbreviations: BMI = Body Mass Index; SD = Standard Deviation; SSRI/SNRI = Selective Serotonin Reuptake Inhibitor and Serotonin and Norepinephrine Reuptake Inhibitor; CNS = Central Nervous System. Table 1 is the original content created by the author for this thesis.

4.2.1 Study I

This sub-study contained 31 randomly selected (n = 22 females, n = 9 males) participants from the pool of 125 newborns (Figure 4).

4.2.2 Study II

Among the 88 participants who had a direction 60 DTI scan, 84 participants (42 girls and 42 boys) whose mothers had completed the EPDS questionnaire at GW 14, 24, and 34 during pregnancy met the necessary criteria for the subsequent DTI image analyses (Figure 4). Among these infants, 11 had a history of mild asphyxia, and 3 required cardiopulmonary resuscitation and respirator treatment. This sub-study incorporated various obstetric information in the analyses, including maternal use of selective serotonin reuptake inhibitors (SSRIs), serotonin and norepinephrine reuptake inhibitors (SNRIs), and other CNS-affecting medications. Additional factors considered were maternal age at the due date, economic situation based on parent(s) perspective obtained through questionnaires, maternal pre-pregnancy body mass index (BMI), infant 5-min Apgar score, infant weight at birth, and infant age at scan time counted from birth date.

4.2.3 Study III

For this sub-study, 40 newborn DTI images (20 females and 20 males) who underwent valid eye-tracking assessments at 8 months of age were included (Figure 4). Additionally, infant age at the time of the MRI scan was adjusted during statistical analyses.

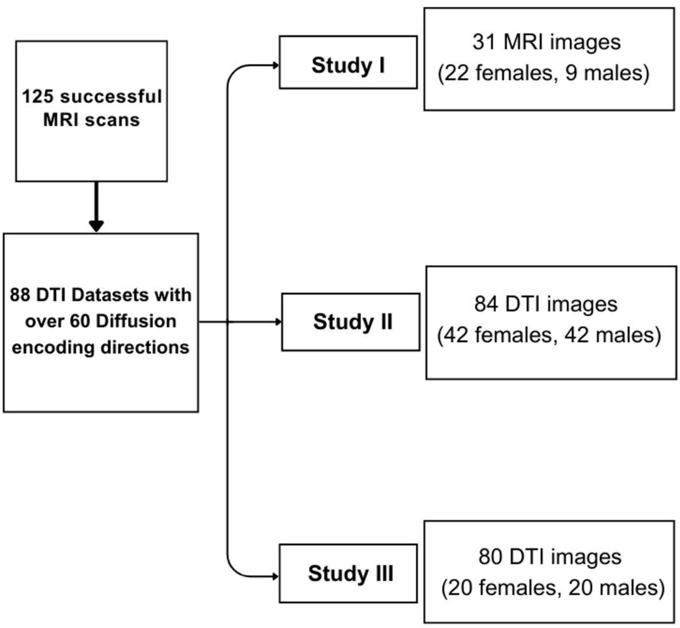

Figure 4. Inclusion of participants in sub-studies I–III Author’s illustration.

4.3 Measures

4.3.1 Prenatal maternal depressive symptoms

In study II, PMDS were assessed at GW 14, 24, and 34 using the EPDS questionnaire (Cox et al., 1987). The EPDS is a validated 10-item self-reported questionnaire designed to evaluate depressive symptoms experienced over the previous 7 days (Adouard et al., 2005; Cox et al., 1987). Each item is scored on a 4-point scale, resulting in a total score range of 0 to 30. The EPDS is widely used for detecting both prenatal and postnatal depressive symptoms. A score of 10 or more has been used as an indicator of clinically meaningful symptoms of depression (Garcia-Esteve et al., 2003). However, in this sub-study, we did not establish specific clinical cut-off scores for depressive symptoms to ensure the inclusivity of participants with subclinical levels of these symptoms. This approach was adopted to consider the potential impact of PMDS on fetal brain development. The EPDS scores are listed in Table 2.

Table 2. Descriptive information from the prenatal maternal depressive questionnaires.

Variables	**Total sample N = 84**	**Girls N = 42**	**Boys N = 42**	**P**
EPDS (GW 14), mean (SD), range	5.9 (5.5), 0-25	5.8 (6.0)	6.0 (5.1)	0.6
EPDS (GW 24), mean (SD), range	6.0 (5.6), 0-25	6.1 (6.2)	5.9 (5.0)	0.8
EPDS (GW 34), mean (SD), range	5.9 (5.3), 0-20	5.7 (5.5)	6.0 (5.1)	0.9

Table 2 footnote | Table 2 is modified from the original publication I with the permission of the copyright holders.

4.3.2 Infant attention to faces and distractors

In study III, an eye-tracking experiment was used to assess infant attention to faces and distractions. During the experiment, the infants were seated on their parent's lap, positioned at 50–70 cm from the eye-tracker (EyeLink1000+, SR Research Ltd, Toronto, Ontario, Canada), with the optimal camera-to-eye distance ranging from 40–70 cm. Monocular data from the right eye was collected at a sampling frequency of 500 Hz. Before each measurement, a five-point calibration procedure was utilized, which included an audiovisual animation displayed in five different locations on the screen. Calibration could be repeated before the actual testing and during the measurement process as necessary, with the option for small breaks if needed. The researcher conducted the measurements in the dimly lit room shared by the infant and parent. To prevent interference, a curtain was used to separate the parent and their infant from the researcher.

The overlap paradigm (Peltola et al., 2008) was used to find out how infants focus on emotional faces. The overlap paradigm examines how the infants stopped paying attention to a face or a scrambled non-face control picture in the middle of the screen when a lateral distraction was shown. The stimuli included images of two distinct women displaying happy, fearful, and neutral facial expressions, as well as scrambled non-face control images (Peltola et al., 2008). A total of 48 trials were shown in semi-random order, with 12 trials per condition (emotion and control) consisting of 18 photographs of each woman and 12 scrambled non-face control pictures.

During each trial, the infant was initially presented with either a face picture or a scrambled non-face control picture in the center of the screen for 1000 ms (Figure 5). Following that, for 3000 ms, a lateral distractor, either a black and white checkerboard or circles, is displayed on either the left or right side of the face at a viewing angle of 13.6°, simultaneously with the face. Each trial had a duration of 4000 ms. The images depicting emotions measured 15.4° x 10.8°, while the distractor stimuli measured 15.4° x 4.3°. Following each trial, a brief animation was displayed to re-engage the infant's attention at the center of the screen. Once the infant's gaze was centered, the researcher proceeded to initiate the next trial. The configuration of the central stimuli was semi-randomized to prevent the repeated delivery of the same stimulus more than three times consecutively. Furthermore, in each trial, the lateral stimulus was chosen and shown in a random manner.

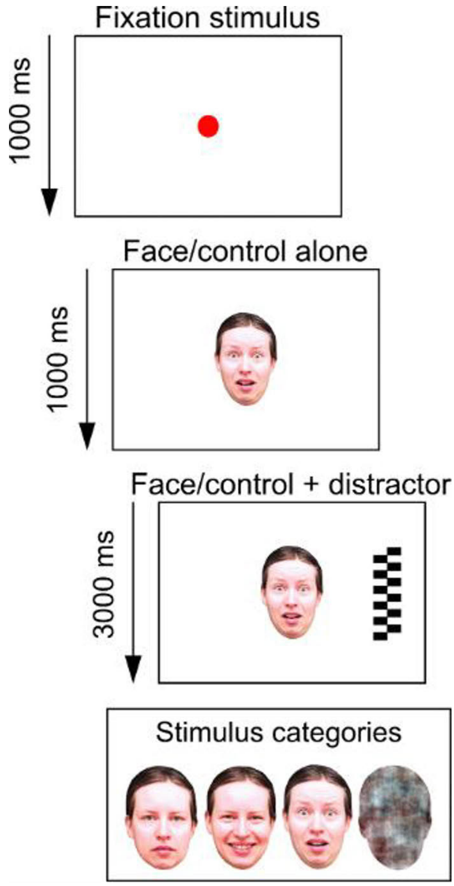

Figure 5. The overlap paradigm. After the infant focused on a fixation stimulus in the center of the screen (red circle), a face or a scrambled face as a control stimulus was displayed. After 1000 ms from the face/control commencement, a distractor appeared to the right or left of the focal stimulus. The core stimulus was delivered until the conclusion of each trial (4000 ms), overlapping in time with the distractor. The figure is adapted from (Yrttiaho et al., 2014) and is reprinted with the permission of the copyright holders.

4.4 MRI acquisition

The newborns underwent the MRI scans at 11 to 54 days after birth. The scans were acquired at the Medical Imaging Center of the Hospital District of Southwest Finland between November 2012 and January 2016. Before the scan, the infants were given breastmilk or formula until they fell asleep, and then carefully wrapped in a vacuum mattress to minimize limb movements. No anesthetics were administered during the procedure. To ensure the safety and comfort of the infants, a comprehensive hearing protection protocol was implemented. This included providing double protection, which included wax plugs and custom-sized earmuffs. Standard earmuffs were also offered to parents, who typically remained in the scanning room during the entire session. Observation of the scanning procedure was conducted by personnel from the control room, facilitated by a window. Communication with parents was enabled through a microphone and loudspeaker system installed in the scanner room. If an infant woke up during the scan, the session was immediately halted. An experienced neuroradiologist reviewed each set of structural infant images to detect any potential incidental findings. Following the study protocol, radiology reports were conveyed to the researchers, who subsequently communicated the results to the families within 1-4 weeks of the scans. In instances where incidental findings were identified, parents were referred to a child neurologist for a comprehensive neurological assessment, in accordance with the study protocol. Notably, throughout the study period, none of the infants displayed clinically significant neurological symptoms or deficits in neurological development (Merisaari et al., 2019).

The MRI scans were acquired using the Siemens Magnetom Verio 3T scanner (manufactured by Siemens Medical Solutions, Erlangen, Germany). The scanning protocol included axial PD-T2-TSE (Dual-Echo Turbo Spin Echo) and sagittal 3D-T1 magnetization prepared rapid acquisition gradient echo (MPRAGE) sequences, providing whole-brain coverage with isotropic 1.0 mm^3 voxels. In the PD-T2-TSE sequence, the use of two effective echo times (TE) of 13 ms and 102 ms, in conjunction with a repetition time (TR) of 12,070 ms, facilitated the acquisition of PD-weighted and T2-weighted images with a resolution of 1x1x1mm^3. A total of 128 slices, each 1 mm thick, were obtained. The 3D-T1-MPRAGE sequence utilized a TR of 1,900 ms, a TE of 3.26 ms, and an inversion time (TI) of 900 ms, resulting in the acquisition of 176 slices. The sequence parameters were fine-tuned to enable the utilization of the "whisper" gradient mode in both the PD-T2-TSE and 3D-T1 sequences, aiming to decrease acoustic noise levels during the scan. This enhancement was intended to improve the quality and comfort of the imaging procedure. Total MRI acquisition time was 32 minutes.

4.5 Amygdala and hippocampus segmentation

Manual segmentation is the gold standard in identifying brain structures (Morey et al., 2009). However, manual brain segmentation is a time-consuming and difficult task in the fields of neuroscience and brain research. This challenging procedure necessitates precisely segmenting and recognizing distinct brain structures from medical images, which requires significant expertise in brain anatomical structures. We created a protocol with content for each step to aid in manual segmentation, which took us approximately two years. All subcortical structures were manually segmented, including bilateral hippocampi, amygdalae, caudate nuclei, putamina, globi pallidi, and thalami (Figure 6). These segmentations were later used to create the openly accessible FinnBrain neonatal (FBN-125) multi-contrast high-resolution template (upsampled from 1x1x1 mm^3 to 0.5 x 0.5 x 0.5 mm^3), and labeled atlases, which include T1- and T2-weighted images, along with DTI data. Only the amygdala and hippocampus were employed in this thesis.

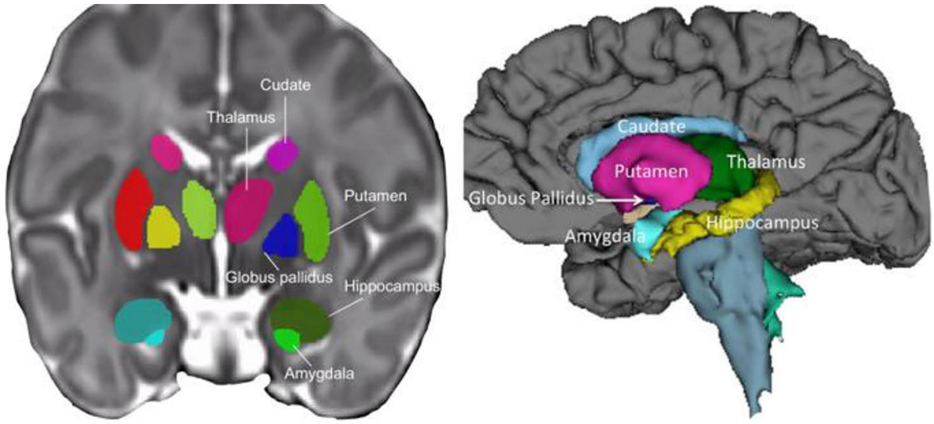

Figure 6. The figure on the left illustrates manual segmentation of subcortical structures on one of the infant MR images. The right figure shows the subcortical structures in 3D. It was adapted from (Jung et al., 2014) and is reprinted with the permission of the copyright holders.

4.5.1 Study I

We transformed the raw MRI DICOM images into Neuroimaging Informatics Technology Initiative (NIfTI) format using dcm2nii software to perform the manual segmentation. The T1- and T2-weighted volumes were co-registered using FSL's flirt (Jenkinson et al., 2012) with 6 degrees of freedom. The orientation of the images was adjusted to match the UNC (University of Carolina) infant template in order to align all the images in the same upright orientation. Next, the NIfTI images underwent conversion to MINC (Medical Imaging NetCDF) format utilizing MINC Tools version 1.5.1, which was created at the McConnell Brain Imaging Centre in Montreal, Canada (https://bic-mni.github.io/). The segmentation process was performed on an iMac operating system X 10.11.6, equipped with a 4 GHz Intel Core i7 processor and an AMD Radeon R9 M395 graphics card with 2048 MB of memory. Using the Display software in MINC Tools, version 2.0, the amygdala and hippocampus were manually segmented from 31 T2-weighted MR images of infants. For precise segmentation, a brush size of 0.5 mm was selected (images have a resolution of 1 mm^3). The axial, coronal, and sagittal planes were evaluated simultaneously. Slice by slice, the amygdala and hippocampus were carefully segmented to precisely trace the anatomical borders. The segmentation of the amygdala and hippocampus on each MR image took, on average, about two days of work. To guarantee the segmentations were harmonized in three dimensions, the images were assessed and edited in the axial, coronal, and sagittal planes. Following the completion of segmentations, a thorough review of amygdala and hippocampus delineations was conducted for both hemispheres, and any required adjustments were implemented. Subsequently, the volumes of the amygdala and hippocampus were computed. The segmentation of the amygdala and hippocampus was performed by the primary rater (NH). Two novice raters, who were trained by NH, independently conducted segmentations for inter-rater assessment. These segmentations were then reviewed by another expert rater (JJT).

4.5.1.1 Amygdala manual segmentation

The olive-shaped amygdala is above and anterior to the hippocampus in both brain hemispheres' medial temporal lobes. The amygdala is located within the superomedial temporal lobe, situated at the junction where the basal ganglia and entorhinal cortex connect, toward the posterior and inferior boundaries (Pruessner et al., 2000). A slice-by-slice tracing approach using all three planes is needed to determine the amygdala's borders.

In each T2-weighted MRI dataset, approximately ten slices containing the amygdala were identified. The tracing of the amygdala in the sagittal plane commenced from the point where the thalamus began to assume its distinctive walnut shape, extending towards the superomedial edges above the hippocampus. In the axial orientation, the top boundary of the amygdala is linked to the ambient cistern, rendering the axial view for the most reliable differentiation. To ensure uniformity, a single row of voxels located in the cerebral cortex anterior to the amygdala was intentionally excluded during delineation. In the coronal plane, the inferior and anterior boundaries of the amygdala and hippocampus were defined by the temporal horn of the lateral ventricle. Progressing anteriorly in the coronal plane, the lateral and inferior aspects of the amygdala were identified. Removal or addition of any over-segmented or empty voxels was performed carefully to achieve precise and consistent segmentation. Amygdala manual segmentation steps are shown in Figure 7.

4.5.1.2 Hippocampus manual segmentation

Hippocampus segmentation contained the dentate gyrus, hippocampus proper, cornu ammonis (CA), CA4 region (hilus), CA3, CA2, CA1, and subiculum between CA1 and fornix (Figure 8). Three main anatomical elements make up the hippocampus: the head, body, and tail. In this approach, the hippocampus included the posterior uncus, the hooked structure near the parahippocampal gyrus' anterior end. The posterior hippocampus's white matter track of the fimbria is segmented until it forms the fornix (De Macedo Rodrigues et al., 2015). Careful exclusion of the white matter fibers from the fornix and parahippocampal gyrus was performed during segmentation. The hippocampus was delineated using the most lateral slice in the sagittal plane. Identification of the hippocampus tail was based on the definition provided by the lateral ventricle, while the appearance of the temporal horn near the head was noted (C. Konrad et al., 2009).White matter presence was observed along the body of the hippocampus. To ensure accurate delineation, the contrast difference between the hippocampus and white matter was considered when defining the hippocampus's inferior boundary. Tracing of the hippocampal mass continued inferiorly in the sagittal plane until the appearance of the amygdala's boundaries and the identification of the hippocampus head by the lateral ventricle's horn. In coronal and axial planes, the superomedial hippocampus margins are readily discernible from the lateral ventricle. Hippocampus manual segmentation steps are shown in Figure 7.

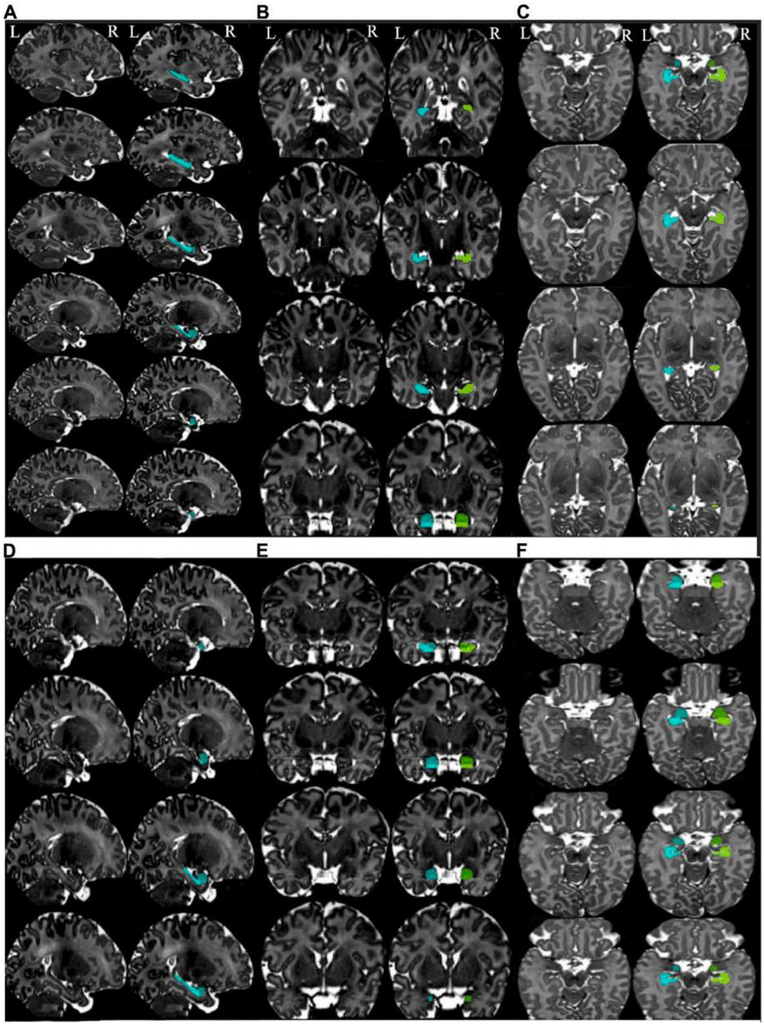

Figure 7. Summary of the steps for segmenting the hippocampus and amygdala in the various planes. Summary of the steps for segmentation of the hippocampus in the sagittal (A), coronal (B), and axial planes (C). Summary of the steps for segmentation of the amygdala in the sagittal (D), coronal (E), and axial planes (F). The images on the left are the templates (non-segmented), and the images on the right side present segmented structures. The left hippocampus is shown in cyan, and the left amygdala is shown in blue. The right hippocampus is presented in chartreuse, and the right amygdala is in green. The figure appears in the original publication of study I and is reprinted with the permission of the copyright holders.

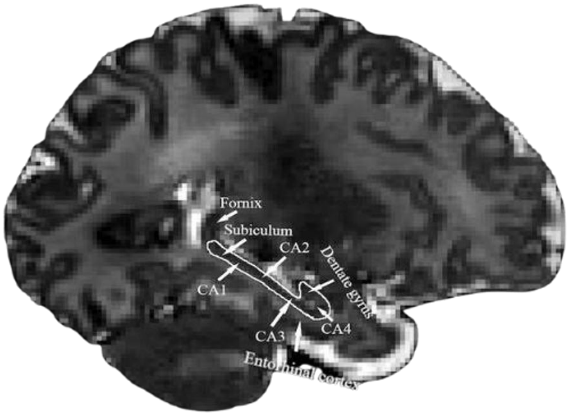

Figure 8. Structures of the left fornix, entorhinal cortex, subiculum, CA1, CA2, CA3, CA4, and dentate gyrus are shown on one of the infant's MR images. CA is the cornu ammonis. The figure appears in the original publication of study I and is reprinted with the permission of the copyright holders.

4.5.1.3 Automated segmentation of the amygdala and hippocampus

To evaluate the consistency between manual and automated segmentation techniques for the amygdala and hippocampus, ten T2-weighted MR images of newborns were segmented using iBEAT software (Dai et al., 2013). The iBEAT software was created exclusively for automatic segmentation of T2-weighted newborn brain images. iBEAT is open-source software accessible on Linux platforms, employing sophisticated image processing methodologies for tasks including voxel analysis and labeling of newborn brain structures. MR images were reoriented and adjusted for non-parametric non-uniform intensity normalization (N3) intensity. An iBEAT module was then used to extract the skull. Following that, tissue segmentation was conducted. Finally, iBEAT labeled the various brain regions using an infant-specific AAL (Automatic Anatomical Labeling) atlas. Subsequently, the volumes of the amygdala and hippocampus were computed.

4.5.2 Study II and III

The FinnBrain Neonate (FBN-125) template was created using the methods described below. The FBN-125 is aligned symmetrically with the Talairach-like MNI-152 template. Moreover, the atlas labels provided, derived from meticulous manual segmentations of subcortical structures, aim to serve the neuroscience community by offering valuable resources for future research on achieving precise and dependable spatial normalization and automated computational methods to measure neonate brain structure (Tuulari et al., 2024).

4.5.2.1 Creation of an Unbiased Population-Specific Template

The analysis utilized measurements obtained through a fusion-based approach that relies on a labeled template. These methods necessitate precise registration between subjects and templates, which becomes increasingly challenging when the template's resemblance to the subjects diminishes. Consequently, a template tailored to the participants in this study was developed. This involved creating a population-specific dual-contrast template incorporating data from all 125 MRIs (Figure 9), similar to the previous study (Fonov et al., 2011). Using a sequence of MRI volumes, iteratively produce a template aimed at two objectives. The first objective was to minimize the mean squared intensity difference between the template and each subject's MRI. The second objective was to minimize the magnitude of all deformations used to align the template with each subject's MRI. This approach was used on T1 images. The T1 scans were subjected to linear registration with the Montreal Neurological Institute (MNI) 152 template. Following this, the average scaling factor from the MRIs to the MNI 152 template was calculated. This scaling factor was then used inversely to adjust the size of the MNI 152 template to match the average size of the research population. This modified template was subsequently utilized as the starting point for constructing the population-specific template. The T1 template was then created using an iterative template construction technique, as well as non-linear changes between each T1 and the T1 template. After that, the T2 scans were registered to the T1 scans, and the resulting transform was concatenated with the linear and non-linear transforms that took that T1 to the T1 template. The T2 scans were then mapped to template space and averaged to construct the T2 template using these composite modifications.

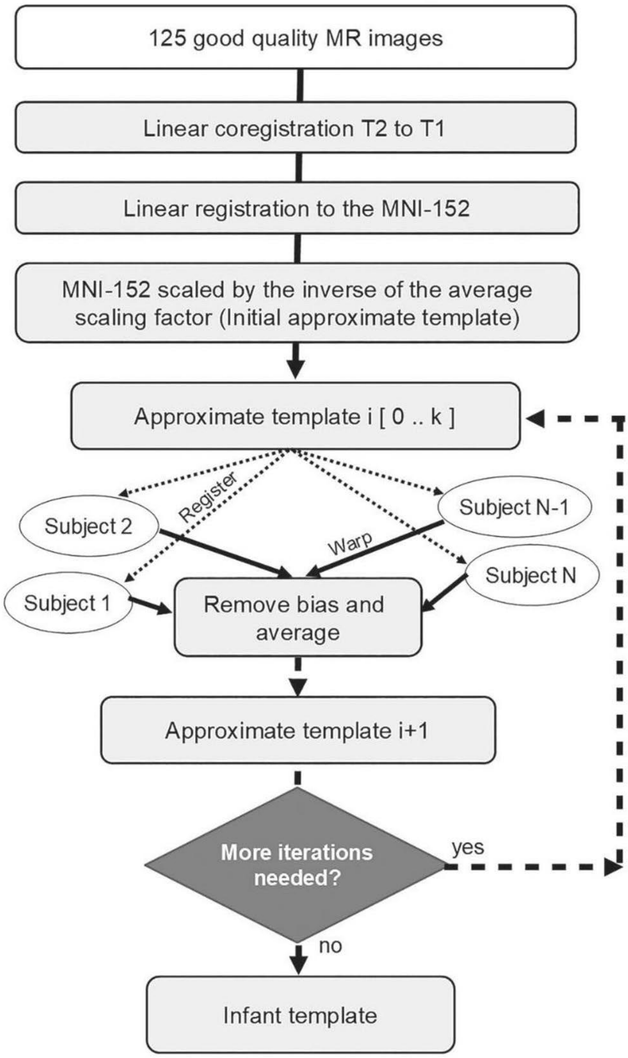

Figure 9. The construction of the infant template. The figure is adapted from (Acosta, Kantojärvi, et al., 2020) and is reprinted with the permission of the copyright holders.

4.5.2.2 Template labeling

Manual segmentations were performed on the structures of interest, namely the amygdalae and hippocampi, on the dual-contrast template. To confirm the accuracy of the manual labeling, many warped variations of the template (Figure 10) were created to replicate the morphological heterogeneity in the population, and each variant was manually labeled. Each variation represented a non-linear modification of the template to align with a specific subject in the population. The non-linear transformations derived from the template generation process were utilized to categorize participants into 21 groups, where the anatomical variability within each group was minimized compared to the variability between groups. This method aimed to capture morphological variations in the data accurately. The Jacobian of the non-linear transformation, which mapped each subject to the template, was computed as the foundation for clustering. Subsequently, the Jacobian values were extracted as a vector for every voxel within the template brain mask. Ward's clustering approach (Ward Jr, 1963) was employed to cluster these Jacobian vectors using a balanced combination of cosine similarity and Euclidean distance, with the total number of clusters set at 21. The total squared distances from each subject to every other subject were calculated inside each cluster. The subject with the smallest sum of squared distances was chosen as the central-most representative of the cluster. Subsequently, the dual-contrast template from the preceding step was adapted to match these 21 representative subjects and was made accessible for manual segmentation (Figure 9).

Sections 4.5.1.1 and 4.5.1.2 describe the segmentation approaches used. While the processes for amygdala and hippocampus segmentation were similar, the change in image resolution from 1 mm^3 to 0.5 mm^3 allowed for substantially better precision in the segmentations. One template was segmented first by the primary rater, then by a senior rater, and finally by another senior rater. After the first segmentation was approved, the other templates were segmented. Afterward, the 21 manual segmentations were wrapped back to the standard template, and voxel labeling was determined based on the majority vote across all 21 manual segmentations. This process yielded the definitive labels for the amygdalae and hippocampi on the standard template. To assess inter-rater agreement regarding spatial overlap on the newborn template, the Generalized Conformity Index (GCI) was introduced (hippocampus: GCI = 0.76, amygdala: GCI = 0.70). CGI ratings ranging from 0.7 to 1.0 are considered to represent high agreement across raters (Kouwenhoven et al., 2009; Visser et al., 2019).

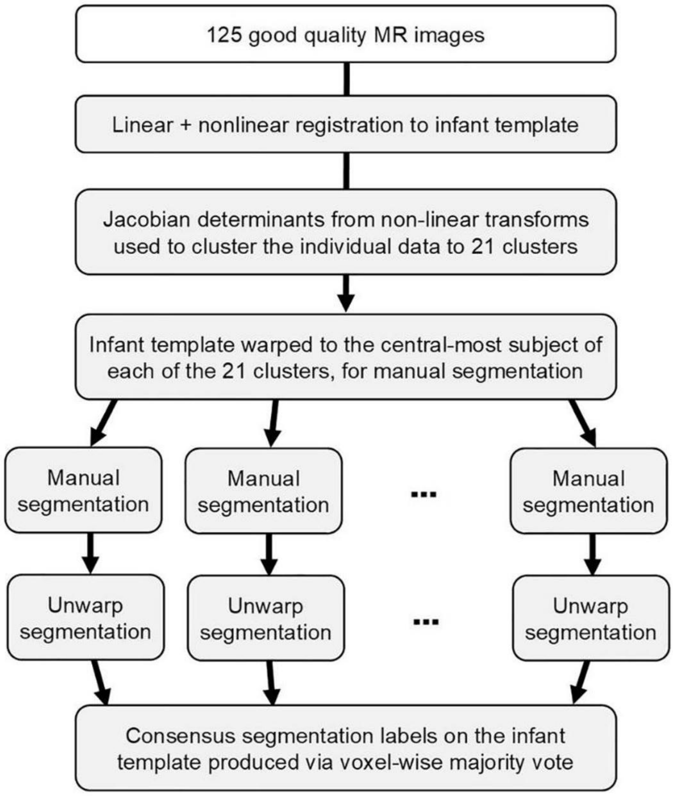

Figure 10. Labeling the infant template. The figure is from (Acosta, Kantojärvi, et al., 2020). It was reprinted with the permission of the copyright holders.

4.5.2.3 Subject labeling

Each subject underwent segmentation of the left and right amygdalae and hippocampi using a labeling technique based on label fusion. This technique was initially introduced by (Coupé et al., 2011) and further refined by subsequent studies led by Weier et al., 2014 and Lewis et al., 2019). The technique utilizes a specialized template library tailored to the population. This library was constructed by grouping deformation fields derived from the nonlinear transformations generated during the template construction process. The central-most subject from each cluster was then utilized to form the entries within the template library. Clustering was performed using an expanded mask encompassing the amygdalae and hippocampi to capture the anatomical intricacies of nonlinear registration in that specific brain region. As previously noted, the representative subject for each cluster was carefully chosen. To address hemispheric asymmetries, this process was repeated for each hemisphere. Consequently, the template library comprehensively captured the spectrum of hippocampal and amygdala deformations observed within the population.

The non-linear transform for the center-most subject was used to warp the template along with the segmentation defined on it to construct the library entry for a cluster, and this pair was put into the template library. The template library was thus a collection of warped copies of the template, each with its own warped segmentation. After establishing the template library, every individual in the population underwent non-linear registration to the most similar templates within the library (in this case, n = 7). The resulting transformations were then applied to adjust their respective segmentations, and the ultimate labeling was determined through patch-based label fusion. The process was also conducted independently for each hemisphere. An example of such labeling is illustrated in Figure 11. Subsequently, the volumes of each final labeling were calculated and adjusted to native space using the scaling factors from the subject's linear transformations.

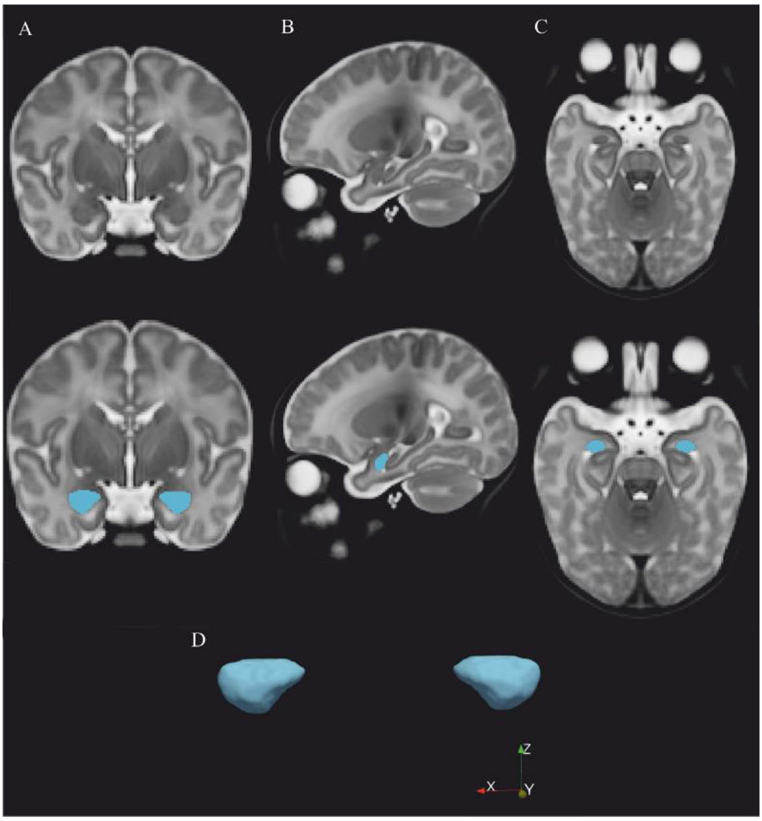

Figure 11. An example of the amygdala's segmentations in the coronal, axial, and sagittal planes is shown from left to right. The first row presents the newborn brain without segmentation: (a) coronal, (b) sagittal, and (c) axial. The second row presents the segmentation of the amygdala, and (d) shows three-dimensional segmentation of the amygdala. The figure appears in the original publication of study II and is reprinted with the permission of the copyright holders.

4.6 DTI data preprocessing

Susceptibility artifacts can lead to distortion in echo planar imaging (EPI). Although our dataset showed minimal distortion, we chose not to perform distortion correction because some field maps were corrupted by motion, posing a potential risk to data quality.

The diffusion-weighted imaging (DWI) procedure included 96 diffusion encoding directions divided into three parts with varied numbers of directions (31, 32, and 33). These directions were equally dispersed in 3D space, resulting in a full 96-direction protocol for each part, lasting roughly 6 minutes. The matrix size is 104 x 104 for each slice in the DWI sequence. Acquisiton time was approximately 18 minutes.

We chose 60 diffusion directions at b = 1000 s/mm^2 for our work, along with three b = 0 s/mm^2 images, because a greater number of diffusion directions allows for more robust tensor model fitting and improves outcome accuracy in infant data. The sequences were obtained using a 2 mm^3 isotropic spin echo EPI sequence (field of view 208 mm; 64 slices; repetition time 8500 ms; echo time 90 ms). Then, good quality b0 volumes were aligned, averaged, and shifted to the beginning of the four-dimensional (4D) series in each of the three DWI segments. FSL (FMRIB Software Library v. 5.0.9) and FSL's Brain Extraction Tool were used to produce a brain mask from the specified b0 volume (Smith, 2002). To assess the quality of each diffusion dataset, the DTIprep program version 1.2.4 was employed (Oguz et al., 2014).

By co-registering and averaging the b0 volumes of each segment, the three DWI segments containing quality-controlled data were combined. The related DWI data were converted, and the b-matrix was adjusted to account for the rotational component of the transforms. These merged datasets had a varying number of diffusion encoding directions, more than 60 in some cases, which were then decreased while retaining an equitable distribution of encoding directions and maximizing angular resolution (Roalf et al., 2016). FSL tools were used to perform motion and eddy current adjustments, and the residual motion correlation was determined to be small (Merisaari et al., 2019). Finally, we produced MD metrics by running the 4D diffusion dataset via FSL's dtifit, ensuring that the modeling was constrained to brain tissue alone by using the brain mask.

4.6.1 Mean diffusivity metrics

The diffusion data were aligned with the T1-weighted data to extract the amygdala MD metrics. We isolated the b0 volume containing raw T2 signal with no diffusion weighting from the diffusion datasets and aligned it with the nonuniformity-corrected T1-weighted data in its native space. Then, the resulting transformation was combined with the transformation from native to a stereotaxic group average template space, and this combined transformation was applied to each DTI map, overlaying them onto the T1-weighted data in stereotaxic space. The diffusion data were captured at a resolution of 2 mm^3 isotropic. Removing partial volume effects completely would have led to the exclusion of many measurements within small structures such as the amygdala. To address this, we applied a 1.5 mm erosion to the amygdala labels. This erosion helped mitigate most of these effects while still allowing us to retain enough DTI measures for statistical analysis. Subsequently, we used these eroded labels as masks to compute the mean of the remaining measures in each DTI map.

4.7 Statistical methods

4.7.1 Study I

The objective of this study was to develop a practical manual segmentation method for the amygdala and hippocampus in infant brain MRI scans. The protocol was evaluated using both T1- and T2-weighted MR images. Additionally, we conducted a comparative analysis between data segmented using iBEAT software and manually segmented data. The manual segmentation volumes were analyzed descriptively, presenting mean and standard deviation (SD) values. Hemispheric volume disparities for both the right and left amygdala and hippocampus were examined using a paired t-test, with statistical significance defined as p-values ≤ 0.05. The data distribution of the sample did not significantly differ from a normal distribution and was evaluated through visual confirmation and the Shapiro-Wilk test. The statistical analyses were performed using SPSS version 24, Armonk, NY, United States. Additionally, the Dice Similarity Coefficient (DSC), introduced by Dice in 1945, was calculated using Python version 2.7 to estimate the level of volumetric overlap between the delineations.

4.7.1.1 Intra-rater reliability

Re-segmentation on 12 randomly selected MR images from 12 different participants assessed stability and intra-rater reliability. Six of these MR images were segmented at 1-month intervals, while the other six were segmented at 6-month intervals. Intra-rater reliability assessments for the left and right amygdala and hippocampus were determined utilizing the two-way mixed-model and absolute agreement Intraclass Correlation Coefficient (ICC) method, along with the Dice Similarity Coefficient (DSC) (Shrout & Fleiss, 1979).

4.7.1.2 Reliability between the raters

Two novice raters re-segmented 20 randomly selected MR images from the initial 31 images to assess inter-rater reliability. Each rater segmented the amygdala and hippocampus in 10 brains, blind to gender and age. A two-way mixed-model, absolute agreement, and multiple rater ICC were used to calculate inter-rater reliability using segmented structure volumes (Koo & Li, 2016; Shrout & Fleiss, 1979). DSC was also used to assess the volumetric overlap of the left and right amygdala and hippocampus between rater 1 and the primary rater, as well as between rater 2 and the primary rater.

4.7.1.3 T1- and T2-weighted MR image manual segmentation

Following the protocol produced, manual segmentation was performed on a set of 10 T1- and T2-weighted images derived from identical participants. This discrepancy in contrast between T1- and T2-weighted images arises due to the ongoing myelination process and increased water content within the infant brain, leading to a reduced contrast in T1-weighted images in comparison to T2-weighted images (Dean et al., 2018). In infants, the intensity pattern of white and gray matter in T1-weighted images resembles that of adult T2-weighted images, where white matter appears with lower intensity than gray matter (Dean et al., 2018; Paus et al., 2001). On the contrary, the distinction between the white and gray matter in T2-weighted images of infants within this age range resembles that observed in T1-weighted images of adults.

Through modifications to the image's brightness and contrast settings, it becomes possible to distinguish the amygdala and hippocampus in T1-weighted images, although this clarity falls short of that achieved in T2-weighted images. The volume differences between the left and right hippocampus and amygdala in both T1 and T2 images of identical participants were derived from the segmentation data. To assess the coherence between T1 and T2 manual segmentation, calculations for the ICC and DSC were performed. While T2-weighted MR images provide better tissue contrast during this developmental stage, T1-weighted MR images were included in the protocol to explore their potential interchangeability, particularly in cases where T2-weighted images may be affected by motion artifacts.

4.7.1.4 Manual versus automated segmentation

Automated segmentation was performed using the iBEAT software, while manual segmentations were carried out through the Display software, both applied to 10 T2-weighted MR images. Due to iBEAT's limitation in accepting infants' T1-weighted images, solely T2-weighted images were employed for the comparative analysis with manual segmentation. To validate the accuracy of iBEAT's automated segmentation outcomes for the limbic structures (specifically, the hippocampus and amygdala), a comparison was made between the volumetric outcomes obtained from iBEAT and the volumes manually defined.

The volumetric outcomes from both iBEAT's software and manual segmentation were compared. Furthermore, the discrepancy in outcomes between automated and manual segmentation was quantified as a percentage through the formula %VD = (T.Va - Vm) / Vm * 100% (Schoemaker et al., 2016). In this formula, negative percentages signify an underestimation of automated segmentation volumes in relation to manual segmentation, while positive percentages indicate an overestimation of volumes in comparison to manual segmentation. Additionally, ICC and DSC analyses were conducted on the extracted volumes for both automated and manual segmentations.

4.7.2 Study II

This study investigated the impact of PMDS on the amygdala MD metrics in infants aged 11–54 days, assessed through the EPDS questionnaire, across GW 14, 24, and 34. Moreover, potential sexually dimorphic associations between PMDS and amygdala MD metrics were explored.

IBM SPSS version 25 (IBM Corp., Armonk, NY) and R version 3.6.3 (http://www.r-project.org/) were used for statistical analyses. The production of figures was facilitated by ParaView, ITK-SNAP, and FSLeyes software (Ayachit, 2015; Jenkinson et al., 2012b; Yushkevich et al., 2006).

The distribution normality of MD metrics across participants was assessed, and no statistically significant deviations from normal distributions were observed ($p > 0.05$). Associations among maternal and infant demographics, EPDS, and MD metrics were reported through bivariate Pearson correlations, one-way ANOVA, and two-sample t-tests between measurement variables and nominal variables.

Covariates were examined with both EPDS and MD, and those that had a significant association with either EPDS scores or MD metrics were chosen for further analysis. Maternal use of SSRIs, SNRIs, other CNS-affecting medications, maternal age at due date, economic situation based on parent(s) perspective obtained through questionnaires, maternal pre-pregnancy BMI, infant 5-min Apgar score, and infant weight at birth were all considered for inclusion in the models. All analyses included newborn age at scan time, infant GW at birth, and infant sex in the models.

Multiple linear regression models were employed to investigate the connections between EPDS score timepoints (GW14, 24, and 36) and MD metrics of the right and left amygdala. Associations were analyzed separately for each side of the amygdala and for each pregnancy time point (GW14, GW24, and GW34). Consequently, a total of 6 models were employed for the main effects analysis, and 6 models were used for investigating sex-specific associations. Sex interactions with EPDS scores and amygdala MD metrics were examined using models that introduced a sex-EPDS score interaction term. False-discovery rate (FDR) corrections (Benjamini & Hochberg, 1995) were applied to p-values to address multiple comparisons. Separate FDR corrections were conducted for the six main effects analyses (MD ~ EPDS + covariates) and the six sex interactions analyses (MD ~ EPDS*sex + covariate). The threshold for statistical significance was set at 0.05 for both uncorrected and corrected p-values.

For significant outcomes, sensitivity analyses were conducted by iteratively adding and removing the individual covariates mentioned above in a leave-one-out manner within the multiple linear regression tests. Multiple comparison corrections were not applied in the sensitivity analysis.

4.7.3 Study III

The purpose of this study was to explore the relationship between infants' amygdalae MD metrics measured between 11 and 54 days after birth and their attention to facial expressions at 8 months. Following that, we investigated gender-specific associations.

Statistical analyses were performed using R v. 3.6.3 (http://www.r-project.org/). The Kolmogorov-Smirnov statistics, skewness, and kurtosis of the main interest variables did not violate the assumptions of normality, so parametric methods were used to analyze the associations. First, multiple linear regression was used to examine the associations between right and left amygdala MD metrics and disengagement probability in control, neutral, happy, and fearful faces after controlling for infant age at the MRI scan (age from birth). Second, a sex-specific interaction between infant sex and disengagement probability from faces was examined. The level of statistical significance in all analyses was set at 0.05.

5 Results

5.1 Manual segmentation protocol and comparison with automated methods (study I)

To evaluate intra-rater reliability, we computed ICC and DSC scores at two time points (1-month and 6-month intervals). The volumes of the segmented left and right amygdala and hippocampus at these intervals are represented in Figure 12. The ICC and DSC scores for intra-rater reliability revealed high levels of consistency (ICC ranging from 0.91 and DSC between 0.89 and 0.94). This signifies the robust replicability of manual tracings by a single rater. Notably, strong ICC and satisfactory DSC outcomes for hippocampus tracings were reported among raters (ICC of 0.90 and DSC of 0.75). The amygdala tracing also exhibited high ICC scores (ICC of 0.92), although the DSC scores indicated moderate agreement between the raters for amygdala segmentation (DSC of 0.52). The outcomes suggest that there were no notable variations in volumes among these structures (Figure 13).

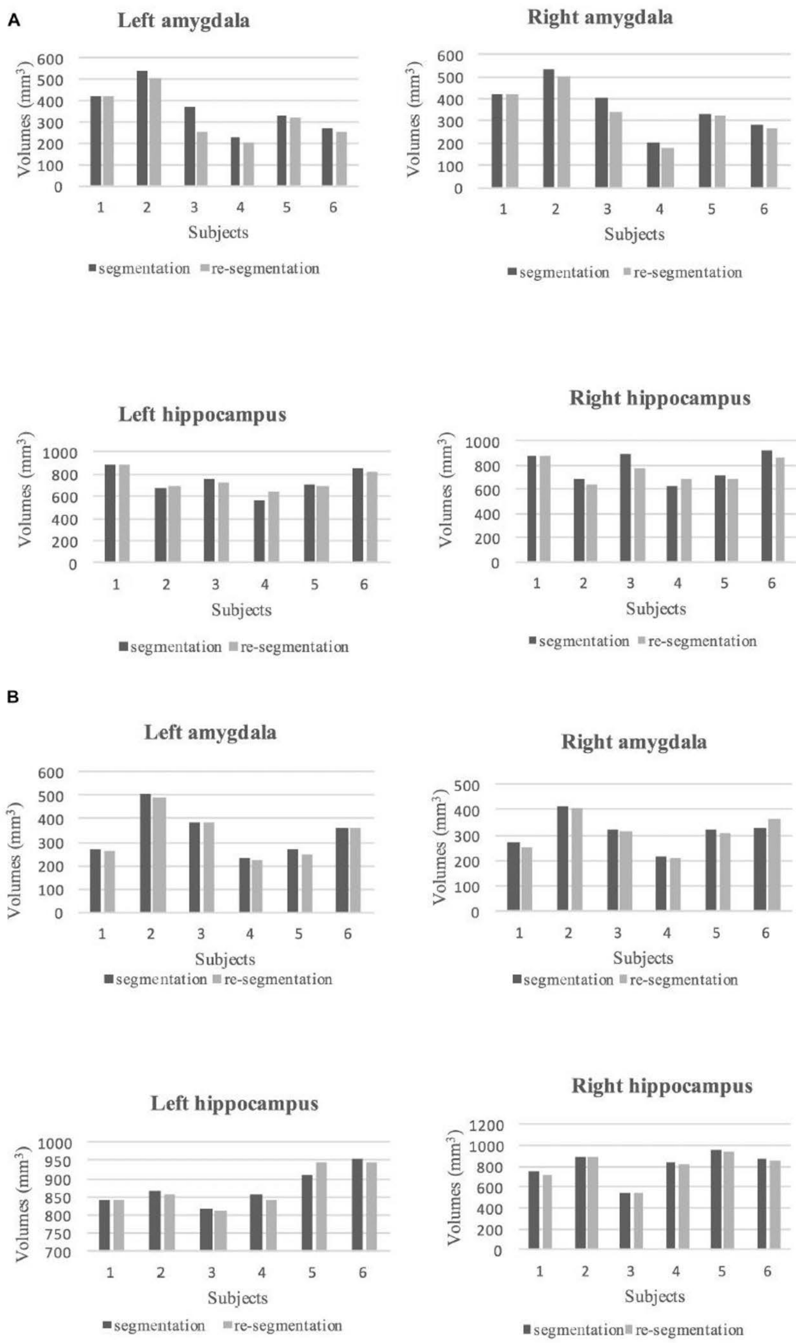

Figure 12. A) The measurements of the segmented (dark gray) and re-segmented (light gray) volumes of the left and right amygdala and hippocampus at 1-month intervals, and B) 6-month intervals after the initial segmentation. The figure appears in the original publication of study I and is reprinted with the permission of the copyright holders.

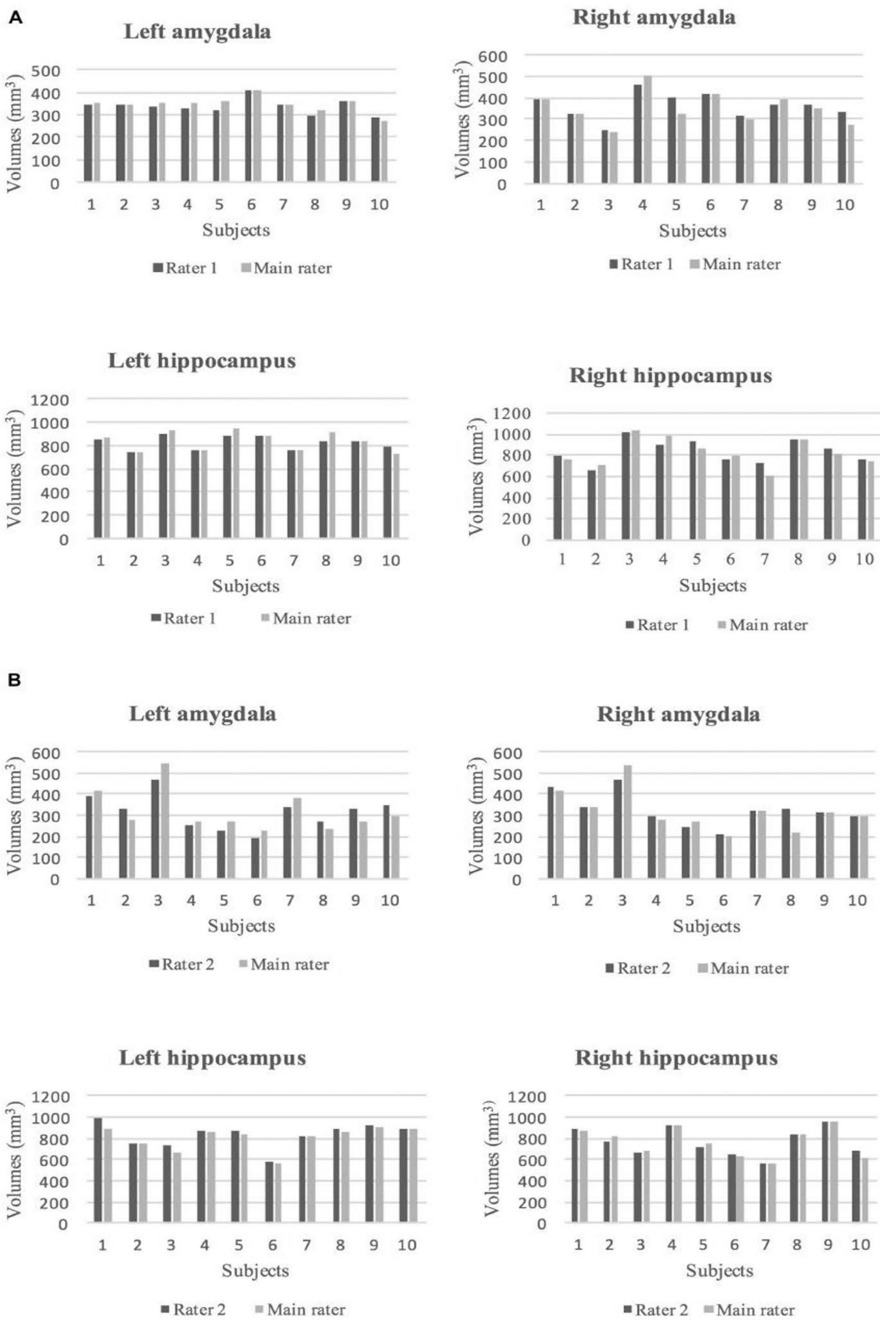

Figure 13. Displayed are segmented volumes of the left and right amygdala and hippocampus for 10 subjects in T2 images. (A) Rater 1 (dark gray) and primary rater (light gray) results are shown. (B) Rater 2 (dark gray) and primary rater (light gray) results are depicted. The figure appears in the original publication of study I and is reprinted with the permission of the copyright holders.

5.1.1 Comparing manual segmentation in T1- vs. T2-weighted MR images

Manual segmentation of the amygdala and hippocampus volumes within T1- and T2-weighted MR images of the same participants yielded slightly discrepant results. Generally, the volumes derived from manual segmentation in T2 images exhibited lower values, likely attributed to enhanced border contrast. Consequently, the manual segmentation performed on T1 images slightly overestimated the volumes of both the left and right amygdala and hippocampus. Robust ICC and DSC scores were evident in amygdala and hippocampus segmentation within both T1 and T2 images (ICC $\geq$ 0.90 and DSC $\geq$ 0.74).

5.1.2 Automated vs. manual segmentation

Manual delineation yielded different hippocampus and amygdala structural volumes than iBEAT automated segmentation. Automated segmentation resulted in significantly higher volumes for both the left and right amygdala and hippocampus when contrasted with manual segmentation. The average percentage volume difference for the left amygdala was 111.8% with a standard deviation of 71.6, while for the right amygdala it was 55.9% with a standard deviation of 70.5. For the left hippocampus, the mean percentage volume difference was 130.3% with a standard deviation of 32.8, and for the right hippocampus, it was 128.4% with a standard deviation of 39.3. The ICC and DSC results between manual segmentation and automated segmentation methods for the left and right amygdala and hippocampus were not strong (ICC = 0.07 and DSC = 0.39) (Figure 14 and Figure 15).

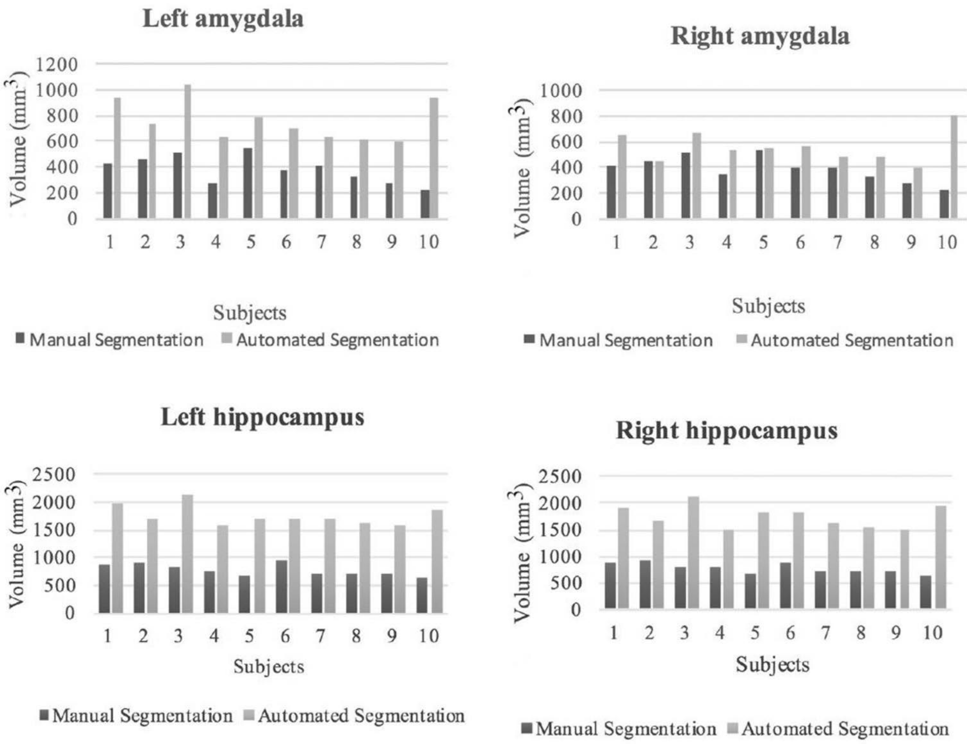

Figure 14. Left and right amygdala and hippocampus volumes from manual and automatic segmentation for all 10 subjects. Light and dark gray volumes represent automated and manual segmentation, respectively. The figure appears in the original publication of study I and is reprinted with the permission of the copyright holders.

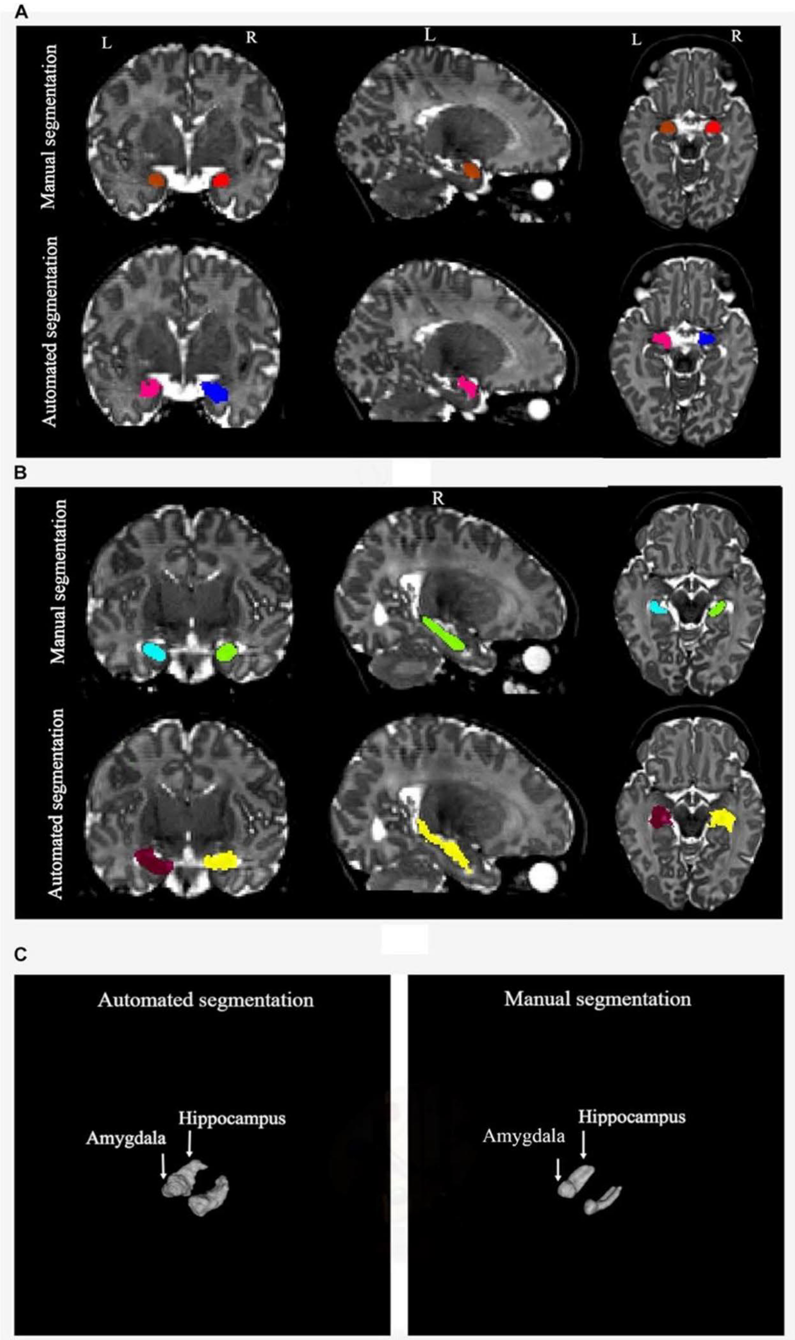

Figure 15. Manual and automated amygdala (A) and hippocampus (B) segmentation in T2 images. A comparison of automated and manual segmentation in a 3D surface render (C). The figure appears in the original publication of study I and is reprinted with the permission of the copyright holders.

Summary: A neonatal MR image segmentation protocol for the amygdala and hippocampus was developed. Its reliability was evaluated for both inter- and intra-rater assessments. Intra-rater reliability demonstrated high consistency, and inter-rater reliability was found to be satisfactory. Furthermore, a comparison of manual and automatic segmentation using iBEAT revealed a lack of agreement.

5.2 PMDS and amygdala diffusion properties (study II)

Mothers with lower EPDS scores had a better economic status during GW 24 and 34. Maternal age was negatively correlated with EPDS scores during GW 14. In infants, there was a negative correlation between maternal EPDS scores at gestational week 34 and 5-minute Apgar scores. Additionally, greater MD measurements of the left amygdala were strongly linked with child age from birth at scan time (Table 3).

Multiple linear regression analyses indicated no significant main effects of EPDS scores (GW 14, 24, and 34) on MD metrics in the left or right amygdala, after accounting for prenatal and postnatal factors. A notable sex interaction effect was identified for EPDS GW 14 scores on MD in the left amygdala (Table 4). Boys showed a stronger positive link between EPDS GW 14 and left amygdala MD than girls after controlling for prenatal and postnatal factors (Figure 16). The significance of the sex interaction effect persisted in sensitivity analyses ($p < 0.050$).

Table 3. Correlations between the EPDS scores, the amygdala mean diffusivity (MD), and the demographics (* p < .05, ** p < .01).

Variables	**EPDS GW 14**	**EPDS GW 24**	**EPDS GW 34**	**MD LA**	**MD RA**
Maternal pre-pregnancy BMI, r	-0.06	-0.00	0.07*	0.94	0.19
Mother's age at due date (years), r	-0.32**	-0.23*	-0.19	-0.12	0.01
Infant gestational age at birth (week), r	-0.01	0.05	0.05	0.15	-0.14
Infant age at the scan date (days), r	0.03	0.02	0.00	-0.42**	-0.05
Birth weight (grams), r	-0.07	0.01	0.06	0.01	-0.06
Apgar, 5 min, r	-0.08	-0.12	-0.14*	-0.12	0.02
Economic situation, p	P = 0.01	P = 0.04	P = 0.03	P = 0.80	P = 0.33
Very good, mean (SD)	3.5 (3.4)	2.0 (1.7)	3.2 (2.6)	1.05 (0.04)	1.05 (0.02)
Fairly good, mean (SD)	5.1 (5.5)	5.2 (5.4)	4.6 (5.1)	1.04 (0.04)	1.04 (0.04)
Not good, mean (SD)	6.2 (5.0)	6.2 (5.0)	6.1 (4.8)	1.04 (0.04)	1.05 (0.03)
Fairly bad, mean (SD)	9.9 (6.0)	9.9 (6.0)	12.0 (4.4)	1.04 (0.04)	1.07 (0.04)
Very bad, mean (SD)	0.0 (NA)	0.0 (NA)	0.0 (NA)	0.0 (NA)	0.0 (NA)
Prenatal medication use of SSRI and SNRIS, p	P = 0.02	P = 0.38	P = 0.31	P = 0.13	P = 0.90
yes, mean (SD)	8.2 (6.1)	8.2 (5.6)	8.8 (7.4)	1.07 (0.08)	8.2 (5.6)
no, mean (SD)	5.4 (5.1)	5.4 (5.1)	5.4 (5.0)	1.04 (0.03)	1.05 (0.03)

Table 3 footnote | Table 3 is adopted from original publication II with the permission of the copyright holders.

Table 4. The interaction effect of EPDS and sex after controlling for maternal use of SSRIs and SNRIs, other CNS-affecting medications, maternal age at the due date, economic situation, maternal pre-pregnancy BMI, infant 5-min Apgar score, infant weight at birth, maternal age at the due date, infant age at scan, infant GW at birth, and infant sex on amygdala MD metrics is presented. Estimates (β), standard error (SE), uncorrected p-values (P), and FDR-corrected p-values (P(FDR)) * p < .05).

Multiple regression model	Left amygdala				Right amygdala			
	β	SE	P	P(FDR)	β	SE	P	P(FDR)
SEX * EPDS GW 14 + CONTROL VARIABLES	-.005	.002	.006*	.036*	-.002	.002	.283	.351
SEX * EPDS GW 24 + CONTROL VARIABLES	-.002	.002	.351	.351	-.003	.002	.224	.351
SEX * EPDS GW 34 + CONTROL VARIABLES	-.002	.002	.344	.351	-.003	.002	.147	.351

Table 4 footnote | Table 4 is adopted from original publication II with the permission of the copyright holders.

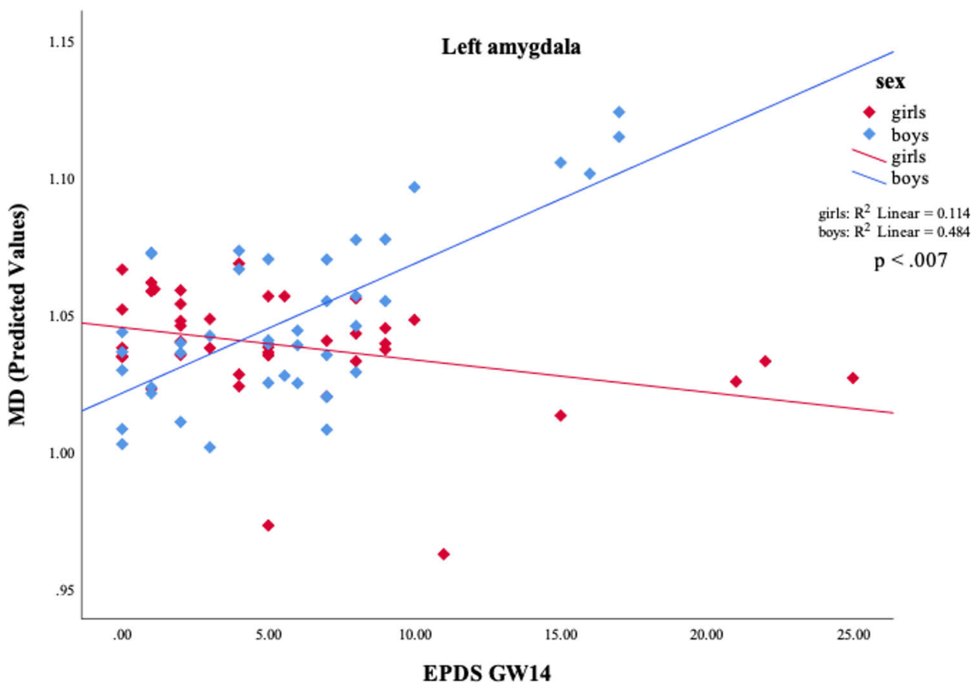

Figure 16. The interaction between EPDS scores at GW 14 and infant sex in relation to the MD of the left amygdala in infants is illustrated, following adjustment for both prenatal and postnatal factors. The figure appears in the original publication of study II and is reprinted with the permission of the copyright holders.

Summary: We found no main EPDS effects on the amygdala MD after accounting for prenatal and postnatal factors. A significant sex interaction showed boys had a stronger positive link between EPDS GW 14 and left amygdala MD than girls, surviving multiple comparisons and sensitivity analyses ($p < 0.05$).

5.2 Emotional face perception and amygdala diffusion properties (study III)

Left and right amygdala MD measurements were correlated ($r = .70$, $p = .001$). The scrambled non-face control picture disengagement probability was negatively connected with infants' birth weight ($r = -.38$, $p = .019$). A negative connection was seen between left amygdala MD and MRI age ($r = -.41$, $p = .007$). Age at eye-tracking date was negatively linked with scrambled non-face control picture disengagement ($r = -.37$, $p = .024$) and positively with infants' birth weight ($r = -.34$, $p = .042$). Table 5 shows variable intercorrelations.

Table 5. The Pearson correlations were calculated for various variables, including disengagement probability (DP) from scrambled non-face control pictures (Cs), neutral (Ne), happy (Ha), and fearful (Fe) pictures, mean diffusivity (MD) measures of the left (MD LA) and right amygdala (MD RA), birth weight (BW), age at the MRI date (MRI Age), head circumference (HC), and age at eye-tracking (ET Age). Significance levels were indicated by asterisks (* p < .05, ** p < .01).

	DP CS	DP Ne	DP Ha	DP Fe	MD LA	MD RA	BW	MRI Age	HC	ET Age
DP CS	1									
DP Ne	.397*	1								
DP Ha	.611**	.692**	1							
DP Fe	.282	.690**	.426**	1						
MD LA	.188	-.087	-.004	-.061	1					
MD RA	.121	-.290	-.170	-.311	.708**	1				
BW	-.380*	-.222	-.101	-.122	-.020	-.060	1			
MRI Age	-.187	-.159	-.285	-.067	-418**	-.096	-.104	1		
HC	-.077	-.215	-.117	.028	.240	.246	.463**	-.092	1	
ET Age	-.371*	-.088	-.144	.025	-.202	-.204	.346*	.153	.299	1

Table 5 footnote | Table 5 is adopted from the original publication III with the permission of the copyright holders.

Infants exhibited a significant tendency to sustain attention towards fearful (the mean probability of attention disengagement, M = .40) rather than happy (M = .53), neutral (M = .56), or scrambled non-face control pictures (M = .75), indicative of an age-typical inclination towards fearful facial expression. In the overall sample, significant associations emerged between the right amygdala MD values and disengagement probability from fearful faces, after controlling for infant age at the time of MRI scans. A negative correlation was found between the probability of disengagement from fearful faces and the measures of MD in the right amygdala (ß = -.058, p = .047), as depicted in Figure 17. However, no significant associations were observed between MD measures in either the left or right amygdala and disengagement probabilities in other conditions ($p > .05$).

Additionally, analyses considering sex interactions did not reveal any significant relationships between amygdala MD measures and the likelihood of attentional disengagement from faces depicting fear, happiness, or neutrality. Nevertheless, a significant sex-interaction emerged in relation to disengagement probabilities from scrambled non-face control pictures after controlling for infant age at the time of MRI scans. Specifically, among girl participants, there was a significant correlation observed between MD values in both the right and left amygdala and a heightened likelihood of disengagement from scrambled non-face control pictures (for right amygdala MD, ß = .130, p = .021, and for left amygdala MD, ß = .19, p = .013) (Figure 18).

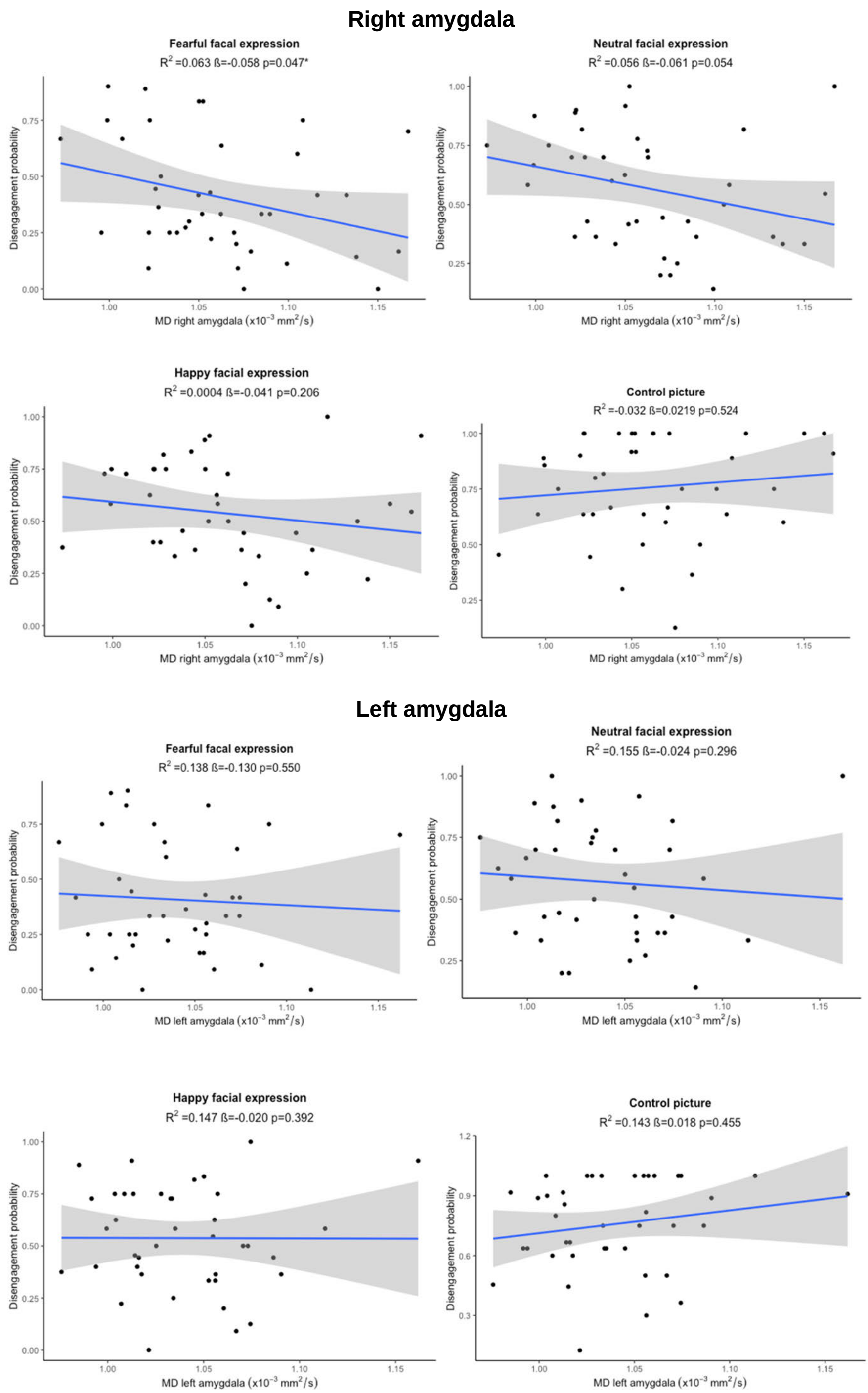

Figure 17. The disengagement probability from fearful, non-fearful (happy and neutral), and scrambled non-face control pictures in the overall sample is associated with the right and left amygdala MD values. In this figures, ß represents an unstandardized coefficient. The figure appears in the original publication of study III and is reprinted with the permission of the copyright holders.

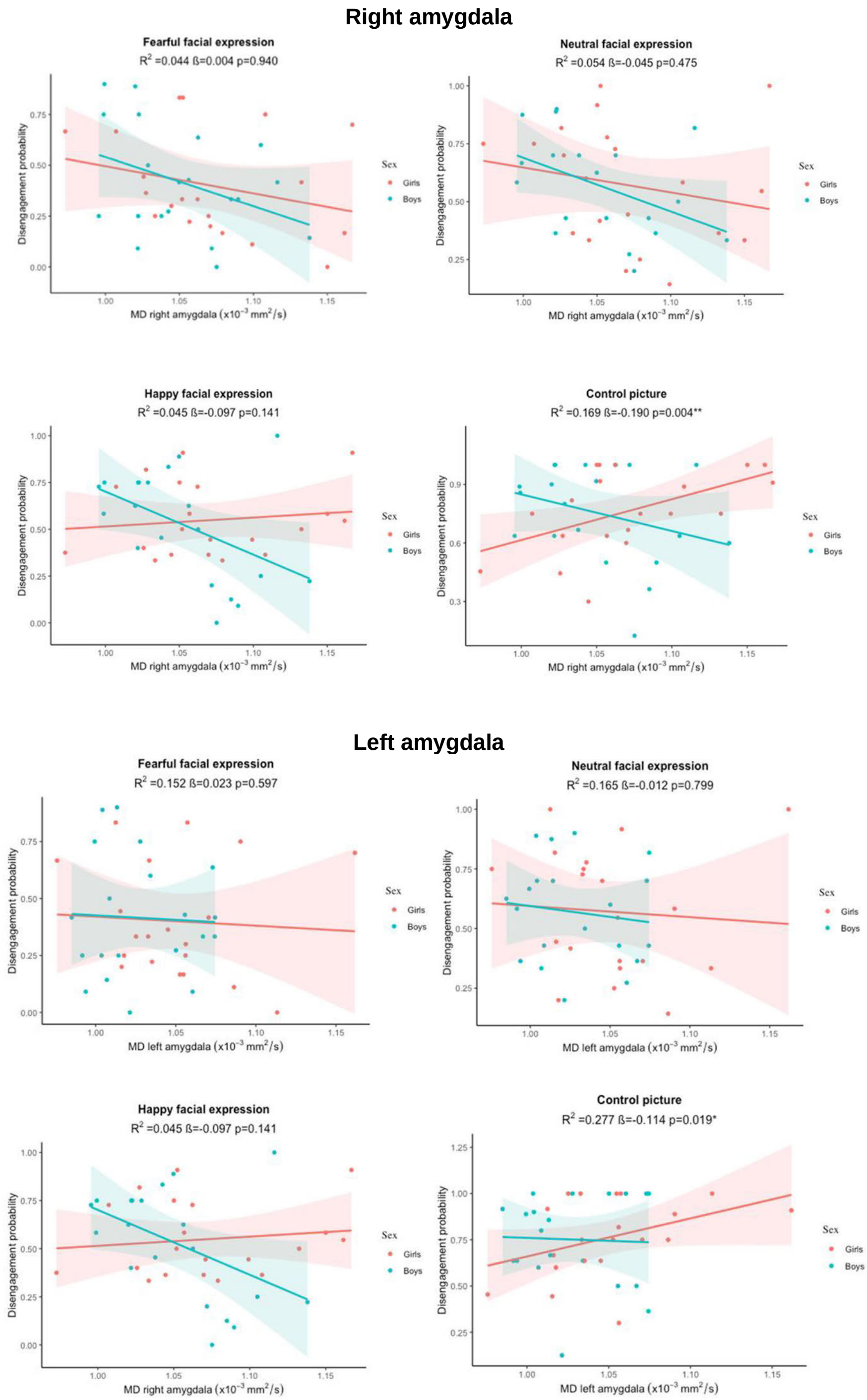

Figure 18. Right and left amygdala mean diffusivity (MD) values and disengagement probability from fearful, non-fearful (neutral and happy), and scrambled non-face control pictures in male and female infants. The figure appears in the original publication of study III and is reprinted with the permission of the copyright holders.

Summary: Increased right amygdala MD values were associated with lower disengagement from fearful faces in infants. In terms of sex differences, elevated MD levels in both the right and left amygdala correlate with heightened disengagement probability from scrambled non-face control pictures in girl participants.

6 Discussion

6.1 Manual segmentation protocol and evaluation of manual versus automated segmentation methods (study I)

We established a robust protocol for manual segmentation of the amygdala and hippocampus structures in MR images of infants, yielding precise delineations for a single rater. Inter-rater assessments for the hippocampus demonstrated high ICC and DSC values, while those for the amygdala demonstrated high ICC and satisfactory DSC values. These findings are likely attributable to systematic disparities between raters and the amygdala's smaller dimensions and intricate characteristics. Despite suboptimal alignment between manual tracings and automated segmentation results, we express confidence in the efficacy of iBEAT software for the majority of brain segmentation tasks (Lehtola et al., 2019). This underscores the crucial need for a thorough assessment of automated segmentation software and its results.

Based on our observations, we found that the general structure of infants' amygdala and hippocampus resembles that of adults, nevertheless, the identification of the lower and lateral boundaries of both structures presents greater challenges. Our segmentation protocol was designed to incorporate macro-anatomical features and boundaries, with a specific focus on excluding the fornix and parahippocampal gyrus from the hippocampus and accurately delineating the boundaries of the amygdala and hippocampus near the temporal horn of the lateral ventricles. We systematically used all three planes (sagittal, axial, and coronal) for the identification of structures and boundaries, in contrast to some other studies that primarily rely on a default view and only incorporate additional planes when deemed necessary (Alexander et al., 2017; De Macedo Rodrigues et al., 2015b; Gousias et al., 2012). This protocol underwent testing by two raters with limited prior experience in brain manual segmentation, and they swiftly adopted this approach.

The protocol was used to compare manually segmenting T1- and T2-weighted images of the same participants. Unlike T1-weighted images, manual delineation of infant T2-weighted images was easier due to better boundary contrast. Although T1- and T2-weighted image segmentations were similar, there were slight differences. T1-weighted image-based amygdala and hippocampus volumes slightly overestimated those from T2-weighted images. The robust correlation and high DSC scores observed between T1- and T2-weighted images provide compelling evidence that these two imaging types can be seamlessly substituted for one another in related studies when either is unavailable.

We evaluated the iBEAT software's accuracy compared to manual segmentations, considered the "gold standard." Unfortunately, iBEAT's automatic segmentation could not be validated against manual segmentation. iBEAT significantly overestimated amygdala and hippocampus volumes, likely due to limited infant brain MR image contrast.

6.2 PMDS and amygdala diffusion properties (study II)

We employed a longitudinal approach to measure PMDS at various stages of pregnancy, providing a comprehensive assessment of its prevalence across the gestational period. We also investigated potential sex differences. Our studies revealed no significant effects of EPDS scores on amygdala MD. However, a significant sex interaction effect was observed. Higher PMDS levels at GW 14 were associated with a significant increase in left amygdala MD in boys compared to girls. Notably, these findings remained significant after undergoing multiple comparisons and sensitivity analyses.

It is uncertain why PMDS affects fetal development differently in boys and girls. Based on our findings, it appears that boys may exhibit a greater susceptibility to the effects of PMDS. This could be explained by different placental responses to glucocorticoids in male and female pregnancies (Clifton, 2010). Elevated maternal cortisol levels can change placental gene expression and protein synthesis, limiting female fetus growth and survival (Clifton, 2010). On the other hand, pregnancies with male fetuses, result in fewer placental function alterations, which ensures growth in an adverse maternal environment, while increasing the possibility of other risk factors (Clifton, 2010). Moreover, shortly after birth, male infants display greater volumes of cortical gray matter, white matter, and subcortical gray matter in comparison to female infants, with these distinctions emerging during prenatal brain development (Gilmore et al., 2007). This phenomenon potentially leads to the development of more neural connections, myelin, and synapses in male brains, making them more susceptible to the adverse effects of PMDS and increasing the risk of neurodevelopmental disorders (Alonso-Nanclares et al., 2008). Additionally, male infants exposed to elevated levels of PMDS during infancy may experience increased anxiety, impaired motor skills, and sleep disturbances (Gerardin et al., 2011; Hay et al., 2019). The type, severity, timing, and age of the offspring at the time of the study affect whether girls or boys are more vulnerable to PMDS (Bale et al., 2015; Glover et al., 2010).

Maternal cortisol can cross the placenta and alter the fetal hypothalamic-pituitary-adrenal (HPA) axis permanently, impacting cognitive and behavioral function later in life (Glover et al., 2010; Rakers et al., 2016). The enzyme 11-beta hydroxysteroid dehydrogenase 2 (11β-HSD2) controls placental glucocorticoid metabolism, converting cortisol into its inactive form (Benediktsson et al., 1997; V. E. Murphy & Clifton, 2003). While it typically deactivates most of maternal cortisol, the fetus has less protection during early pregnancy when placental 11β-HSD2 levels are lower or inactive (Rakers et al., 2016). Our findings indicate that PMDS may have more pronounced effects when experienced in early pregnancy rather than later stages. The negative impacts of early pregnancy exposure to cortisol are likely more related to maternal susceptibility than fetal susceptibility, given that the fetal HPA axis doesn't produce cortisol until late gestation (Magyar et al., 1980; Rakers et al., 2016). Studying PMDS at various pregnancy stages will help to pinpoint vulnerable prenatal periods.

6.3 Emotional face perception and amygdala diffusion properties (study III)

Our study found the first substantial connection between the amygdala MD and infants' disengagement probability from fearful faces. Infants with higher right amygdala MD were less likely to shift their attention away from fearful stimuli towards salient lateral distractors compared to non-fearful stimuli (happy or neutral). These results support past research that indicates the amygdala's attentional bias in processing fearful facial emotions relative to other facial expressions (Tuulari et al., 2020; Vuilleumier, 2005; Whalen et al., 2001). Although the precise neural processes responsible for directing newborns' attention to fearful faces are not yet fully understood, recent studies propose that both the amygdala and orbitofrontal cortex play roles in processing a wide range of facial emotions, rather than exclusively the facial expressions related to fear (D. A. Fitzgerald et al., 2006). The sensitivity of the infant amygdala to emotional cues plays a crucial role in early emotional and social development. Consequently, the amygdala's involvement in emotion perception and recognition appears to be more modulatory and temporally protracted (Adolphs, 2010). This shows that the amygdala's role in emotion processing entails influencing and managing emotional responses over time rather than simply recognizing emotions instantly. It implies that the amygdala not only identifies emotions but also shapes and extends the emotional experience.

In our sex-interaction analysis, female infants showed stronger connections between the probability of disengaging attention from scrambled non-face control images and MD of both the right and left amygdala compared to male infants. Specifically, higher MD was linked to increased attention disengagement from the scrambled images to distractors. The underlying mechanisms of these findings remain unclear. Killgore et al., 2001 found sex variations in amygdala responses to faces and emotional stimuli. Women have a higher bilateral amygdala response to emotional stimuli than men (Hamann, 2005; Killgore et al., 2001). Women's increased emotional reactivity may be due to sex variations in amygdala reactions to faces (Hall & Matsumoto, 2004). However, the evidence is inconclusive. Other studies indicate that the amygdala tends to show higher activation in men, particularly in response to emotional stimuli (Derntl et al., 2009; Kret et al., 2011). These results indicate that amygdala responses to emotional stimuli vary by sex, but additional research is needed to better understand these differences.

6.4 Laterality of the amygdala in response to PMDS and fearful stimuli (studies II and III)

In study II, we found that the left amygdala MD is associated with PMDS, while in study III, the right amygdala MD is associated with the probability of disengagement from fearful facial stimuli. Prior research on the lateralization of amygdala function in each hemisphere shows that left and right amygdalae interpret information differently (Baas et al., 2004). The left amygdala's susceptibility to the effects of PMDS may be linked to the left hemisphere's accelerated growth during the prenatal phase (Andescavage et al., 2017). Furthermore, patients with major depressive disorder often exhibit reduced connectivity with more regions than the right amygdala (Ramasubbu et al., 2014). Additionally, positive associations have been identified between PMDS and the left amygdala's connectivity with other brain regions (Qiu et al., 2015). Furthermore, elevated pregnancy-specific anxiety relates to reduced left amygdala volumes in offspring (Acosta et al., 2019). This consistency in findings strengthens the argument that PMDS can influence the left amygdala and its connectivity with other brain regions. Similarly, some studies have indicated that the left amygdala shows a primary response to fearful events and faces (Hardee et al., 2008; Tuulari et al., 2020). On the contrary, multiple studies have demonstrated that the presentation of fearful facial expressions elicits greater activation in the right amygdala compared to the left amygdala (Framorando et al., 2021; Liddell et al., 2005; Morris et al., 1999). The potential reason for the right amygdala's reaction to fearful facial expressions may be attributed to its connectivity with the brain's visual processing regions. The aforementioned association facilitates the prompt and efficient identification and reaction to stimuli that are perceived as threatening or inducing fear. Consequently, this leads to an intensified response from the extrastriata cortex, achieved by the quick transmission of signals from the amygdala to the visual regions. While the initial recognition of stimuli is primarily attributed to the right amygdala, the left amygdala, characterized by a slower response, may assume a more substantial role in the subsequent processing and interpretation of the identified stimuli (Bonnet et al., 2015; Sergerie et al., 2008). However, the matter of laterality is frequently not explicitly addressed due to variations in stimuli, task design, and data analysis across different experiments. (Hardee et al., 2008). As a result, there remains limited understanding regarding potential distinctions between the roles of the left and right amygdala in responses to PMDS exposure or the processing of fearful stimuli.

6.5 Amygdala MD in response to PMDS and fearful stimuli (studies II and III)

In study II, higher PMDS levels were linked to increased left amygdala MD in boys. In study III, higher right amygdala MD was associated with lower disengagement probability from fearful stimuli, and also correlated with increased attention shift from scrambled non-face control pictures in girls. These findings indicate a correlation between PMDS and changes in amygdala microstructure in infants, highlighting the potential impact of maternal mental health on developing brains. Moreover, the higher MD measures in the amygdala could be an early sign of vulnerability to difficulties in regulating fear responses. This vulnerability may manifest as challenges in disengaging from potential threats, particularly during infancy, when emotional regulation is developing.

Although the specific MD changes in these contexts are not entirely clear, previous studies have suggested various physiological mechanisms could potentially account for these alterations. Typically, there is a trend of decreasing MD in infancy, childhood, and adolescence, which is often a sign of normal brain maturation and higher functional adaptation (Aeby et al., 2009; Dubois et al., 2008; Lebel et al., 2010; Moura et al., 2016; Pohl et al., 2016; Takeuchi et al., 2016; Taki et al., 2013; Tamnes et al., 2010; Yoshida et al., 2013). Therefore, increased MD may indicate delayed development of the amygdala, suggesting that fear processing functions are less developed compared to what is typically expected for that age (Cismaru et al., 2016). Factors such as the distribution of water content within intracellular and extracellular compartments can affect the diffusion of water molecules and therefore impact the MD signal (Gillespie et al., 2017). An elevated MD value suggests enhanced facilitation and accelerated mobility of water molecules in the tissues (Cherubini et al., 2010). The elevation in MD could potentially be attributed to underlying mechanisms, including disturbances in the integrity of tissue microstructure, enlargement of extracellular spaces, reduction in neuronal size, and alterations in synaptic activity (Cherubini et al., 2010; De Gennaro et al., 2011; Gillespie et al., 2017; Kantarci et al., 2005).

Anxiety, traumatic brain injury, cognitive impairment, and Alzheimer's disease have all been linked to increased amygdala MD, which is associated with decreased microstructural integrity (Cherubini et al., 2010; Juranek et al., 2012). Interestingly, the increased MD levels have also been associated with improved empathy, cooperativeness, and cognitive capability (Takeuchi et al., 2019). Moreover, electroconvulsive therapy has been shown to reduce left amygdala MD in individuals with treatment-resistant depression, implying potential microstructural integrity normalization (Yrondi et al., 2019).

It's noteworthy that as these infants grow older, the discrepancies in amygdala MD may tend to align more closely with typical developmental patterns. However, further longitudinal studies are needed to elucidate the long-term trajectory of amygdala development and its implications. Furthermore, incorporating the wider perspective of intergenerational effects on early brain development is essential for comprehensively assessing the implications of amygdala MD changes in infancy. While increased amygdala MD values may indicate disruptions in microstructural properties, it is evident that the implications of increased amygdala MD are complex, uncertain, and require further investigation.

6.6 Significance of the findings

These three studies provide insights into various aspects of infant brain development. The first study focused on producing a segmentation protocol for the amygdala and hippocampus in neonatal MR images, highlighting the need for improved automated segmentation procedures for infant brain imaging. The second study revealed a sex-dependent relationship between PMDS and amygdala microstructure, with potential implications for neuropsychiatric outcomes. Finally, the third study uncovers associations between amygdala microstructure and infants' responsiveness to emotional face stimuli, shedding light on the early neural basis of emotional development. Together, these findings contribute to our understanding of infant brain development and its links to prenatal factors, emotional processing, and neural microstructure.

6.7 Strengths and limitations

One of the main strengths of this thesis is the development of manual segmentation techniques used for the amygdala and hippocampus delineations, which proved highly accurate. These techniques were specifically adapted for the unique infant brain anatomy, reflecting two years of dedicated work, and ensuring the results' robustness and precision.

Although the primary interest was amygdala and hippocampus segmentation, it's noteworthy that we also conducted manual segmentation for all subcortical structures. The segmentation was then used for developing the FinnBrain Neonate (FBN-125) template and generating labeled atlases.

Additionally, the up-sampled high-resolution MR images with a voxel size of 0.5 mm^3 and DTI data with a spatial resolution of 2 mm^3 provide exceptional levels of detail. The improved amygdala labeling procedure and the applied 1.5 mm erosion technique likely reduced partial volume effects, enhancing data accuracy. The use of a high number of diffusion directions (60) further strengthened the precision of tensor model fitting and improved outcome accuracy, which is particularly advantageous in infant brain imaging, characterized by lower resolution and potential motion artifacts. Another strength of the thesis lies in the use of DTI, particularly in its focus on amygdala MD metrics, a measure previously unexplored in studies of a similar nature. With the isotropic nature of diffusion in gray matter, MD provides a more informative assessment of amygdala microstructure and other gray matter structures.

Another advantage of this thesis is the longitudinal design, which provides valuable insights into the prevalence of PMDS throughout the pregnancy, including all trimesters, addressing previous limitations. Furthermore, we explored sex as a contributing factor, enhancing our understanding of potential sex differences in PMDS exposures. Additionally, the inclusion of eye-tracking as a tool for assessing infant attention is a noteworthy strength. It offers an accurate method for studying attention and emotional processing in infants who have not yet developed language skills.

Several limitations are present in this thesis. The manual segmentation protocol demonstrated high Dice coefficient scores in the intra-rater test. However, when evaluating inter-rater reliability for the amygdala, the Dice coefficient values were not as high. This discrepancy is likely linked to systematic variations between raters and the inherent complexities associated with delineating the amygdala due to its small size. These limitations could involve DTI's resolution parameters being insufficient to capture the intricacies of such areas, necessitating improvements in techniques to overcome these challenges (Salat, 2013).

While we improved data quality using up-sampled high-resolution MRI images (0.5 mm^3) for amygdala delineation, we only analyzed the entire amygdala without segmenting its individual nuclei, missing insights into their roles in emotional processes. The basolateral and central nuclei of the amygdala, for example, are important in fear learning and the expression of fear reactions (Beyeler & Dabrowska, 2020; Yau et al., 2021), as are the effects of depression on the amygdala, especially on the medial nucleus (Roddy et al., 2021). However, this is challenging in infants due to their small brain size and lower brain MR and DTI image resolution.

Another drawback of this thesis is the reliance on self-reported PMDS data, which may introduce potential biases and inaccuracies due to recall bias or social desirability bias. Furthermore, the study's geographical focus on a region characterized by high income and relatively strong social support may restrict the applicability of its findings to a more diverse population.

7 Conclusions

Study 1: Accurate segmentation techniques are indispensable for studying developing brains. The absence of both manual and automated segmentation protocols tailored for infants poses a significant challenge in the field of pediatric neuroimaging. This study provides a manual segmentation protocol to create a validation dataset for neonatal brain imaging. This protocol aims to improve manual segmentation and assess automated segmentation techniques.

Study 2: This study revealed links between PMDS and infant amygdala microstructure development. Notably, early pregnancy PMDS was associated with increased MD in the left amygdala among boys but not girls. Further research is needed to elucidate the mechanisms and potential impacts of these alterations in the amygdala on the mental health of offspring.

Study 3: In conclusion, this study explored how amygdala microstructure is related to attention disengagement, both in response to emotional faces and non-emotional stimuli during infancy. Higher right amygdala MD was associated with delayed attention disengagement from fearful faces in the entire sample, and in girls, greater bilateral amygdala MD facilitated higher disengagement from non-face stimuli. Future research should explore the underlying mechanisms behind observed results and the factors influencing predictive value for emotional and social behaviors in offspring. This includes considerations of genetics, environment, and social dynamics to enrich our understanding.

7.1 Future directions

Future research should prioritize the development of both manual and automated segmentation techniques tailored specifically for infant brain imaging. Enhancing these segmentation methods is crucial for precise brain structure delineation and advancing our understanding of early neurodevelopment in infants. Enhancing DTI techniques is essential, and considering biophysical tissue modeling, such as neurite orientation and dispersion density imaging (NODDI), may be more suitable for studying gray matter microstructure (Stoye et al., 2020).

Since the second study was the first to uncover associations between PMDS measured at different pregnancy time points and infant amygdala MD properties, further investigations are needed to elucidate the underlying mechanisms and potential long-term effects. Future research should focus on exploring the long-term behavioral and mental health outcomes of offspring affected by maternal depressive symptoms, as this can provide valuable insights into the broader impact of such conditions. Additionally, given that PMDS was self-reported in the study, it is imperative to further investigate the precise regulation of the placental barrier for cortisol through the measurement of 11β-HSD2 activity, offering a more accurate assessment (Acosta et al., 2019). Moreover, integrating markers of the HPA axis activity alongside psychological assessments can provide a more comprehensive understanding of the intricate relationship between maternal mental health, placental function, and its effects on offspring brain measures.

Considering the interplay of genetic and epigenetic factors in offspring, alongside gene-environment interactions, is essential. This approach allows for a nuanced examination of how these variables might contribute to the effects of PMDS and the processing of emotions like fear on offspring brain development, influencing the likelihood of adverse mental outcomes. Additionally, exploring other factors alongside PMDS, such as pregnancy-specific anxiety, general anxiety, prenatal education and income levels that may influence maternal and fetal well-being, can provide a more comprehensive understanding of the complex interplay between maternal mental health and pregnancy outcomes.

Additionally, replicating the studies with a larger sample size could enhance their robustness and reliability. In the field of pediatric neuroimaging, technical challenges often lead to a substantial reduction in the available data. Therefore, the implementation of standardized scanning protocols specifically designed to suit the distinctive features of the pediatric population would enhance data acquisition and ensure data quality.

The studies in this thesis were the first to report findings in their respective areas. They have opened doors to future longitudinal research directions aimed at enhancing our understanding of pediatric brain development, maternal influences on fetal neurodevelopment, and the early neural basis of emotional processes. These future directions have the potential to shape clinical practice and interventions, ultimately benefiting maternal and child well-being.

Acknowledgements

I would like to express my appreciation to Professor Hasse Karlsson and Professor Linnea Karlsson for providing me with the opportunity to be a part of the FinnBrain research group. The serendipitous encounter with Hasse during a lecture back in 2017 was an incredible stroke of luck that changed my academic career forever. Hasse, you are one of the most exceptional people I know. You value individuality, listen carefully, and give everyone equal opportunities. Your belief in the potential of those around you and your constant support have been invaluable to me. I feel incredibly fortunate to have gotten to know you and to have you as my supervisor and mentor. Thank you for everything. Linnea, I also want to express my gratitude for your kindness and support. Yours and Hasse’s outstanding contributions to our research, have significantly deepened our understanding and made a lasting, inspirational impact.

I would like to thank my second supervisor, Dr. Jetro Tuulari. As we began the manual segmentation journey, we were initially a humble team of two with little clarity on the path ahead. Yet, your supervision and encouragement transformed this long endeavor into a great achievement, leading to the publication of numerous impactful works.

I'm grateful to my third supervisor, Dr. Harri Merisaari, for his support and expertise in image processing and analysis, which have greatly benefited this thesis. Regardless of the circumstances, Harri always finds time to accommodate last-minute meetings, showing his invaluable dedication to the projects. He is always there with a helping hand and a brilliant solution.

I would like to thank Dr. Eeva-Leena Kataja, who played a crucial role in the third project of this thesis. Her support was essential in helping me master the intricacies of statistics. Beyond her professional guidance, she has also been a great friend. Her kindness and openness to my ideas have been invaluable. I consider myself fortunate to have had the opportunity to work with such an exceptional mentor and friend.

I thank Dr. Henriette Acosta for her mentorship, wisdom, and kindness. She's not just a mentor but also a dear friend who has supported me in both academic and personal matters.

I would like to express my gratitude to my Nueroimaging lab colleagues: Isabella, Ilka, Ru, Hilya, Elmo, Aylin, Elena, Silja, Ashmeet, and Aaron. Our trip to Vienna and the incredible memories we created together are unforgettable. Each one of you is such an amazing person, and your friendships have made this academic journey filled with joy and laughter. I would like to thank all my co-authors—Rikka Korja, Noora Scheinin, Satu Lehtola, Jani Saunavaara, Tuire Lähdesmäki, Riitta Parkkola, Tuomo Häikiö, Saara Nolvi, Kristian Lidauer, Iiris Luukkonen, and Maria Keskinen—for their invaluable feedback on the manuscripts. I am also thankful to my collaborators, Dr. Vladimir S. Fonov, Professor D. Louis Collins, and Professor Alan Evans. Special thanks to Dr. John Lewis for his role on my advisory committee, for his constructive comments, and for his expertise and guidance through the projects. Your prompt responses to my questions have been invaluable. Thank you for always being so attentive.

Special thanks to the assisting personnel in the FinnBrain project: Eija Jossandt, Katja Tervahartiala, Susanne Sinisalo, Kaisu Kaistinen, Teemu Kemppainen, Tuomo-Artturi Autere, Juho Pelto, Laura Perasto, Rojin Shokriehzadeh, and Saija Terro. Saija, thank you for your help with the dissertation practicality. Your kindness and friendship have been incredibly valuable to me. Moreover, I want to acknowledge the remarkable FinnBrain researchers, to name a few: Elisabeth Nordenswan, Anna soveri, Eeva Eskola, Hetti Lahtela, Venla Huovinen, Viivi Mondolin, Emma Puosi, Susanna Kortesluoma, Minna Lukkarinen, Matias Mäkinen, Shashank Shekhar, and Anna Aatsinki. Each of you has been exceptional and has made a significant impact on the success of our research. Paula Mustonen, I'm truly grateful for your kindness and all our discussions about the dissertation process.

Grateful acknowledgment is given to the members of the University of Turku, especially the Faculty of Medicine. Thank you, Outi Irjala, Tiia Forsström, and Mikko Tähtö-Pakkanen, for helping me with the dissertation process. You were always kind and helpful.

I appreciate the unique experience I had through the University of Turku peer support group, where we shared and learned many valuable insights. Special thanks to Kia Lundqvist, Johanna Mäkinen, and Katarzyna Piatek for being such integral parts of this journey. I also cherish how our friendships continued beyond that, enriching both my personal and professional lives.

I would like to extend my gratitude to my examiners, Dr. Isabelle Rosso and Dr. Kiran Thapaliya, for their positive and insightful comments. Thank you, Dr. Predrag Petrovic. I am honored to have you as my opponent, and I deeply appreciate the time and effort you have dedicated to this process.

I thank all the FinnBrain families; this work would not have been possible without your participation. Next, I would like to thank the Orion Foundation, Finnish State Grants for Clinical Research, and the University of Turku Graduate School for their financial support, which made this work possible.

I would like to thank my friends and family: Shruti Jain, Marvin, Kaisa, Luis, Afsane, Souzan, Maryam, Mehdi, Ame Fateme, Ame Soosan, Lidia, Brunon, my grandparents, and many others. Your support has been invaluable. Special thanks to Dr. Neda Esmaelifar—your insights have made a significant difference in my life. My heart overflows with gratitude for my beloved best friend and husband, Konrad. You are the absolute light of my life. Your support has been my guiding star. I am forever thankful to you for being the extraordinary human being that you are. You inspire me to become a better person every day. My dearest Emilia, I cannot express enough appreciation for your presence in my life and making me a mommy! Your presence has filled my life with hope, making me more resilient and stronger than I ever thought possible. Maman, thank you for everything you did for us. Thanks for coming to Finland and supporting me during the dissertation process and preparations. Your support during the time I spent in Vancouver, writing this thesis in our home, has been invaluable. Narci, my little sister, your presence means so much. Lastly, I dedicate this thesis to the cherished memory of my dad, who was the reason behind my journey to Finland and academic career. He left us too soon, but he instilled in me the values of determination and ambition. His unwavering love, guidance, and the opportunities he provided for me will forever hold a special place in my heart.

Niloofar
August 1st, 2024
Kaarina, Finland

References

Achiron, R., Yagel, S., Rotstein, Z., Inbar, O., Mashiach, S., & Lipitz, S. (1997). Cerebral lateral ventricular asymmetry: Is this a normal ultrasonographic finding in the fetal brain? *Obstetrics and Gynecology*, *89*(2), 233–237. https://doi.org/10.1016/S0029-7844(96)00506-6

Ackerman, S. (1992). Discovering the Brain. In *Washington (DC): National Academies Press (US)*. https://doi.org/10.2307/j.ctt1t891n1.3

Acosta, H., Kantojärvi, K., Hashempour, N., Pelto, J., Scheinin, N. M., Lehtola, S. J., Lewis, J. D., Fonov, V. S., Collins, D. L., Evans, A., Parkkola, R., Lähdesmäki, T., Saunavaara, J., Karlsson, L., Merisaari, H., Paunio, T., Karlsson, H., & Tuulari, J. J. (2020). Partial Support for an Interaction Between a Polygenic Risk Score for Major Depressive Disorder and Prenatal Maternal Depressive Symptoms on Infant Right Amygdalar Volumes. *Cerebral Cortex*, 1–14. https://doi.org/10.1093/cercor/bhaa158

Acosta, H., Tuulari, J. J., Scheinin, N. M., Hashempour, N., Rajasilta, O., Lavonius, T. I., Pelto, J., Saunavaara, V., Parkkola, R., Lähdesmäki, T., Karlsson, L., & Karlsson, H. (2019). Maternal Pregnancy-Related Anxiety Is Associated With Sexually Dimorphic Alterations in Amygdala Volume in 4-Year-Old Children. *Frontiers in Behavioral Neuroscience*, *13*(August), 1–16. https://doi.org/10.3389/fnbeh.2019.00175

Acosta, H., Tuulari, J., Scheinin, N., Hashempour, N., Rajasilta, O., Lavonius, T., Pelto, J., Saunavaara, V., Parkkola, R., Lähdesmäki, T., Karlsson, L., & Karlsson, H. (2020). Prenatal maternal depressive symptoms are associated with smaller amygdalar volumes of four-year-old children. *Psychiatry Research - Neuroimaging*, *304*(July), 111153. https://doi.org/10.1016/j.pscychresns.2020.111153

Adolphs, R. (2010). What does the amygdala contribute to social cognition? *Annals of the New York Academy of Sciences*, *1191*(1), 42–61. https://doi.org/10.1111/j.1749-6632.2010.05445.x

Adolphs, R., Tranel, D., Hamann, S., Young, A. W., Calder, A. J., Phelps, E., Anderson, A., Lee, G. P., & Damasio, A. R. (1999). Recognition of Facial Emotion in Nine Subjects with Bilataral Amygdala Damage. *Neuropsychologia*, *37*, 1111–1117.

Adouard, F., Glangeaud-Freudenthal, N. M. C., & Golse, B. (2005). Validation of the Edinburgh postnatal depression scale (EPDS) in a sample of women with high-risk pregnancies in France. *Archives of Women's Mental Health*, *8*(2), 89–95. https://doi.org/10.1007/s00737-005-0077-9

Aeby, A., Liu, Y., De Tiège, X., Denolin, V., David, P., Balériaux, D., Kavec, M., Metens, T., & Van Bogaert, P. (2009). Maturation of thalamic radiations between 34 and 41 weeks' gestation: A combined voxel-based study and probabilistic tractography with diffusion tensor imaging. *American Journal of Neuroradiology*, *30*(9), 1780–1786. https://doi.org/10.3174/ajnr.A1660

Aggleton, J. P., Burton, M. J., & Passingham, R. E. (1980). Cortical and subcortical afferents to the amygdala of the rhesus monkey (Macaca mulatta). *Brain Research*, *190*(2), 347–368. https://doi.org/https://doi.org/10.1016/0006-8993(80)90279-6

Albi, E., Arcuri, C., Kobayashi, T., Tomishige, N., Cas, M. D., Paroni, R., Signorelli, P., Cerquiglini, L., Troiani, S., Gizzi, C., Ceccarini, M. R., Mirarchi, A., Cossignani, L., Gil, M. G., Beccari, T., & Cataldi, S. (2022). Sphingomyelin in Human Breast Milk might be Essential for the Hippocampus Maturation. *Frontiers in Bioscience - Landmark*, *27*(8). https://doi.org/10.31083/j.fbl2708247

Alexander, B., Murray, A. L., Loh, W. Y., Matthews, L. G., Adamson, C., Beare, R., Chen, J., Kelly, C. E., Rees, S., Warfield, S. K., Anderson, P. J., Doyle, L. W., Spittle, A. J., Cheong, J. L. Y., Seal, M. L., & Thompson, D. K. (2017). A new neonatal cortical and subcortical brain atlas: the Melbourne

Children's Regional Infant Brain (M-CRIB) atlas. *NeuroImage*, *147*, 841–851. https://doi.org/10.1016/j.neuroimage.2016.09.068

Alonso-Nanclares, L., Gonzalez-Soriano, J., Rodriguez, J. R., & DeFelipe, J. (2008). Gender differences in human cortical synaptic density. *Proceedings of the National Academy of Sciences of the United States of America*, *105*(38), 14615–14619. https://doi.org/10.1073/pnas.0803652105

Andescavage, N. N., du Plessis, A., McCarter, R., Serag, A., Evangelou, I., Vezina, G., Robertson, R., & Limperopoulos, C. (2017). Complex Trajectories of Brain Development in the Healthy Human Fetus. *Cerebral Cortex (New York, N.Y. : 1991)*, *27*(11), 5274–5283. https://doi.org/10.1093/cercor/bhw306

Ayachit, U. (2015). The ParaView Guide: A Parallel Visualization Application. *Clifton Park, NY: Kitware, Inc*, 2015.

Baas, D., Aleman, A., & Kahn, R. S. (2004). Lateralization of amygdala activation: A systematic review of functional neuroimaging studies. *Brain Research Reviews*, *45*(2), 96–103. https://doi.org/10.1016/j.brainresrev.2004.02.004

Bale, T. L., Neill Epperson, C., & Neurosci, N. (2015). Sex differences and stress across the lifespan HHS Public Access Author manuscript. *Nat Neurosci*, *18*(10), 1413–1420. https://doi.org/10.1038/nn.4112

Barkovich, M. J., Li, Y., Desikan, R. S., Barkovich, A. J., & Xu, D. (2019). Challenges in pediatric neuroimaging. *NeuroImage*, *185*, 793–801. https://doi.org/10.1016/j.neuroimage.2018.04.044

Barnea-Goraly, N., Menon, V., Eckert, M., Tamm, L., Bammer, R., Karchemskiy, A., Dant, C. C., & Reiss, A. L. (2005). White matter development during childhood and adolescence: A cross-sectional diffusion tensor imaging study. *Cerebral Cortex*, *15*(12), 1848–1854. https://doi.org/10.1093/cercor/bhi062

Basser, P. J., Mattiello, J., & LeBihan, D. (1994). MR diffusion tensor spectroscopy and imaging. *Biophysical Journal*, *66*(1), 259–267. https://doi.org/10.1016/S0006-3495(94)80775-1

Batalle, D., O'Muircheartaigh, J., Makropoulos, A., Kelly, C. J., Dimitrova, R., Hughes, E. J., Hajnal, J. V, Zhang, H., Alexander, D. C., Edwards, A. D., & Counsell, S. J. (2019). Different patterns of cortical maturation before and after 38 weeks gestational age demonstrated by diffusion MRI in vivo. *NeuroImage*, *185*, 764–775. https://doi.org/https://doi.org/10.1016/j.neuroimage.2018.05.046

Baysal Akin, S. A., & Onat, F. (1995). A N A TO M Y and FUNCTIONS OF LIMBIC Role of Acetylcholine Role o i Dopamine. *Marmara Medical Journal*, *8*(2), 100–105.

Benediktsson, R., Calder, A. A., Edwards, C. R. W., & Seckl, J. R. (1997). Placental 11β-hydroxysteroid dehydrogenase: A key regulator of fetal glucocorticoid exposure. *Clinical Endocrinology*, *46*(2), 161–166. https://doi.org/10.1046/j.1365-2265.1997.1230939.x

Bennett, H. A., Einarson, A., Taddio, A., Koren, G., & Einarson, T. R. (2004). Prevalence of depression during pregnancy: Systematic review. *Obstetrics and Gynecology*, *103*(4), 698–709. https://doi.org/10.1097/01.AOG.0000116689.75396.5f

Bertoni, M. A. (2012). *Neuroimaging of the Amygdala: Quantitative Mechanistic Approach* (B. Ferry, Ed.; p. Ch. 2). IntechOpen. https://doi.org/10.5772/48644

Bethlehem, R. A. I., Seidlitz, J., White, S. R., Vogel, J. W., Anderson, K. M., Adamson, C., Adler, S., Alexopoulos, G. S., Anagnostou, E., Areces-Gonzalez, A., Astle, D. E., Auyeung, B., Ayub, M., Bae, J., Ball, G., Baron-Cohen, S., Beare, R., Bedford, S. A., Benegal, V., … Alexander-Bloch, A. F. (2022). Brain charts for the human lifespan. *Nature*, *604*(7906), 525–533. https://doi.org/10.1038/s41586-022-04554-y

Beyeler, A., & Dabrowska, J. (2020). Neuronal diversity of the amygdala and the bed nucleus of the stria terminalis. In *Handbook of Behavioral Neuroscience* (1st ed., Vol. 26). Elsevier B.V. https://doi.org/10.1016/B978-0-12-815134-1.00003-9

Bonari, L., Pinto, N., Ahn, E., Einarson, A., Steiner, M., & Koren, G. (2004). Perinatal Risks of Untreated Depression During Pregnancy. *Can J Psychiatry*, *49*(11).

Buss, C., Poggi, E., Shahbaba, B., Pruessner, J. C., Head, K., & Sandman, C. A. (2012). *Maternal cortisol over the course of pregnancy and subsequent child amygdala and hippocampus volumes and affective problems*. *109*(20). https://doi.org/10.1073/pnas.1201295109/-/DCSupplemental.www.pnas.org/cgi/doi/10.1073/pnas.1201295109

Cardinale, E. M., Reber, J., O'Connell, K., Turkeltaub, P. E., Tranel, D., Buchanan, T. W., & Marsh, A. A. (2021). Bilateral amygdala damage linked to impaired ability to predict others' fear but preserved moral judgements about causing others fear. *Proceedings. Biological Sciences*, *288*(1943), 20202651. https://doi.org/10.1098/rspb.2020.2651

Cherubini, A., Péran, P., Spoletini, I., Di Paola, M., Di Iulio, F., Hagberg, G. E., Sancesario, G., Gianni, W., Bossù, P., Caltagirone, C., Sabatini, U., & Spalletta, G. (2010). Combined volumetry and DTI in subcortical structures of mild cognitive impairment and Alzheimer's disease patients. *Journal of Alzheimer's Disease*, *19*(4), 1273–1282. https://doi.org/10.3233/JAD-2010-091186

Chung, T. K. H., Lau, T. K., Yip, A. S. K., Chiu, H. F. K., & Lee, D. T. S. (2001). Antepartum depressive symptomatology is associated with adverse obstetric and neonatal outcomes. *Psychosomatic Medicine*, *63*(5), 830–834. https://doi.org/10.1097/00006842-200109000-00017

Cismaru, A. L., Gui, L., Vasung, L., Lejeune, F., Barisnikov, K., Truttmann, A., Borradori Tolsa, C., & Hüppi, P. S. (2016). Altered amygdala development and fear processing in prematurely born infants. *Frontiers in Neuroanatomy*, *10*(MAY). https://doi.org/10.3389/fnana.2016.00055

Clark, K. A., Nuechterlein, K. H., Asarnow, R. F., Hamilton, L. S., Phillips, O. R., Hageman, N. S., Woods, R. P., Alger, J. R., Toga, A. W., & Narr, K. L. (2011). Mean diffusivity and fractional anisotropy as indicators of disease and genetic liability to schizophrenia. *Psychiatr Res*, *23*(1), 1–7. https://doi.org/10.1161/CIRCULATIONAHA.110.956839

Clifton, V. L. (2010). Review: Sex and the Human Placenta: Mediating Differential Strategies of Fetal Growth and Survival. *Placenta*, *31*(SUPPL.), S33–S39. https://doi.org/10.1016/j.placenta.2009.11.010

Coupé, P., Manjón, J. V., Fonov, V., Pruessner, J., Robles, M., & Collins, D. L. (2011). Patch-based segmentation using expert priors: Application to hippocampus and ventricle segmentation. *NeuroImage*, *54*(2), 940–954. https://doi.org/10.1016/j.neuroimage.2010.09.018

Cox, J. L., Holden, J. M., & Sagovsky, R. (1987). Detection of Postnatal Depression: Development of the 10-item Edinburgh Postnatal Depression scale. *British Journal of Psychiatry*, *150*(JUNE), 782–786. https://doi.org/10.1192/bjp.150.6.782

Dai, Y., Shi, F., Wang, L., Wu, G., & Shen, D. (2013). IBEAT: A toolbox for infant brain magnetic resonance image processing. *Neuroinformatics*, *11*(2), 211–225. https://doi.org/10.1007/s12021-012-9164-z

Davalos, D. B., Yadon, C. A., & Tregellas, H. C. (2012). Untreated prenatal maternal depression and the potential risks to offspring: A review. *Archives of Women's Mental Health*, *15*(1), 1–14. https://doi.org/10.1007/s00737-011-0251-1

De Gennaro, L., Cipolli, C., Cherubini, A., Assogna, F., Cacciari, C., Marzano, C., Curcio, G., Ferrara, M., Caltagirone, C., & Spalletta, G. (2011). Amygdala and hippocampus volumetry and diffusivity in relation to dreaming. *Human Brain Mapping*, *32*(9), 1458–1470. https://doi.org/10.1002/hbm.21120

de Graaf-Peters, V. B., & Hadders-Algra, M. (2006). Ontogeny of the human central nervous system: What is happening when? *Early Human Development*, *82*(4), 257–266. https://doi.org/10.1016/j.earlhumdev.2005.10.013

De Macedo Rodrigues, K., Ben-Avi, E., Sliva, D. D., Choe, M. S., Drottar, M., Wang, R., Fischl, B., Grant, P. E., & Zöllei, L. (2015). Afreesurfer-compliantconsistentmanualsegmentationofinfantbrainsspanningthe0–2yearagerange. *Frontiers in Human Neuroscience*, *9*(FEB), 1–12. https://doi.org/10.3389/fnhum.2015.00021

De Macedo Rodrigues, K., Ben-Avi, E., Sliva, D. D., Choe, M. S., Drottar, M., Wang, R., Fischl, B., Grant, P. E., & Zöllei, L. (2015). Afreesurfer-compliantconsistentmanualsegmentationofinfantbrainsspanningthe0–2yearagerange. *Frontiers in Human Neuroscience*, *9*(FEB), 1–12. https://doi.org/10.3389/fnhum.2015.00021

Dean, D. C., Planalp, E. M., Wooten, W., Kecskemeti, S. R., Adluru, N., Schmidt, C. K., Frye, C., Birn, R. M., Burghy, C. A., Schmidt, N. L., Styner, M. A., Short, S. J., Kalin, N. H., Goldsmith, H. H., Alexander, A. L., & Davidson, R. J. (2018). Association of Prenatal Maternal Depression and Anxiety Symptoms with Infant White Matter Microstructure. *JAMA Pediatrics*, *172*(10), 973–981. https://doi.org/10.1001/jamapediatrics.2018.2132

Derntl, B., Habel, U., Windischberger, C., Robinson, S., Kryspin-Exner, I., Gur, R. C., & Moser, E. (2009). General and specific responsiveness of the amygdala during explicit emotion recognition in females and males. *BMC Neuroscience*, *10*, 1–14. https://doi.org/10.1186/1471-2202-10-91

Devi, C. N., Chandrasekharan, A., Sundararaman, S., & Alex, Z. C. (2017). Automatic segmentation of infant brain MR images: With special reference to myelinated white matter. *Biocybernetics and Biomedical Engineering*, *37*(1), 143–158. https://doi.org/10.1016/j.bbe.2016.11.004

Diego, M. A., Field, T., Hernandez-Reif, M., Schanberg, S., Kuhn, C., & Gonzalez-Quintero, V. H. (2009). Prenatal depression restricts fetal growth. *Early Human Development*, *85*(1), 65–70. https://doi.org/10.1016/j.earlhumdev.2008.07.002

Dieleman, N., Koek, H. L., & Hendrikse, J. (2017). Short-term mechanisms influencing volumetric brain dynamics. In *NeuroImage: Clinical* (Vol. 16, pp. 507–513). Elsevier Inc. https://doi.org/10.1016/j.nicl.2017.09.002

Douros, K., Moustaki, M., Tsabouri, S., Papadopoulou, A., Papadopoulos, M., & Priftis, K. N. (2017). Prenatal maternal stress and the risk of asthma in children. *Frontiers in Pediatrics*, *5*(September), 1–9. https://doi.org/10.3389/fped.2017.00202

Dubois, J., Dehaene-Lambertz, G., Perrin, M., Mangin, J. F., Cointepas, Y., Duchesnay, E., Le Bihan, D., & Hertz-Pannier, L. (2008). Asynchrony of the early maturation of white matter bundles in healthy infants: Quantitative landmarks revealed noninvasively by diffusion tensor imaging. *Human Brain Mapping*, *29*(1), 14–27. https://doi.org/10.1002/hbm.20363

Duvernoy, H. M., Cattin, F., Naidich, T. P., Raybaud, C., Risold, P. Y., Salvolini, U., Scarabine, U., York, N., & Springer, : (2005). *The Human Hippocampus: Functional Anatomy, Vascularization and Serial Sections with MRI, 3rd edition* (Vol. 26).

Farroni, T., Johnson, M. H., Menon, E., Zulian, L., Faraguna, D., & Csibra, G. (2005). Newborns' preference for face-relevant stimuli: Effects of contrast polarity. *Proceedings of the National Academy of Sciences of the United States of America*, *102*(47), 17245–17250. https://doi.org/10.1073/pnas.0502205102

Fitzgerald, D. A., Angstadt, M., Jelsone, L. M., Nathan, P. J., & Phan, K. L. (2006). Beyond threat: Amygdala reactivity across multiple expressions of facial affect. *NeuroImage*, *30*(4), 1441–1448. https://doi.org/10.1016/j.neuroimage.2005.11.003

Fitzgerald, E., Hor, K., & Drake, A. J. (2020). Maternal influences on fetal brain development: The role of nutrition, infection and stress, and the potential for intergenerational consequences. *Early Human Development*, *150*, 105190. https://doi.org/https://doi.org/10.1016/j.earlhumdev.2020.105190

Fonov, V., Evans, A. C., Botteron, K., Almli, C. R., McKinstry, R. C., & Collins, D. L. (2011). Unbiased average age-appropriate atlases for pediatric studies. *NeuroImage*, *54*(1), 313–327. https://doi.org/10.1016/j.neuroimage.2010.07.033

Forstmann, B. U., de Hollander, G., van Maanen, L., Alkemade, A., & Keuken, M. C. (2017). Towards a mechanistic understanding of the human subcortex. *Nature Reviews Neuroscience*, *18*(1), 57–65. https://doi.org/10.1038/nrn.2016.163

Framorando, D., Moses, E., Legrand, L., Seeck, M., & Pegna, A. J. (2021). Rapid processing of fearful faces relies on the right amygdala: evidence from individuals undergoing unilateral temporal lobectomy. *Scientific Reports*, *11*(1), 1–9. https://doi.org/10.1038/s41598-020-80054-1

Fricker, M., Tolkovsky, A. M., Borutaite, V., Coleman, M., & Brown, G. C. (2018). Neuronal cell death. *Physiological Reviews*, *98*(2), 813–880. https://doi.org/10.1152/physrev.00011.2017

Garcia-Esteve, L., Ascaso, C., Ojuel, J., & Navarro, P. (2003). Validation of the Edinburgh Postnatal Depression Scale (EPDS) in Spanish mothers. *Journal of Affective Disorders*, *75*(1), 71–76. https://doi.org/10.1016/S0165-0327(02)00020-4

Gerardin, P., Wendland, J., Bodeau, N., Galin, A., Bialobos, S., Tordjman, S., Mazet, P., Darbois, Y., Nizard, J., Dommergues, M., & Cohen, D. (2011). Depression during pregnancy: Is the developmental impact earlier in boys? A prospective case-control study. *Journal of Clinical Psychiatry*, *72*(3), 378–387. https://doi.org/10.4088/JCP.09m05724blu

Giedd, J. N., Blumenthal, J., Jeffries, N., Castellanos, F., Liu, H., Zijdenbos, A., Paus, T., Evans, A., & Rapoport, J. (1999). Brain development during childhood and adolescence: a longitudinal MRI study. In *Nature neuroscience* (Vol. 2, Issue 10, pp. 861–863). https://doi.org/10.1038/13158

Giedd, J. N., Snell, J. W., Lange, N., Rajapakse, J. C., Casey, B. J., Kozuch, P. L., Vaituzis, A. C., Vauss, Y. C., Hamburger, S. D., Kaysen, D., & Rapoport, J. L. (1996). Quantitative magnetic resonance imaging of human brain development: Ages 4-18. *Cerebral Cortex*, *6*(4), 551–560. https://doi.org/10.1093/cercor/6.4.551

Gillespie, N. A., Neale, M. C., Hagler, D. J., Eyler, L. T., Fennema-Notestine, C., Franz, C. E., Lyons, M. J., McEvoy, L. K., Dale, A. M., Panizzon, M. S., & Kremen, W. S. (2017). Genetic and environmental influences on mean diffusivity and volume in subcortical brain regions. *Human Brain Mapping*, *38*(5), 2589–2598. https://doi.org/10.1002/hbm.23544

Gilmore, J. H., Lin, W., Prastawa, M. W., Looney, C. B., Vetsa, Y. S. K., Knickmeyer, R. C., Evans, D. D., Smith, J. K., Hamer, R. M., Lieberman, J. A., & Gerig, G. (2007). Regional gray matter growth, sexual dimorphism, and cerebral asymmetry in the neonatal brain. *Journal of Neuroscience*, *27*(6), 1255–1260. https://doi.org/10.1523/JNEUROSCI.3339-06.2007

Glover, V., O'Connor, T. G., & O'Donnell, K. (2010). Prenatal stress and the programming of the HPA axis. *Neuroscience and Biobehavioral Reviews*, *35*(1), 17–22. https://doi.org/10.1016/j.neubiorev.2009.11.008

Gousias, I. S., Edwards, A. D., Rutherford, M. A., Counsell, S. J., Hajnal, J. V., Rueckert, D., & Hammers, A. (2012). Magnetic resonance imaging of the newborn brain: Manual segmentation of labelled atlases in term-born and preterm infants. *NeuroImage*, *62*(3), 1499–1509. https://doi.org/10.1016/j.neuroimage.2012.05.083

Gousias, I. S., Edwards, A. D., Rutherford, M. A., Counsell, S. J., Hajnal, J. V., Rueckert, D., & Hammers, A. (2012). Magnetic resonance imaging of the newborn brain: Manual segmentation of labelled atlases in term-born and preterm infants. *NeuroImage*, *62*(3), 1499–1509. https://doi.org/10.1016/j.neuroimage.2012.05.083

Govaert, P., Triulzi, F., & Dudink, J. (2020). The developing brain by trimester. In *Handbook of Clinical Neurology* (1st ed., Vol. 171). Elsevier B.V. https://doi.org/10.1016/B978-0-444-64239-4.00014-X

Gupta, D. (2017). *Chapter 1 - Neuroanatomy* (H. B. T.-E. of N. Prabhakar, Ed.; pp. 3–40). Academic Press. https://doi.org/https://doi.org/10.1016/B978-0-12-805299-0.00001-4

Gupta, D. (2017). *Chapter 1 - Neuroanatomy* (H. B. T.-E. of N. Prabhakar, Ed.; pp. 3–40). Academic Press. https://doi.org/https://doi.org/10.1016/B978-0-12-805299-0.00001-4

Gur, R. C., Turetsky, B. I., Matsui, M., Yan, M., Bilker, W., Hughett, P., & Gur, R. E. (1999). Sex Differences in Brain Gray and White Matter in Healthy Young Adults: Correlations with Cognitive Performance. *The Journal of Neuroscience*, *19*(10), 4065 LP – 4072. https://doi.org/10.1523/JNEUROSCI.19-10-04065.1999

Hall, J. A., & Matsumoto, D. (2004). Gender Differences in Judgments of Multiple Emotions From Facial Expressions. In *Emotion* (Vol. 4, Issue 2, pp. 201–206). American Psychological Association. https://doi.org/10.1037/1528-3542.4.2.201

Hamann, S. (2005). Sex differences in the responses of the human amygdala. *Neuroscientist*, *11*(4), 288–293. https://doi.org/10.1177/1073858404271981

Hardee, J. E., Thompson, J. C., & Puce, A. (2008). The left amygdala knows fear: laterality in the amygdala response to fearful eyes. *Social Cognitive and Affective Neuroscience*, *3*(1), 47–54. https://doi.org/10.1093/scan/nsn001

Hariri, A. R., Bookheimer, S. Y., & Mazziotta, J. C. (2000). Modulating emotional responses: effects of a neocortical network on the limbic system. *Neuroreport*, *11*(1), 43. https://doi.org/0.1097/00001756-200001170-00009

Hasegawa, M., Houdou, S., Mito, T., Takashima, S., Asanuma, K., & Ohno, T. (1992). Development of myelination in the human fetal and infant cerebrum: A myelin basic protein immunohistochemical study. *Brain and Development*, *14*(1), 1–6. https://doi.org/10.1016/S0387-7604(12)80271-3

Hay, R. E., Letourneau, N., Dewey, D., & Lebel, C. (2019). Examining the relationship between prenatal depression, amygdala-prefrontal structural connectivity and behaviour in preschool children. *BioRxiv*, *403*.

Hering-Hanit, R., Achiron, R., Lipitz, S., & Achiron, A. (2001). Asymmetry of fetal cerebral hemispheres: in utero ultrasound study. *Archives of Disease in Childhood. Fetal and Neonatal Edition*, *85*(3), F194-6. https://doi.org/10.1136/fn.85.3.f194

Hochberg, Z., & Konner, M. (2020). Emerging Adulthood, a Pre-adult Life-History Stage. *Frontiers in Endocrinology*, *10*(January), 1–12. https://doi.org/10.3389/fendo.2019.00918

Huang, H., Zhang, J., Wakana, S., Zhang, W., Ren, T., Richards, L. J., Yarowsky, P., Donohue, P., Graham, E., van Zijl, P. C. M., & Mori, S. (2006). White and gray matter development in human fetal, newborn and pediatric brains. *NeuroImage*, *33*(1), 27–38. https://doi.org/10.1016/j.neuroimage.2006.06.009

Humphrey, T. (1968). The development of the human amygdala during early embryonic life,. *Journal of Comparative Neurology*, *132*(1), 135–165. https://doi.org/10.1002/cne.901320108

Jenkinson, M., Beckmann, C. F., Behrens, T. E. J., Woolrich, M. W., & Smith, S. M. (2012). Fsl. *NeuroImage*, *62*(2), 782–790. https://doi.org/10.1016/j.neuroimage.2011.09.015

Jenkinson, M., Beckmann, C. F., Behrens, T. E. J., Woolrich, M. W., & Smith, S. M. (2012). Fsl. *NeuroImage*, *62*(2), 782–790. https://doi.org/10.1016/j.neuroimage.2011.09.015

Jernigan, T. L., Baaré, W. F. C., Stiles, J., & Madsen, K. S. (2011). Chapter 5 - Postnatal brain development: Structural imaging of dynamic neurodevelopmental processes. In O. Braddick, J. Atkinson, & G. M. B. T.-P. in B. R. Innocenti (Eds.), *Gene Expression to Neurobiology and Behavior: Human Brain Development and Developmental Disorders* (Vol. 189, pp. 77–92). Elsevier. https://doi.org/https://doi.org/10.1016/B978-0-444-53884-0.00019-1

Jeurissen, B., Leemans, A., Tournier, J. D., Jones, D. K., & Sijbers, J. (2013). Investigating the prevalence of complex fiber configurations in white matter tissue with diffusion magnetic resonance imaging. *Human Brain Mapping*, *34*(11), 2747–2766. https://doi.org/10.1002/hbm.22099

Joffe, T. H., Tarantal, A. F., Rice, K., Leland, M., Oerke, A. K., Rodeck, C., Geary, M., Hindmarsh, P., Wells, J. C. K., & Aiello, L. C. (2005). Fetal and infant head circumference sexual dimorphism in primates. *American Journal of Physical Anthropology*, *126*(1), 97–110. https://doi.org/10.1002/ajpa.20035

Johnson, M. H., Dziurawiec, S., Ellis, H., & Morton, J. (1991). Newborns' preferential tracking of face-like stimuli and its subsequent decline. *Cognition*, *40*(1–2), 1–19. https://doi.org/10.1016/0010-0277(91)90045-6

Juranek, J., Johnson, C. P., Prasad, M. R., Kramer, L. A., Saunders, A., Filipek, P. A., Swank, P. R., Cox, C. S., & Ewing-Cobbs, L. (2012). Mean diffusivity in the amygdala correlates with anxiety in pediatric TBI. *Brain Imaging Behav*, *6*(1), 36–48. https://doi.org/10.1007/s11682-011-9140-5

Kantarci, K., Petersen, R. C., Boeve, B. F., Knopman, D. S., Weigand, S. D., O'Brien, P. C., Shiung, M. M., Smith, G. E., Ivnik, R. J., Tangalos, E. G., & Jack, C. R. (2005). DWI predicts future progression to Alzheimer disease in amnestic mild cognitive impairment. *Neurology*, *64*(5), 902–904. https://doi.org/10.1212/01.WNL.0000153076.46126.E9

Karlsson, L., Tolvanen, M., Scheinin, N. M., Uusitupa, H. M., Korja, R., Ekholm, E., Tuulari, J. J., Pajulo, M., Huotilainen, M., Paunio, T., & Karlsson, H. (2018). Cohort Profile: The FinnBrain Birth Cohort Study (FinnBrain). *International Journal of Epidemiology*, *47*(1), 15–16j. https://doi.org/10.1093/ije/dyx173

Killgore, W. D. S., Oki, M., & Yurgelun-Todd, D. A. (2001). Sex-specific developmental changes in amygdala responses to affective faces. *NeuroReport*, *12*(2), 427–433. https://doi.org/10.1097/00001756-200102120-00047

Kinney, D. K., Munir, K. M., Crowley, D. J., & Miller, A. M. (2008). Prenatal stress and risk for autism. *Neuroscience and Biobehavioral Reviews*, *32*(8), 1519–1532. https://doi.org/10.1016/j.neubiorev.2008.06.004

Kivilevitch, Z., Achiron, R., & Zalel, Y. (2010). Fetal brain asymmetry: in utero sonographic study of normal fetuses. *American Journal of Obstetrics and Gynecology*, *202*(4), 359.e1-359.e8. https://doi.org/10.1016/j.ajog.2009.11.001

Klawiter, E. C., Schmidt, R. E., Trinkaus, K., Liang, H. F., Budde, M. D., Naismith, R. T., Song, S. K., Cross, A. H., & Benzinger, T. L. (2011). Radial diffusivity predicts demyelination in ex vivo multiple sclerosis spinal cords. *NeuroImage*, *55*(4), 1454–1460. https://doi.org/10.1016/j.neuroimage.2011.01.007

Ko, J. Y., Farr, S. L., Dietz, P. M., & Robbins, C. L. (2012). Depression and treatment among U.S. pregnant and nonpregnant women of reproductive age, 2005-2009. *Journal of Women's Health (2002)*, *21*(8), 830–836. https://doi.org/10.1089/jwh.2011.3466

Konrad, C., Ukas, T., Nebel, C., Arolt, V., Toga, A. W., & Narr, K. L. (2009). Defining the human hippocampus in cerebral magnetic resonance images-An overview of current segmentation protocols. In *NeuroImage* (Vol. 47, Issue 4, pp. 1185–1195). https://doi.org/10.1016/j.neuroimage.2009.05.019

Konrad, K., Firk, C., & Uhlhaas, P. J. (2013). Brain development during adolescence. *Deutsches Arzteblatt International*, *110*(25), 425–431. https://doi.org/10.3238/arztebl.2013.0425

Koo, T. K., & Li, M. Y. (2016). A Guideline of Selecting and Reporting Intraclass Correlation Coefficients for Reliability Research. *Journal of Chiropractic Medicine*, *15*(2), 155–163. https://doi.org/10.1016/j.jcm.2016.02.012

Kouwenhoven, E., Giezen, M., & Struikmans, H. (2009). Measuring the similarity of target volume delineations independent of the number of observers. *Physics in Medicine and Biology*, *54*(9), 2863–2873. https://doi.org/10.1088/0031-9155/54/9/018

Kret, M. E., Pichon, S., Grèzes, J., & de Gelder, B. (2011). Men fear other men most: Gender specific brain activations in perceiving threat from dynamic faces and bodies-an fMRI study. *Frontiers in Psychology*, *2*(JAN), 1–11. https://doi.org/10.3389/fpsyg.2011.00003

Lebel, C., Caverhill-Godkewitsch, S., & Beaulieu, C. (2010). Age-related regional variations of the corpus callosum identified by diffusion tensor tractography. *NeuroImage*, *52*(1), 20–31. https://doi.org/10.1016/j.neuroimage.2010.03.072

Lehtola, S., Tuulari, J., Karlsson, L., Parkkola, R., Merisaari, H., Saunavaara, J., Lähdesmäki, T., Scheinin, N., & Karlsson, H. (2019). Associations of age and sex with brain volumes and asymmetry in 2–5-week-old infants. *Brain Structure and Function*, *224*(1), 501–513. https://doi.org/10.1007/s00429-018-1787-x

Leibovitz, Z., Lerman-Sagie, T., & Haddad, L. (2022). Fetal Brain Development: Regulating Processes and Related Malformations. *Life*, *12*(6). https://doi.org/10.3390/life12060809

Lewis, J. D., Fonov, V. S., Collins, D. L., Evans, A. C., & Tohka, J. (2019). Cortical and subcortical T1 white/gray contrast, chronological age, and cognitive performance. *NeuroImage*, *196*(April), 276–288. https://doi.org/10.1016/j.neuroimage.2019.04.022

Libertus, K., Landa, R. J., & Haworth, J. L. (2017). Development of attention to faces during the first 3 years: Influences of stimulus type. *Frontiers in Psychology*, *8*(NOV), 1–10. https://doi.org/10.3389/fpsyg.2017.01976

Liddell, B. J., Brown, K. J., Kemp, A. H., Barton, M. J., Das, P., Peduto, A., Gordon, E., & Williams, L. M. (2005). A direct brainstem-amygdala-cortical "alarm" system for subliminal signals of fear. *NeuroImage*, *24*(1), 235–243. https://doi.org/10.1016/j.neuroimage.2004.08.016

Liu, T., Gao, F., Zheng, W., You, Y., Zhao, Z., Lv, Y., Chen, W., Zhang, H., Ji, C., & Wu, D. (2021). Diffusion MRI of the infant brain reveals unique asymmetry patterns during the first-half-year of development. *NeuroImage*, *242*(August), 118465. https://doi.org/10.1016/j.neuroimage.2021.118465

Lombardo, M. V., Ashwin, E., Auyeung, B., Chakrabarti, B., Taylor, K., Hackett, G., Bullmore, E. T., & Baron-Cohen, S. (2012). Fetal testosterone influences sexually dimorphic gray matter in the human brain. *Journal of Neuroscience*, *32*(2), 674–680. https://doi.org/10.1523/JNEUROSCI.4389-11.2012

Loomans, E. M., Van Dijk, A. E., Vrijkotte, T. G. M., Van Eijsden, M., Stronks, K., Gemke, R. J. B. J., & Van Den Bergh, B. R. H. (2013). Psychosocial stress during pregnancy is related to adverse birth outcomes: Results from a large multi-ethnic community-based birth cohort. *European Journal of Public Health*, *23*(3), 485–491. https://doi.org/10.1093/eurpub/cks097

Lupien, S. J., McEwen, B. S., Gunnar, M. R., & Heim, C. (2009). Effects of stress throughout the lifespan on the brain, behaviour and cognition. *Nature Reviews Neuroscience*, *10*(6), 434–445. https://doi.org/10.1038/nrn2639

Magyar, D. M., Fridshal, D., Elsner, C. W., Glatz, T., Eliot, J., Klein, A. H., Lowe, K. C., Buster, J. E., & Nathanielsz, P. W. (1980). Time-trend analysis of plasma cortisol concentrations in the fetal sheep in relation to parturition. *Endocrinology*, *107*(1), 155–159. https://doi.org/10.1210/endo-107-1-155

Marecková, K., Klasnja, A., Bencurova, P., Andrýsková, L., Brázdil, M., & Paus, T. (2019). Prenatal Stress, Mood, and Gray Matter Volume in Young Adulthood. *Cerebral Cortex (New York, N.Y. : 1991)*, *29*(3), 1244–1250. https://doi.org/10.1093/cercor/bhy030

Marschner, A., Kalisch, R., Vervliet, B., Vansteenwegen, D., & Büchel, C. (2008). Dissociable Roles for the Hippocampus and the Amygdala in Human Cued versus Context Fear Conditioning. *The Journal of Neuroscience*, *28*(36), 9030 LP – 9036. https://doi.org/10.1523/JNEUROSCI.1651-08.2008

Maselko, J., Sikander, S., Bhalotra, S., Bangash, O., Ganga, N., Mukherjee, S., Egger, H., Franz, L., Bibi, A., Liaqat, R., Kanwal, M., Abbasi, T., Noor, M., Ameen, N., & Rahman, A. (2015). Effect of an early perinatal depression intervention on long-term child development outcomes: Follow-up of the Thinking Healthy Programme randomised controlled trial. *The Lancet Psychiatry*, *2*(7), 609–617. https://doi.org/10.1016/S2215-0366(15)00109-1

Matsuzawa, J., Matsui, M., & Konishi, T. (2001). brain volume changes infancy and childhood. *Cereb Cortex*, *11*(4), 335–342.

Merisaari, H., Tuulari, J. J., Karlsson, L., Scheinin, N. M., Parkkola, R., Saunavaara, J., Lähdesmäki, T., Lehtola, S. J., Keskinen, M., Lewis, J. D., Evans, A. C., & Karlsson, H. (2019). Test-retest reliability of Diffusion Tensor Imaging metrics in neonates. *NeuroImage*, *197*, 598–607. https://doi.org/10.1016/j.neuroimage.2019.04.067

Morey, R. A., Petty, C. M., Xu, Y., Pannu, J., Wagner, H. R., Lewis, D. V, Labar, K. S., Styner, M., & Mccarthy, G. (2009). NeuroImage A comparison of automated segmentation and manual tracing for quantifying hippocampal and amygdala volumes. *NeuroImage*, *45*(3), 855–866. https://doi.org/10.1016/j.neuroimage.2008.12.033

Morey, R. A., Petty, C. M., Xu, Y., Pannu, J., Wagner, H. R., Lewis, D. V, Labar, K. S., Styner, M., & Mccarthy, G. (2009). NeuroImage A comparison of automated segmentation and manual tracing for quantifying hippocampal and amygdala volumes. *NeuroImage*, *45*(3), 855–866. https://doi.org/10.1016/j.neuroimage.2008.12.033

Morris, J. S., Frith, C. D., Perrett, D. I., Rowland, D., Young, A. W., Calder, A. J., & Dolan, R. J. (1996). Differential response of amygdala to fearful and happy facial expressions. In *Nature* (Vol. 383, pp. 812–815).

Morris, J. S., Öhman, A., & Dolan, R. J. (1999). A subcortical pathway to the right amygdala mediating "unseen" fear. *Proceedings of the National Academy of Sciences of the United States of America*, *96*(4), 1680–1685. https://doi.org/10.1073/pnas.96.4.1680

Morrow, J., Mosher, C., & Gothard, K. (2019). Multisensory neurons in the primate amygdala. *Journal of Neuroscience*, *39*(19), 3663–3675. https://doi.org/10.1523/JNEUROSCI.2903-18.2019

Mortamet, B., Zeng, D., Gerig, G., Prastawa, M., & Bullitt, E. (2005). Effects of Healthy Aging Measured By Intracranial Compartment Volumes Using a Designed MR Brain Database Bénédicte. *Med Image Comput Comput Assist Interv*, *8*(Pt 1), 383. https://doi.org/10.1007/11566465_48. PMID: 16685869; PMCID: PMC2430269

Moura, L. M., Kempton, M., Barker, G., Salum, G., Gadelha, A., Pan, P. M., Hoexter, M., Del Aquilla, M. A. G., Picon, F. A., Anés, M., Otaduy, M. C. G., Amaro, E., Rohde, L. A., McGuire, P., Bressan, R. A., Sato, J. R., & Jackowski, A. P. (2016). Age-effects in white matter using associated diffusion tensor imaging and magnetization transfer ratio during late childhood and early adolescence. *Magnetic Resonance Imaging*, *34*(4), 529–534. https://doi.org/10.1016/j.mri.2015.12.021

Müller, F., & O'Rahilly, R. (2006). The amygdaloid complex and the medial and lateral ventricular eminences in staged human embryos. *Journal of Anatomy*, *208*(5), 547–564. https://doi.org/10.1111/j.1469-7580.2006.00553.x

Munakata, S., Okada, T., Okahashi, A., Yoshikawa, K., Usukura, Y., Makimoto, M., Hosono, S., Takahashi, S., Mugishima, H., & Okuhata, Y. (2013). Gray matter volumetric MRI differences late-preterm and term infants. *Brain and Development*, *35*(1), 10–16. https://doi.org/10.1016/j.braindev.2011.12.011

Murphy, G. J., Inger, P., Mark, K., Lin, J., Morrice, W., Gee, C., Gan, S., & Korp, B. (1987). Volumetric asymmetry in the human amygdaloid complex. *Journal Fur Hirnforschung*, *28*(3), 281–289.

Murphy, V. E., & Clifton, V. L. (2003). Alterations in human placental 11β=hydroxysteroid dehydrogenase type 1 and 2 with gestational age and labour. *Placenta*, *24*(7), 739–744. https://doi.org/10.1016/S0143-4004(03)00103-6

Nazzari, S., Fearon, P., Rice, F., Dottori, N., Ciceri, F., Molteni, M., & Frigerio, A. (2019). Beyond the HPA-axis: Exploring maternal prenatal influences on birth outcomes and stress reactivity. *Psychoneuroendocrinology*, *101*(April 2018), 253–262. https://doi.org/10.1016/j.psyneuen.2018.11.018

Nelson, C. A., & Dolgin, K. G. (1985). The generalized discrimination of facial expressions by seven-month-old infants. *Child Development*, *56*(1), 58–61. https://doi.org/10.1111/j.1467-8624.1985.tb00085.x

Oguz, I., Farzinfar, M., Matsui, J., Budin, F., Liu, Z., Gerig, G., Johnson, H. J., & Styner, M. (2014). DTIPrep: quality control of diffusion-weighted images. *Frontiers in Neuroinformatics*, *8*(January), 1–11. https://doi.org/10.3389/fninf.2014.00004

O'Rahilly, R., & Muller, F. (2006). The Embryonic Human Brain. *JohnWiley&Sons:Hoboken,NJ,USA*, *pp*, 31–38.

Paus, T., Collins, D. L., Evans, A. C., Leonard, G., Pike, B., & Zijdenbos, A. (2001). Maturation of white matter in the human brain: A review of magnetic resonance studies. *Brain Research Bulletin*, *54*(3), 255–266. https://doi.org/10.1016/S0361-9230(00)00434-2

Pedraza, O., Bowers, D., & Gilmore, R. (2004). Asymmetry of the hippocampus and amygdala in MRI volumetric measurements of normal adults. *Journal of the International Neuropsychological Society*, *10*(5), 664–678. https://doi.org/10.1017/S1355617704105080

Peltola, M. J., Hietanen, J. K., Forssman, L., & Leppänen, J. M. (2013). The emergence and stability of the attentional bias to fearful faces in infancy. *Infancy*, *18*(6), 905–926. https://doi.org/10.1111/infa.12013

Peltola, M. J., Leppänen, J. M., Mäki, S., & Hietanen, J. K. (2009). Emergence of enhanced attention to fearful faces between 5 and 7 months of age. *Social Cognitive and Affective Neuroscience*, *4*(2), 134–142. https://doi.org/10.1093/scan/nsn046

Peltola, M. J., Leppänen, J. M., Palokangas, T., & Hietanen, J. K. (2008). Fearful faces modulate looking duration and attention disengagement in 7-month-old infants. *Developmental Science*, *11*(1), 60–68. https://doi.org/10.1111/j.1467-7687.2007.00659.x

Phan, K. L., Wager, T., Taylor, S. F., & Liberzon, I. (2002). Functional neuroanatomy of emotion: a meta-analysis of emotion activation studies in PET and fMRI. *NeuroImage*, *16*(2), 331–348. https://doi.org/10.1006/nimg.2002.1087

Pohl, K. M., Sullivan, E. V., Rohlfing, T., Chu, W., Kwon, D., Nichols, B. N., Zhang, Y., Brown, S. A., Tapert, S. F., Cummins, K., Thompson, W. K., Brumback, T., Colrain, I. M., Baker, F. C., Prouty, D., De Bellis, M. D., Voyvodic, J. T., Clark, D. B., Schirda, C., … Pfefferbaum, A. (2016). Harmonizing DTI measurements across scanners to examine the development of white matter microstructure in 803 adolescents of the NCANDA study. *NeuroImage*, *130*, 194–213. https://doi.org/10.1016/j.neuroimage.2016.01.061

Prado, E. L., & Dewey, K. G. (2014). Nutrition and brain development in early life. *Nutrition Reviews*, *72*(4), 267–284. https://doi.org/10.1111/nure.12102

Pruessner, J. C., Li, L. M., Serles, W., Pruessner, M., Collins, D. L., Kabani, N., Lupien, S., & Evans, A. C. (2000). Volumetry of hippocampus and amygdala with high-resolution MRI and three-dimensional analysis software: Minimizing the discrepancies between laboratories. *Cerebral Cortex*, *10*(4), 433–442. https://doi.org/10.1093/cercor/10.4.433

Prunty, J. E., Jackson, K. C., Keemink, J. R., & Kelly, D. J. (2020). Caucasian infants' attentional orienting to own- and other-race faces. *Brain Sciences*, *10*(1). https://doi.org/10.3390/brainsci10010053

Qiu, A., Anh, T. T., Li, Y., Chen, H., Rifkin-Graboi, A., Broekman, B. F. P., Kwek, K., Saw, S. M., Chong, Y. S., Gluckman, P. D., Fortier, M. V., & Meaney, M. J. (2015). Prenatal maternal depression alters amygdala functional connectivity in 6-month-old infants. *Translational Psychiatry*, *5*(2). https://doi.org/10.1038/tp.2015.3

Rakers, F., Rupprecht, S., Dreiling, M., Bergmeier, C., Witte, O. W., & Schwab, M. (2016). Transfer of maternal psychosocial stress to the fetus. *Neuroscience and Biobehavioral Reviews*. https://doi.org/10.1016/j.neubiorev.2017.02.019

Ramasubbu, R., Konduru, N., Cortese, F., Bray, S., Gaxiola-Valdez, I., & Goodyear, B. (2014). Reduced intrinsic connectivity of amygdala in adults with major depressive disorder. *Frontiers in Psychiatry*, *5*(FEB), 1–11. https://doi.org/10.3389/fpsyt.2014.00017

Raz, N., Gunning-Dixon, F., Head, D., Rodrigue, K. M., Williamson, A., & Acker, J. D. (2004). Aging, sexual dimorphism, and hemispheric asymmetry of the cerebral cortex: replicability of regional differences in volume. *Neurobiology of Aging*, *25*(3), 377–396. https://doi.org/10.1016/S0197-4580(03)00118-0

Ressler, K. J. (2010). Amygdala Activity, Fear, and Anxiety: Modulation by Stress. *Biol Psychiatry*, *67*(12), 1117–1119. https://doi.org/10.1016/j.biopsych.2010.04.027.Amygdala

Reynolds, G. D., & Roth, K. C. (2018). The development of attentional biases for faces in infancy: A developmental systems perspective. *Frontiers in Psychology*, *9*(FEB), 1–16. https://doi.org/10.3389/fpsyg.2018.00222

Rifkin-Graboi, A., Bai, J., Chen, H., Hameed, W. B. R., Sim, L. W., Tint, M. T., Leutscher-Broekman, B., Chong, Y. S., Gluckman, P. D., Fortier, M. V., Meaney, M. J., & Qiu, A. (2013). Prenatal maternal depression associates with microstructure of right amygdala in neonates at birth. *Biological Psychiatry*, *74*(11), 837–844. https://doi.org/10.1016/j.biopsych.2013.06.019

Roalf, D. R., Quarmley, M., Elliott, M. A., Satterthwaite, T. D., Vandekar, S. N., Ruparel, K., Gennatas, E. D., Calkins, M. E., Moore, T. M., Hopson, R., Prabhakaran, K., Jackson, C. T., Verma, R., Hakonarson, H., Gur, R. C., & Gur, R. E. (2016). The impact of quality assurance assessment on diffusion tensor imaging outcomes in a large-scale population-based cohort. *NeuroImage*, *125*, 903–919. https://doi.org/10.1016/j.neuroimage.2015.10.068

Roddy, D., Kelly, J. R., Farrell, C., Doolin, K., Roman, E., Nasa, A., Frodl, T., Harkin, A., O'Mara, S., O'Hanlon, E., & O'Keane, V. (2021). Amygdala substructure volumes in Major Depressive Disorder. *NeuroImage: Clinical*, *31*(July). https://doi.org/10.1016/j.nicl.2021.102781

Ronald, A., Pennell, C. E., & Whitehouse, A. J. O. (2011). Prenatal maternal stress associated with ADHD and autistic traits in early childhood. *Frontiers in Psychology*, *1*(JAN), 1–8. https://doi.org/10.3389/fpsyg.2010.00223

Rosenbloom, M. J., & Pfefferbaum, A. (2008). Magnetic resonance imaging of the living brain: evidence for brain degeneration among alcoholics and recovery with abstinence. *Alcohol Res Health*, 362–376.

Ruiz, N. A. L., Del Ángel, D. S., Olguín, H. J., & Silva, M. L. (2018). Neuroprogression: The hidden mechanism of depression. *Neuropsychiatric Disease and Treatment*, *14*, 2837–2845. https://doi.org/10.2147/NDT.S177973

Saghir, Z., Syeda, J. N., Muhammad, A. S., & Balla Abdalla, T. H. (2018). The Amygdala, Sleep Debt, Sleep Deprivation, and the Emotion of Anger: A Possible Connection? *Cureus*, *10*(7), 10–14. https://doi.org/10.7759/cureus.2912

Salat, D. H. (2013). Diffusion Tensor Imaging in the Study of Aging and Age-Associated Neural Disease. In *Diffusion MRI: From Quantitative Measurement to In vivo Neuroanatomy: Second Edition* (Second Edi). Elsevier. https://doi.org/10.1016/B978-0-12-396460-1.00012-3

Salo, R. A., Belevich, I., Manninen, E., Jokitalo, E., Gröhn, O., & Sierra, A. (2018). Quantification of anisotropy and orientation in 3D electron microscopy and diffusion tensor imaging in injured rat brain. *NeuroImage*, *172*(January), 404–414. https://doi.org/10.1016/j.neuroimage.2018.01.087

Sandman, C. A., WADHWA, P. D., DUNKEL-SCHETTER, C., CHICZ-DeMET, A., BELMAN, J., PORTO, M., MURATA, Y., GARITE, T. J., & CRINELLA, F. M. (1994). Psychobiological Influences of Stress and HPA Regulation on the Human Fetus and Infant Birth Outcomes. *Annals of the New York Academy of Sciences*, *739*(1), 198–210. https://doi.org/10.1111/j.1749-6632.1994.tb19822.x

Saxena, S., & Caroni, P. (2007). Mechanisms of axon degeneration: From development to disease. *Progress in Neurobiology*, *83*(3), 174–191. https://doi.org/10.1016/j.pneurobio.2007.07.007

Schoemaker, D., Buss, C., Head, K., Sandman, C. A., Davis, E. P., Chakravarty, M. M., Gauthier, S., & Pruessner, J. C. (2016). Corrigendum to "Hippocampus and amygdala volumes from magnetic resonance images in children: Assessing accuracy of FreeSurfer and FSL against manual segmentation"[NeuroImage 129 (2016) 1–14] (S1053811916000537) (10.1016/j.neuroimage.2016.01.038)). *NeuroImage*, *173*, 1–2. https://doi.org/10.1016/j.neuroimage.2018.02.009

Shrout, P. E., & Fleiss, J. L. (1979). *Intraclass Correlations : Uses in Assessing Rater Reliability*. *86*(2), 420–428.

Sidebottom, A., Vacquier, M., Larusso, E., Erickson, D., & Hardeman, R. (2020). *Perinatal depression screening practices in a large health system : identifying current state and assessing opportunities to provide more equitable care*.

Singh, R., & Munakomi, S. (2023). *Embryology, Neural Tube*. In: StatPearls [Internet]. Treasure Island (FL): StatPearls Publishing.

Smith, S. M. (2002). Fast robust automated brain extraction. *Human Brain Mapping*, *17*(3), 143–155. https://doi.org/10.1002/hbm.10062

Smith, S. M., & Wylie, V. W. (2006). The role of the hypothalamic-pituitary-adrenal axis in neuroendocrine responses to stress. *Dialogues in Clinical Neuroscience*, *8*(4), 383–395. https://doi.org/10.31887/dcns.2006.8.4/ssmith

Stebbins, G. T. (2010). Diffusion Tensor Imaging in Parkinson's Disease. *Encyclopedia of Movement Disorders*, *109*, 308–310. https://doi.org/10.1016/B978-0-12-374105-9.00020-4

Stiles, J., & Jernigan, T. L. (2010). The basics of brain development. *Neuropsychology Review*, *20*(4), 327–348. https://doi.org/10.1007/s11065-010-9148-4

Stowe, Z. N., & Nemeroff, C. B. (1995). Women at risk for postpartum-onset major depression. *American Journal of Obstetrics and Gynecology*, *173*(2), 639–645. https://doi.org/10.1016/0002-9378(95)90296-1

Sun, T., & Walsh, C. A. (2006). Molecular approaches to brain asymmetry and handedness. *Nature Reviews Neuroscience*, *7*(8), 655–662. https://doi.org/10.1038/nrn1930

Susser, L. C., Sansone, S. A., & Hermann, A. D. (2016). Selective serotonin reuptake inhibitors for depression in pregnancy. *American Journal of Obstetrics and Gynecology*, *215*(6), 722–730. https://doi.org/10.1016/j.ajog.2016.07.011

Tae, W. S., Ham, B. J., Pyun, S. B., Kang, S. H., & Kim, B. J. (2018). Current Clinical Applications of Diffusion-Tensor Imaging in Neurological Disorders. *Journal of Clinical Neurology (Seoul, Korea)*, *14*(2), 129–140. https://doi.org/10.3988/jcn.2018.14.2.129

Takeuchi, H., Taki, Y., Hashizume, H., Asano, K., Asano, M., Sassa, Y., Yokota, S., Kotozaki, Y., Nouchi, R., & Kawashima, R. (2016). Impact of videogame play on the brain's microstructural properties: Cross-sectional and longitudinal analyses. *Molecular Psychiatry*, *21*(12), 1781–1789. https://doi.org/10.1038/mp.2015.193

Takeuchi, H., Taki, Y., Nouchi, R., Yokoyama, R., Kotozaki, Y., Nakagawa, S., Sekiguchi, A., Iizuka, K., Yamamoto, Y., Hanawa, S., Araki, T., Miyauchi, C. M., Sakaki, K., Sassa, Y., Nozawa, T., Ikeda, S., Yokota, S., Daniele, M., & Kawashima, R. (2019). Empathizing associates with mean diffusivity. *Scientific Reports*, *9*(1), 1–13. https://doi.org/10.1038/s41598-019-45106-1

Taki, Y., Thyreau, B., Hashizume, H., Sassa, Y., Takeuchi, H., Wu, K., Kotozaki, Y., Nouchi, R., Asano, M., Asano, K., Fukuda, H., & Kawashima, R. (2013). Linear and curvilinear correlations of brain white matter volume, fractional anisotropy, and mean diffusivity with age using voxel-based and region-of-interest analyses in 246 healthy children. *Human Brain Mapping*, *34*(8), 1842–1856. https://doi.org/10.1002/hbm.22027

Tamnes, C. K., Østby, Y., Fjell, A. M., Westlye, T., Due-tønnessen, P., & Walhovd, K. B. (2010). *Brain Maturation in Adolescence and Young Adulthood : Regional Age-Related Changes in Cortical Thickness and White Matter Volume and Microstructure*. *i*(March). https://doi.org/10.1093/cercor/bhp118

Tanaka, C., Matsui, M., Uematsu, A., Noguchi, K., & Miyawaki, T. (2013). Developmental trajectories of the fronto-temporal lobes from infancy to early adulthood in healthy individuals. *Developmental Neuroscience*, *34*(6), 477–487. https://doi.org/10.1159/000345152

Tao, J., Wang, X., Zhong, Z., Han, H., Liu, S., Wen, S., Guan, N., & Li, L. (2017). Alterations of white matter fractional anisotropy in unmedicated obsessive-compulsive disorder. *Neuropsychiatric Disease and Treatment*, *13*, 69–76. https://doi.org/10.2147/NDT.S123669

Tax, C. M. W., Genc, S., MacIver, C. L., Nilsson, M., Wardle, M., Szczepankiewicz, F., Jones, D. K., & Peall, K. J. (2023). Ultra-strong diffusion-weighted MRI reveals cerebellar grey matter abnormalities in movement disorders. *NeuroImage: Clinical*, *38*. https://doi.org/10.1016/j.nicl.2023.103419

Thomason, M. E. (2020). Development of Brain Networks In Utero: Relevance for Common Neural Disorders. *Biol Psychiatry*, *88*(1), 40–50. https://doi.org/10.1016/j.biopsych.2020.02.007

Thukral, B. B. (2015). Problems and preferences in pediatric imaging. *Indian Journal of Radiology and Imaging*, *25*(4), 359–364. https://doi.org/10.4103/0971-3026.169466

Thukral, B. B. (2015). Problems and preferences in pediatric imaging. *Indian Journal of Radiology and Imaging*, *25*(4), 359–364. https://doi.org/10.4103/0971-3026.169466

Tierney, A. L., & Nelson, C. A. (2009). Brain Development and the Role of Experience in the Early Years. *Zero Three*, *30*(2), 9–13.

Tuulari, J. J., Kataja, E. L., Leppänen, J. M., Lewis, J. D., Nolvi, S., Häikiö, T., Lehtola, S. J., Hashempour, N., Saunavaara, J., Scheinin, N. M., Korja, R., Karlsson, L., & Karlsson, H. (2020). Newborn left amygdala volume associates with attention disengagement from fearful faces at eight months. *Developmental Cognitive Neuroscience*, *45*. https://doi.org/10.1016/j.dcn.2020.100839

Tuulari, J. J., Rosberg, A., Pulli, E. P., Hashempour, N., Ukharova, E., Lidauer, K., Jolly, A., Luotonen, S., Audah, H. K., Vartiainen, E., Bano, W., Suuronen, I., Wigley, I. L. C. M., Fonov, V. S., Collins, D. L., Merisaari, H., Karlsson, L., Karlsson, H., & Lewis, J. D. (2024). The FinnBrain Multimodal Neonatal Template and Atlas Collection: T1, T2, and DTI brain templates, and accompanying cortical and subcortical atlases. *BioRxiv*, 2024.01.18.576325. https://doi.org/10.1101/2024.01.18.576325

Tyler J., T., & Abdijadid, S. (2023). Neuroanatomy , Limbic System. In *StatPearls*.

Uematsu, A., Matsui, M., Tanaka, C., Takahashi, T., Noguchi, K., Suzuki, M., & Nishijo, H. (2012). Developmental Trajectories of Amygdala and Hippocampus from Infancy to Early Adulthood in Healthy Individuals. *PLoS ONE*, *7*(10). https://doi.org/10.1371/journal.pone.0046970

Vachha, B., & Huang, S. Y. (2021). MRI with ultrahigh field strength and high-performance gradients: challenges and opportunities for clinical neuroimaging at 7 T and beyond. In *European Radiology Experimental* (Vol. 5, Issue 1). Springer Science and Business Media Deutschland GmbH. https://doi.org/10.1186/s41747-021-00216-2

Visser, M., Müller, D. M. J., van Duijn, R. J. M., Smits, M., Verburg, N., Hendriks, E. J., Nabuurs, R. J. A., Bot, J. C. J., Eijgelaar, R. S., Witte, M., van Herk, M. B., Barkhof, F., de Witt Hamer, P. C., & de Munck, J. C. (2019). Inter-rater agreement in glioma segmentations on longitudinal MRI. *NeuroImage: Clinical*, *22*(July 2018), 101727. https://doi.org/10.1016/j.nicl.2019.101727

Vuilleumier, P. (2005). How brains beware: Neural mechanisms of emotional attention. *Trends in Cognitive Sciences*, *9*(12), 585–594. https://doi.org/10.1016/j.tics.2005.10.011

Ward Jr, J. H. (1963). Hierarchical Grouping to Optimize an Objective Function. *Journal of the American Statistical Association*, *58*(301), 236–244. https://doi.org/10.1080/01621459.1963.10500845

Watson, C., Kirkcaldie, M., & Paxinos, G. (2010). Higher level functions consciousness, learning, memory, and emotions. *The Brain*, 109–124. https://doi.org/10.1016/b978-0-12-373889-9.50008-5

Weier, K., Fonov, V., Lavoie, K., Doyon, J., & Louis Collins, D. (2014). Rapid automatic segmentation of the human cerebellum and its lobules (RASCAL)-Implementation and application of the patch-based label-fusion technique with a template library to segment the human cerebellum. *Human Brain Mapping*, *35*(10), 5026–5039. https://doi.org/10.1002/hbm.22529

Weisenfeld, N. I., Mewes, A. U. J., & Warfield, S. K. (2006). Highly accurate segmentation of brain tissue and subcortical gray matter from newborn MRI. *Lecture Notes in Computer Science (Including Subseries Lecture Notes in Artificial Intelligence and Lecture Notes in Bioinformatics)*, *4190 LNCS*, 199–206. https://doi.org/10.1007/11866565_25

Wen, D. J., Poh, J. S., Ni, S. N., Chong, Y. S., Chen, H., Kwek, K., Shek, L. P., Gluckman, P. D., Fortier, M. V., Meaney, M. J., & Qiu, A. (2017). Influences of prenatal and postnatal maternal depression on amygdala volume and microstructure in young children. *Translational Psychiatry*, *7*(4). https://doi.org/10.1038/tp.2017.74

Wen, D. J., Poh, J. S., Ni, S. N., Chong, Y. S., Chen, H., Kwek, K., Shek, L. P., Gluckman, P. D., Fortier, M. V., Meaney, M. J., & Qiu, A. (2017). Influences of prenatal and postnatal maternal depression on amygdala volume and microstructure in young children. *Translational Psychiatry*, *7*(4). https://doi.org/10.1038/tp.2017.74

Whalen, P. J., Shin, L. M., McInerney, S. C., Fischer, H., Wright, C. I., & Rauch, S. L. (2001). A Functional MRI Study of Human Amygdala Responses to Facial Expressions of Fear Versus Anger. *Emotion*, *1*(1), 70–83. https://doi.org/10.1037/1528-3542.1.1.70

Yau, J. O. Y., Chaichim, C., Power, J. M., & McNally, G. P. (2021). The Roles of Basolateral Amygdala Parvalbumin Neurons in Fear Learning. *The Journal of Neuroscience : The Official Journal of the Society for Neuroscience*, *41*(44), 9223–9234. https://doi.org/10.1523/JNEUROSCI.2461-20.2021

Yoshida, S., Oishi, K., Faria, A. V., & Mori, S. (2013). Diffusion tensor imaging of normal brain development. *Pediatric Radiology*, *43*(1), 15–27. https://doi.org/10.1007/s00247-012-2496-x

Yrondi, A., Nemmi, F., Billoux, S., Giron, A., Sporer, M., Taib, S., Salles, J., Pierre, D., Thalamas, C., Schmitt, L., Péran, P., & Arbus, C. (2019). Significant decrease in hippocampus and amygdala mean diffusivity in treatment-resistant depression patients who respond to electroconvulsive therapy. *Frontiers in Psychiatry*, *10*(SEP), 1–8. https://doi.org/10.3389/fpsyt.2019.00694

Yrttiaho, S., Forssman, L., Kaatiala, J., & Leppänen, J. M. (2014). Developmental precursors of social brain networks: The emergence of attentional and cortical sensitivity to facial expressions in 5 to 7 months old infants. *PLoS ONE*, *9*(6). https://doi.org/10.1371/journal.pone.0100811

Yushkevich, P. A., Piven, J., Hazlett, H. C., Smith, R. G., Ho, S., Gee, J. C., & Gerig, G. (2006). User-guided 3D active contour segmentation of anatomical structures: Significantly improved efficiency and reliability. *NeuroImage*, *31*(3), 1116–1128. https://doi.org/10.1016/j.neuroimage.2006.01.015

Zeidman, P., & Maguire, E. A. (2016). *Anterior hippocampus: the anatomy of perception, imagination and episodic memory*. https://doi.org/10.1038/nrn.2015.24

Zhao, K., Zhao, J., Zhang, M., Cui, Q., & Fu, X. (2017). Neural responses to rapid facial expressions of fear and surprise. *Frontiers in Psychology*, *8*(MAY), 1–8. https://doi.org/10.3389/fpsyg.2017.00761

Zuckerman, B., Amaro, H., Bauchner, H., & Cabral, H. (1989). Depressive symptoms during pregnancy: Relationship to poor health behaviors. *American Journal of Obstetrics and Gynecology*, *160*(5 PART 1), 1107–1111. https://doi.org/10.1016/0002-9378(89)90170-1

TURUN
YLIOPISTO
UNIVERSITY
OF TURKU

Painosalama, Turku, Finland 2024

ISBN 978-951-29-9863-0 (PRINT)
ISBN 978-951-29-9864-7 (PDF)
ISSN 0355-9483 (Print)
ISSN 2343-3213 (Online)